Department of Molecular Medicine, The Scripps Research Institute, 10550 North Torrey Pines Rd., 92037 La Jolla CA, United States of America

Decorating Antigen with Multivalent CD22 Ligands to Prevent B-cell Mediated Anti-Drug Antibody Formation

Jan-Willem H. Langenbach

Submitted as the minor project thesis for fulfilment of the requirements of the master's degree in Drug Innovation (MBiosciences) at Utrecht University

1st of October 2022

Supervisors: Dr. Shengyang Wang, Prof. J. C. Paulson

1 Contents

2 LIST OF NON-STANDARD TERMS/ABBREVIATIONS

TLC	= thin layer chromatography
rt	= room temperature
LacNAc	= β-D-galactopyranosyl-1→4-*N*-acetyl-β-D-glucopyranosamine
2,3-Sia-	= α-*N*-acetyl-Neuraminic-acid-2,3-
2,6-Sia-	= α-*N*-acetyl-Neuraminic acid-2,6-
OAc	= *O*-acetyl
PE	= petroleum ether
EtOAc	= ethyl acetate
HVAC	= high vacuum
THF	= tetrahydrofuran
TFA	= trifluoroacetic acid
TCA	= trichloroacetic acid
DCM	= dichloromethane

3 ABSTRACT

Over the past few decades, the field of drug discovery has slowly been shifting towards the development of biotherapeutics. They offer many benefits over traditional small molecules imparted by their high specificity such as low off-target effects and low chance of drug-drug interactions. However, because these are large and complex biomolecules, anti-drug antibodies (ADAs) can easily be formed reducing their efficacy and causing moderate to severe side effects. As B-cells are the cells responsible for antibody production, inhibiting their activation may supress or completely forgo ADA formation. To achieve this goal, we opted to link high affinity murine CD22 (mCD22) ligands to the model antigen Ovalbumin (OVA), to examine if costimulatory binding of the inhibitory CD22 receptor can prevent OVA specific antibody formation. A novel synthetic route was developed to synthesize large quantities of a previously reported high affinity mCD22 ligand and novel di- and tetravalent scaffolds were developed based on existing literature and used to multimerize this mCD22 ligand. Microscale thermophoresis showed sub-micromolar binding of these di- and tetravalent ligands to mCD22. The conjugation of these multivalent ligands to OVA was optimized and it was shown to lead to highly increased uptake of the conjugates by splenic B-cells as seen by FACS. *In vivo,* the OVA modified with the di- and tetravalent ligand showed an over ten-fold reduction in anti-OVA IgG1 production. Unfortunately, the total antibody production against the OVA-conjugates, was not changed. This observation likely indicates that antibodies are generated against the linker or ligand, suggesting that this way of presentation does not (fully) supress B-cell activation. The possible reasons as to why this was observed are discussed, and suggestions are made for further research.

4 LAYMAN'S SUMMARY

Over the last 100 years, there has been a great deal of development in the medical sciences. Where a simple paper cut in your finger becoming infected could mean that there was no hope left, these days taking some simple antibiotics can make you feel better in no time. Most drugs like antibiotics consist of 'small molecule drugs', meaning that chemists made this drug which consists of a compound not found in nature that can be made chemically in a laboratory. This compound can then usually bind to a protein in your body or of a pathogen, inhibiting its function and thereby curing the disease.

However, some diseases have proven to be quite difficult to treat this way, and examples include diseases such as cancer, rheumatoid arthritis, or diabetes. In these diseases, binding one part of a protein with a small molecule drug to inhibit it has not proven effective, and thus scientists turned to nature for a solution. In nature, you can find very large and complex molecules like proteins that could in principle cure a disease. Let's look at diabetes for example. Here, people suffer from high blood sugar. To combat this, diabetics are given insulin. This is not a small molecule, but a protein naturally found in the body that can lower blood sugar. Such drugs are called 'biologicals' because they are derived from nature.

Although these biologicals have many advantages and can treat diseases once considered untreatable, they have one major disadvantage. Because these are large molecules coming from nature, some of these drugs can trigger an immune response. The drug is then mistaken as harmful, which elicits antibodies against the drug. These antibodies are produced by immune cells called B-cells, and these antibodies can destroy the drug rendering it ineffective. Furthermore, the immune response itself can be harmful to the patient.

In my research, I explored a way to modify biologicals, so they don't trigger the B-cells and activate the immune system. The way we try to do this is that we put ligands for a receptor called CD22 onto a biological drug. This receptor is found on the B-cells but turns them off when they bind to their ligand. Thus, the idea is that when the B-cells encounter a protein-based drug which has this ligand, they are taught that the drug is safe and does not warrant an immune response, thereby improving the tolerance for the drug.

We successfully synthesized ligands for CD22 and placed these on a food allergen from eggs called Ovalbumin to see if they would prevent the formation of anti-Ovalbumin antibodies. Unfortunately, although the B-cells do seem to bind the CD22 ligands through their CD22 receptor, they still were activated. We think this might be because of the way we presented these ligands on the Ovalbumin and the structures we used to attach them. Therefore, we propose to adapt our strategy and continue the research to make the idea work.

5 ACKNOWLEDGMENTS

First, I would like to thank Shengyang for his excellent supervision. It was great to work with someone with so much synthetic experience and I appreciate the freedom you gave me to try new things. Moreover, we also had a lot of fun both inside and outside the lab, which made me feel very welcome from day 1 and made my time in San Diego a great one. I would like to thank Corwin for all the good conversation on synthesis (among other things), without your help and experience I would never have been able to prepare these compounds so quickly. I would like to thank Maidul for his advice and patience to help me modify the Ovalbumin and design the in vivo experiments. I would like to thank Britni, without whom al the in vivo work would have never been possible, and who was always there to help me learn or to perform some of the the biological parts of this project. You really are a great teacher, and a true curiosity driven scientist. I would also like to thank all the other Paulson Lab members; I had great conversations with all of you about anything from science to politics and everyone was always ready to help, teach or explain me something new. I could not have imagined a better environment for my internship abroad. I would like to thank Anna for all her help in organizing everything non science. It was quite a lot of work sometimes, but no matter what the issue was you always made sure things got done. Finally, I would like to thank Jim for giving me the opportunity to come to his lab and even extend the internship. You were very welcoming from the start to the great baseball game at the end. Through your experience, critical view, and safe atmosphere to ask questions, I learned a great deal about immunology, SigLec biology, experimental design, and the way science as a whole works for which I am very grateful.

6 INTRODUCTION

6.1 BACKGROUND

Over the past few decades, the field of drug discovery has slowly been shifting towards the development of biotherapeutics. Recently the number of approvals has increased drastically, from averaging less than five per year between 2000 and 2010, to over eighteen over the past five years.[1] And although currently only making up 2% of prescriptions, biologicals already account for over a third of net drug spending.[2] They have many advantages over the more traditional small molecules due to their high specificity, such as low off-target effects and low chance of drug-drug interactions. Furthermore, biologicals have been used to treat diseases once considered untreatable. However, they also come with major disadvantages such as decreased stability, increased complexity, and the risk of anti-drug antibody (ADA) formation.[3]

ADA formation can occur because biologicals are large and complex biomolecules, which are easily recognized by the body as foreign. In the case of monoclonal antibodies for example, this phenomenon can occur in up to 70% of patients.[4] These ADAs are problematic, because they can influence the pharmacokinetic properties of a drug and even render the drug ineffective. Moreover, the corresponding immune response can trigger (severe) side effects in patients.[4] Therefore, there is a need to develop a way to mitigate the formation of ADAs.

Unwanted immunogenicity starts when antigen presenting cells (APCs) take up the biological and present part of it as an antigen on the MHC-II receptor. This will activate $CD4^+$ T-cells which will start producing cytokines. Next, these bind to the B-cells that have bound the same antigen via their B-cell receptor (BCR), which actives the B-cell turning it into a plasma cell that will produce antibodies.[5] Figure 1 depicts this route by which ADA formation occurs. Because the biotherapeutic endocytosis can take place through multiple types of APCs, halting the activation of the B-cell was identified as the most viable way of preventing ADA formation. To achieve this, an inhibitory receptor on the B-cell was chosen as the target, namely CD22.

Figure 1. *Mechanism by which unwanted immunogenicity is generated against a biotherapeutic. Endocytosis of the biotherapeutic by an APC activates T-cells, which activate B-cells, which turn into plasma cells that produce the antibody. Figure adapted from*[6,7]

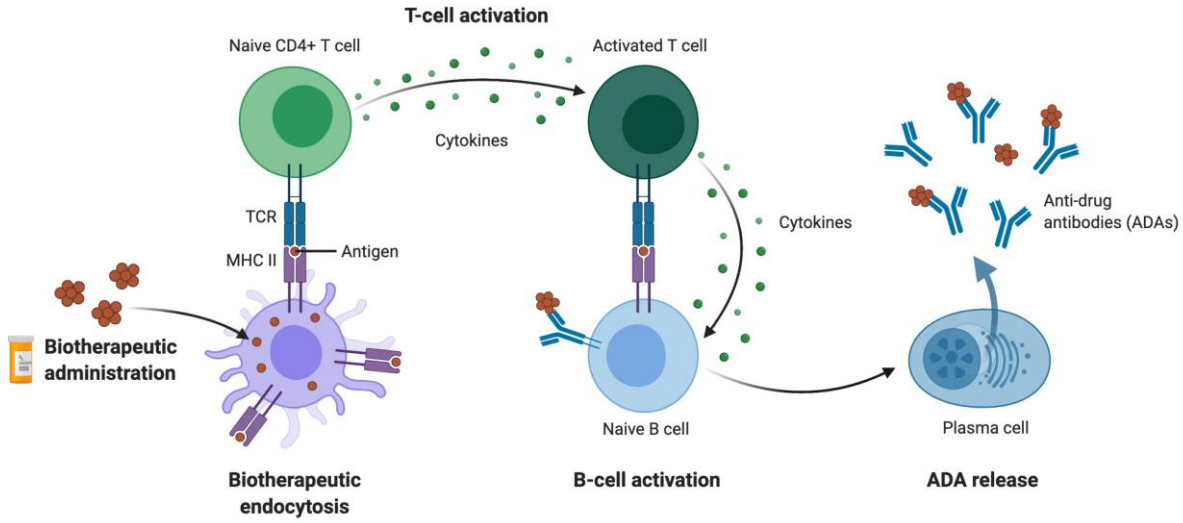

CD22 is a receptor which is found almost exclusively on B-cells, and which is colocalized with the BCR. Figure 2 shows normal B-cell activation, and CD22 based inhibition. Without binding CD22, when the BCR binds an antigen CD79 is phosphorylated which in turn phosphorylates Syk. This phosphorylated Syk then triggers a cascade leading to B-cell activation. However, when the antigen contains a ligand for CD22, CD22 itself is phosphorylated by the surface kinase Lyn. This phosphorylated CD22 can then recruit Shp-I. When the CD22 ligands are in close proximity to the antigen, this Shp-I is also indirectly recruited to the BCR. Here, it can dephosphorylate Syk. As mentioned before, the phosphorylated Syk is part of the cascade leading to B-cell activation, and thus its dephosphorylation stops the B-cell activation.[8]

Figure 2. *Mechanism by which CD22 can supress B-cell activation. A) The normal activation of a B-cell by the BCR. An antigen is bound, which phosphorylates CD79a and -b, which in turn phosphorylate Syk. This triggers B-cell activation downstream. B) When CD22 is bound, Lyn phosphorylates Shp-1, which dephosphorylates Syk halting B-cell activation. Figure was created in Biorender.*

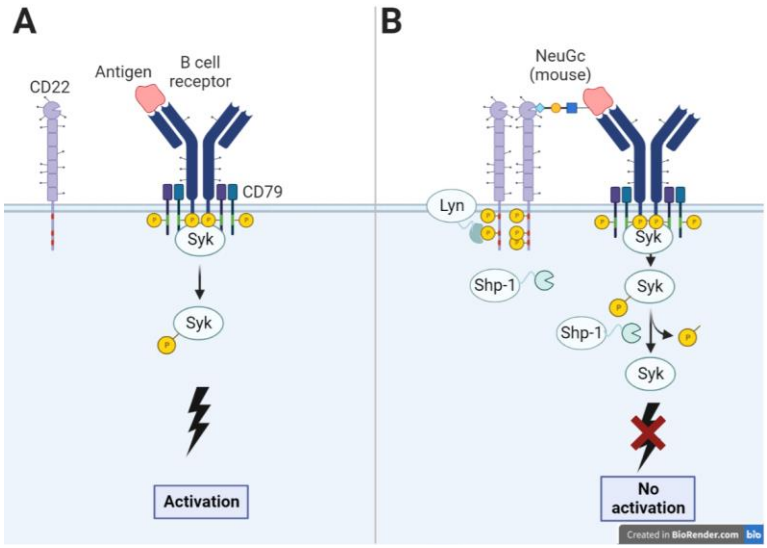

In research by Paulson *et al.*, high affinity ligands for both murine and human CD22 were identified.[9,10] These consist of Sialyl-LacNAc, the natural ligand for CD22, modified at the 5- and 9-position of the sialic acid. Figure 3 shows the chemical structures of the high-affinity murine and human CD22 ligand. In unpublished research, it was shown that attaching this ligand to the model biotherapeutic Ovalbumin which normally causes a strong antibody response in mice, the formation of ADAs could indeed be slightly suppressed. However, the effect was not substantial and the protection only short lasting. To overcome this, the CD22 based suppression thus needs to be improved.

Figure 3. *Chemical structures of the high affinity murine and human CD22 ligand.*

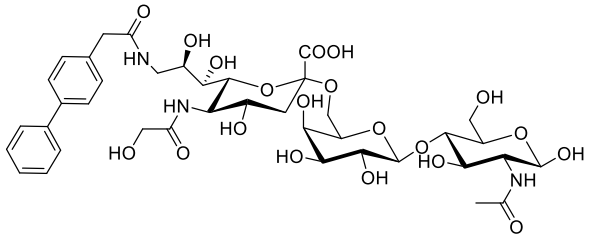

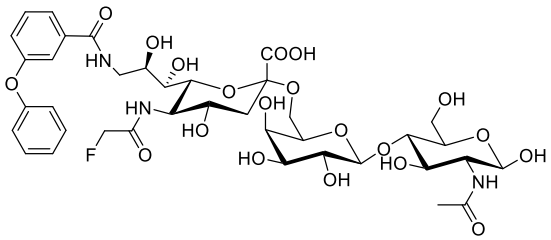

In research by Peng *et al.*, it was shown that by increasing the valency of the ligand by attaching it to a natural N-glycan scaffold, the affinity could be dramatically improved.[11] Furthermore, in research by Harumoto *et al,*. it was shown that by multimerizing the CD22 ligand on an unnatural scaffold, the avidity measured by SPR could be improved even further into the mid- to low nanomolar range.[12] Therefore, these synthetic multivalent CD22 ligands based on the scaffold of Harumoto *et al.* might provide a viable route for successful CD22 mediated B-cell suppression.

7 RESULTS & DISCUSSION

7.1 AIM & GENERAL STRATEGY

Our aim was to synthesize multivalent CD22 ligands analogous to those used by Harumoto *et al.*[12] and attach these to the model antigen Ovalbumin (OVA) to explore if these modifications could suppress anti-OVA antibody formation. Scheme 1 shows an overview for the synthesis of the ovalbumin modified with mCD22 ligands. First, the high affinity ligand is synthesized chemoenzymatically and functionalized with a maleimide linker for conjugation with the scaffolds. These scaffolds are synthesized chemically, consisting largely of polyethylene glycol linkers and two or four thiol moieties, as well as an azide moiety to allow for the use of click chemistry. Combining the scaffold and ligand together then gives the multivalent high affinity mCD22 ligands. In parallel, the model antigen OVA can be modified with bicyclononyne (BCN) groups that allow for copper free click chemistry using the surface exposed amines. Combining the multivalent high affinity ligands with the OVA then clicks the two together to give the modified OVA conjugates.

Scheme 1. *Reaction scheme for the synthesis of 9-azido-5-N-Boc-sialic acid, including the reagents and conditions used and the final yields in which the compound was obtained. This figure was created in Biorender.*

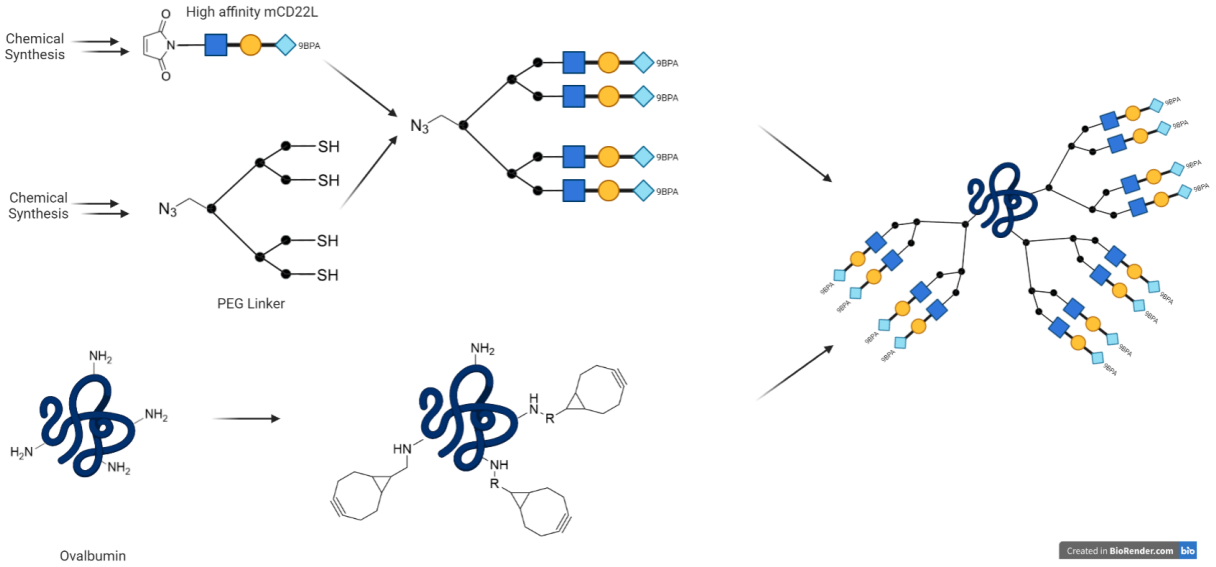

7.2 SYNTHESIS OF N-ACETYL-LACTOSAMINE-B-(N-CBZ-ETHYLAMINE)

Scheme 2A shows the chemoenzymatic synthesis of β-LacNAc-(N-Cbz-ethylamine), which is required for the preparation of the high affinity murine CD22 (mCD22) ligand. First, N-acetyl glucosamine is peracetylated using acetic anhydride in pyridine as a solvent and nucleophilic catalyst. The obtained anomeric mixture is then converted to the α-oxazoline intermediate by activating the anomeric ester using TMSOTf, which is subsequently reacted with N-Cbz-2-aminoethanol to give pure β compound **2**. This compound can then be deacetylated under Zemplén conditions to give modified N-acetyl-glucosamine **3** in good yield. A galactose unit is then installed enzymatically using UPD-glucose and the fusion enzyme lgtb-GalE which isomerizes the UPD-glucose to UDP-galactose, and subsequently transfers it stereo- and regioselectively onto the C4 position of the GlcNAc to give compound **4** in moderate yield. In parallel, the Cbz group can be removed from compound **3** by palladium catalysed hydrogenation to give compound **5** in quantitative yield.

Scheme 2. *Reaction scheme for the synthesis of A) LacNAc-N-Cbz-ethylamine and B) GlcNAc-maleimide including the reagents and conditions used and the final yields in which the compound was obtained.*

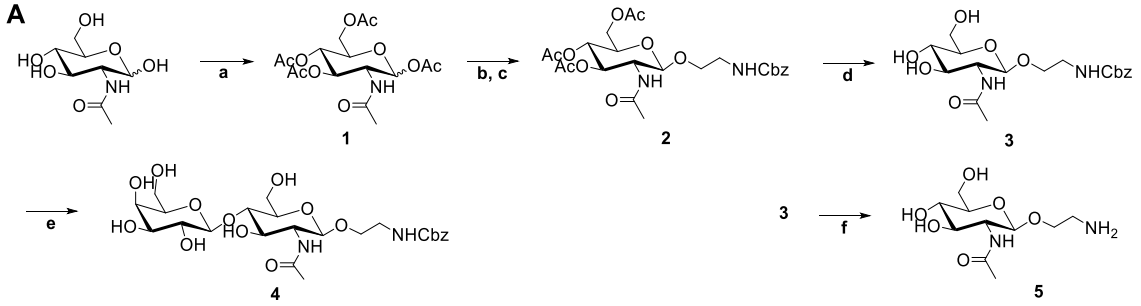

Reagents and Conditions: a) Ac_2O, Pyridine, R.T., 15h **b)** TMSOTf, DCE, molsieves, 50°C, 15h, **c)** TMSOTf, N-CBz-ethanolamine, molsieves, DCM, 20-30°C, 15h, 68% over 3 steps **d)** NaOMe, MeOH, R.T. 3h, 94% **e)** lgtb-GalE, UDP-Glc, Tris pH=7.5, $MnCl_2$, 37°C, 15h, 45% **f)** Pd/C, H_2, H_2O, R.T., 48h, quant.

7.3 SYNTHESIS OF CD22 LIGAND WITH MALEIMIDE LINKER

The synthesis of the high affinity multivalent mCD22 ligand has been reported previously.[13] However, the scale of this approach was limited to few hundred milligrams of modified sialic acid because of an enzymatic step early in the process. As many different high affinity Siglec ligands are used routinely in the Paulson Lab, it was decided to derive a new synthetic route, that would allow for the preparation of multi-gram quantities of a modified sialic acid which could serve as a common intermediate for all these ligands. 9-azido-5-Boc-sialic acid was chosen as the intermediate since all Paulson Lab high affinity Siglec ligands consist of sialic acids modified at the 5- and/or 9-positions on either lactose or N-acetyl-lactosamine and this intermediate could be transferred enzymatically onto these substrates. Furthermore, it contains two orthogonal protecting groups that provide synthetic flexibility. Because sometimes the 5-position of the sialic acid can be changed before enzymatic transfer, the intermediate was left fully protected as compound **10** to allowed for easy exchange of the 5-position.

Scheme 3 shows the synthesis of the maleimide linker modified by a high affinity murine CD22 ligand via the new synthetic route. First, sialic acid is esterified using a Fisher esterification in methanol to give the methyl ester. The obtained solid was subsequently peracetylated using acetic anhydride and pyridine as solvent and nucleophilic catalyst to give compound **7** in excellent yield. Next, the anomeric acetate was activated using BF_3▪Et_2O and reacted with p-thiocresol to form the thioether which serves as a robust protecting group. Deacetylation under Zemplén conditions gave compound **8** in excellent yield. To modify the 9-position, tosyl chloride is used to selectively convert the primary alcohol to the corresponding tosylate. After purification to separate any unreacted and over-tosylated material, it was displaced to azide using sodium azide to give compound **9**. To modify the 5-position, the compound is again peracetylated and Boc_2O was used to install a Boc group onto the amide. The presence of this carbamate severely reduces the stability of the acetamide, which was subsequently removed using K_2CO_3 in methanol. As some loss of acetyl esters was observed, the crude was re-acetylated using acetic anhydride in pyridine. Although the acetylation steps here are not strictly required, they allowed for much easier separation of the compound on silica gel and are presumed to be (nearly) quantitative. After purification, 12.5 grams of compound **10** was obtained which can serve as a common intermediate for many of the published high-affinity ligands for SigLecs. To synthesize the mCD22 ligand, the Boc-group was removed under strongly acidic conditions using TFA and the amine subsequently reacted with O-acetyl-glycolyl chloride under basic conditions to install the protected glycolyl group and give compound **11** quantitatively. The modified sialic acid could then be deprotected, by first performing deacetylation under anhydrous conditions using sodium methoxide, and then the methyl ester was removed using aqueous sodium hydroxide. Finally, the thiocresol ether was oxidized using iodine in neutral phosphate buffer to the tosylate which under the employed conditions quickly hydrolysed to the free alcohol as desired to give compound **13** in excellent yield. This sequence of deprotection steps was found to be crucial, as the removal of the p-thiocresol ether caused an instability of the sialic acid under acidic or basic conditions. Next, the modified sialic acid was transferred onto previously prepared compound **4** by first forming the activated CMP-sialic acid analogue *in situ* using NmCSS and CTP in the presence of $CaCl_2$, and then adding compound **4** and Pd2,6ST to form compound **14** in moderate yield. Next, the azide was reduced to the amine using triphenyl phosphine which allowed for the installation of the biphenyl acetamide group under basic conditions using biphenyl acetic acid N-hydroxy succinimide ester (BPA-NHS). The BPA group cannot be installed before the enzymatic reaction, as the enzyme does not tolerate this modification. Finally, the Cbz-group on the aglycone was removed using palladium catalysed hydrogenation to give compound **15** in moderate yield. The now exposed amine moiety was then reacted with NHS-PEG_6-Maleimide under anhydrous conditions and subsequently purified using HPLC to give compound **16** in moderate yield.

Scheme 3. *Reaction scheme for the synthesis of the maleimide functionalized high affinity murine CD22 ligand, including the reagents and conditions used and the final yields in which the compound was obtained.*

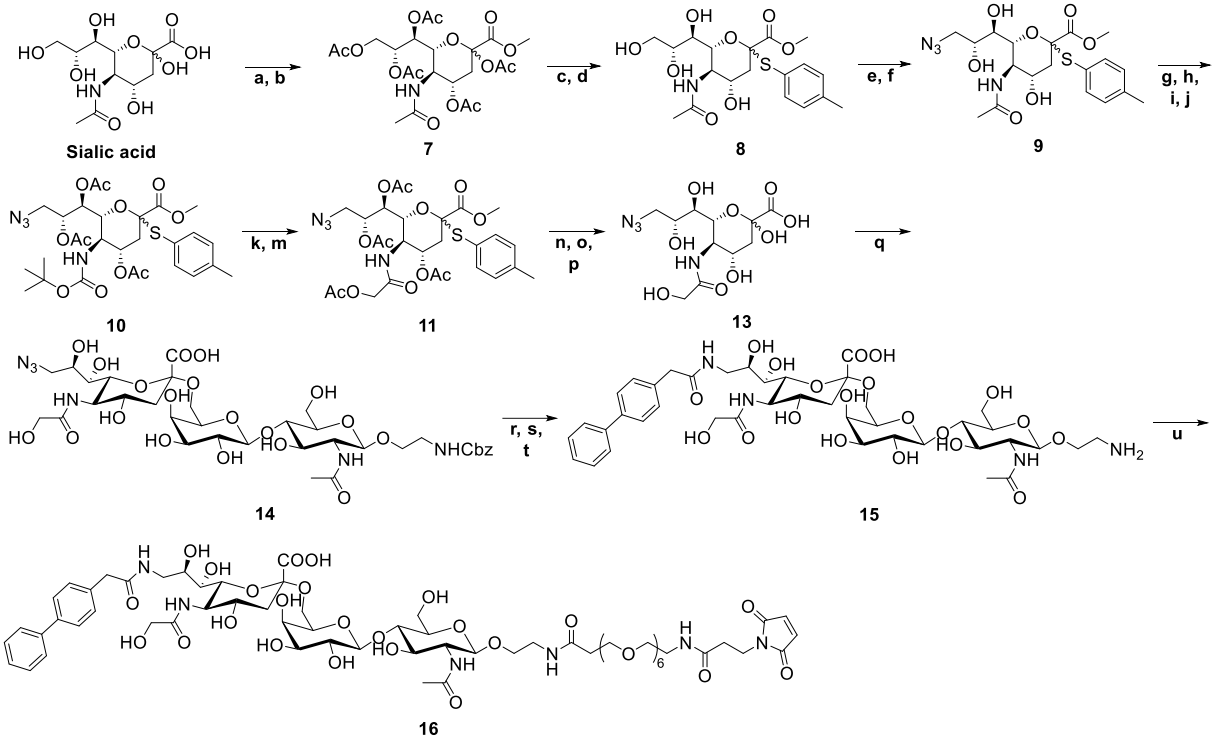

Reagents and Conditions: a) MeOH, Amberlite-H^+, R.T, 48h **b)** Ac_2O, Pyridine, 0°C to R.T., 5h, 94% over two steps **c)** p-thiocresol, BF_3Et_2O, DCM, 48h **d)** NaOMe, MeOH, H^+ workup, R.T., 3h, 91% over two steps **e)** TsCl, Pyridine, 0°C to R.T., 18h, 69% **f)** NaN_3, Acetone/H_2O, 80°C, 48h, 65% **g)** Ac_2O, Pyridine, R.T., 15h **h)** Boc_2O, THF, 60°C, 24h **i)** K_2CO_3, $MeOH^+THF$, R.T., 72h **j)** Ac_2O, Pyridine, R.T., 15h, 80% over 4 steps **k)** TFA, DCM, R.T., 1h **m)** O-acetyl-glycoyl chloride, Et_3N, DCM, R.T., 1h, quant. **n)** NaOMe, MeOH, H^+ workup, R.T., 15h **o)** NaOH, H_2O, R.T. 5h, Quant over 2 steps **p)** I_2, H_2O, R.T., 15h, 95% **q)** Compound **4**, CTP, NmCSS, Pd2,6ST, $CaCl_2$, Tris pH= 9, 37°C, 24h, 77% **r)** PPh_3, H_2O, NaOH, R.T., 24h **s)** I) BPA, NHS, DCC, Et_3N, r.t, 15h II) Et_3N, DCM, 12h **t)** Pd/C, H_2 (balloon), H_2O, 2h, 47% over 3 steps **u)** NHS-$dPEG_6$-Mal, Et_3N, DMSO, 37°C, 6h, 52%

7.4 SYNTHESIS OF DI- AND TETRAVALENT LINKERS

The scaffolds were designed based on research by Harumoto *et al.*[12] Some modifications were made to allow for the use of different click chemistries, ease of synthesis and increased hydrophilicity. Scheme 4 shows the synthesis of the di- and tetravalent scaffolds. First, PEG_3-Cl was converted to PEG_3-N_3 by simple displacement using sodium azide in DMF. Next, the alcohol is activated using tosyl chloride to give compound **17** in moderate yield. The primary reason for the low yield was the incomplete formation of the tosylate under the employed reaction conditions, but any remaining PEG_3-N_3 was recovered. Next, the latter was reacted with 5-hydroxy-dimethyl-isophthalate in order to form the first branching point. Hydrolysing the methyl groups using aqueous sodium hydroxide and neutralisation with hydrochloric acid gave compound **18** in good yield. Next, the two arms were extended using the bifunctional NHBoc-PEG_9-NH_2 using EDCI/DIPEA coupling to activate the acid and form the amides which gave compound **19** in moderate yield. Deprotection of the Boc groups under strongly acidic conditions using TFA gave compound **20** quantitatively. Part of compound **20** was then reacted with S-acetyl-thiopropionic acid NHS ester under slightly basic conditions to install the protected thiopriopionamide groups, which were deprotected using sodium methoxide in methanol to give divalent scaffold **21** in very good yield. In parallel, part of compound **20** was reacted with Boc-Lys(Boc)-OSu to install another branching point and gave compound **22**. Deprotection of the Boc groups under moderately strongly acidic conditions using TFA gave compound **23** quantitatively. Following the same methodology, the latter was then reacted with S-acetyl-thiopropionic acid NHS ester under slightly basic conditions to install the protected thiopriopionamide groups, which were deprotected using sodium methoxide in methanol to give divalent scaffold **24** in good yield.

Scheme 4. *Reaction scheme for the synthesis of the multivalent scaffolds, including the reagents and conditions used and the final yields in which the compound was obtained.*

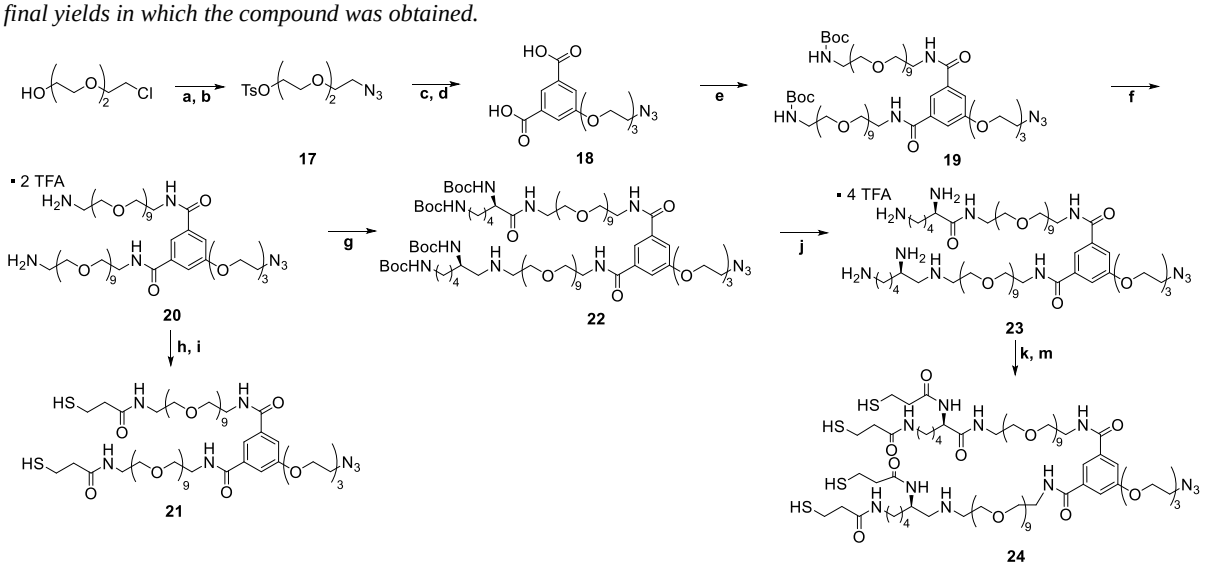

Reagents and Conditions: **a)** NaN_3, DMF, 100°C, 15h **b)** TsCl, Et_3N, DCM, R.T., 15h, 45% over two steps **c)** Dimethyl 5-hydroxyisophtalate, $CsCO_3$, ACN, 80°C, 15h, **d)** I) NaOH, H_2O, R.T., 4h II) HCl 66% over two steps **e)** NH_2-PEG_9-NHBoc, EDCI, DIPEA, THF, R.T., 48h, 49% **f)** TFA, DCM, R.T., 2h, 98% **g)** Boc-Lys(Boc)-OSu, THF, DIPEA, R.T., 15h, 55% **h)** I) Thiopropionic acid, NHS, DCC, Et_3N, r.t, 15h II) Et_3N, DCM, 12h **i)** NaOMe, MeOH, R.T., 5 min, 81% over 2 steps **j)** TFA, DCM, R.T., 2h, quant. **k)** I) Thiopropionic acid, NHS, DCC, Et_3N, r.t, 15h II) Et_3N, DCM, 12h **m)** NaOMe, MeOH, R.T., 5 min, 70% over 2 steps

7.5 SYNTHESIS OF MULTIVALENT MCD22L & CONTROL COMPOUNDS

To synthesize the multivalent ligands, the same general procedure was followed for all compounds. Scheme 5 shows the synthesis of the clickable (multivalent) ligands. For the clickable monovalent ligand, N_3-PEG_3-SH was reacted with monovalent high affinity ligand **16** to form the clicked intermediate, which was stabilized by ring opening hydrolysis in water at pH=9 to give compound **25** in good yield. To synthesize compound **26**, compound **5** was reacted with Mal-PEG_6-NHS to give GlcNAc-Mal. Next, this was reacted with scaffold **21** which after subsequent ring opening hydrolysis gave compound **26**. For the di- and tetravalent compounds, scaffolds **21** and **24** were reacted with monovalent ligand **16**, which gave the clicked intermediates that after ring opening hydrolysis gave compounds **27** and **28** respectively.

Scheme 5. *Reaction scheme for the synthesis of the azido carrying mono-, di- and tetravalent murine CD22 ligands, including the reagents and conditions used and the final yields in which the compound was obtained.*

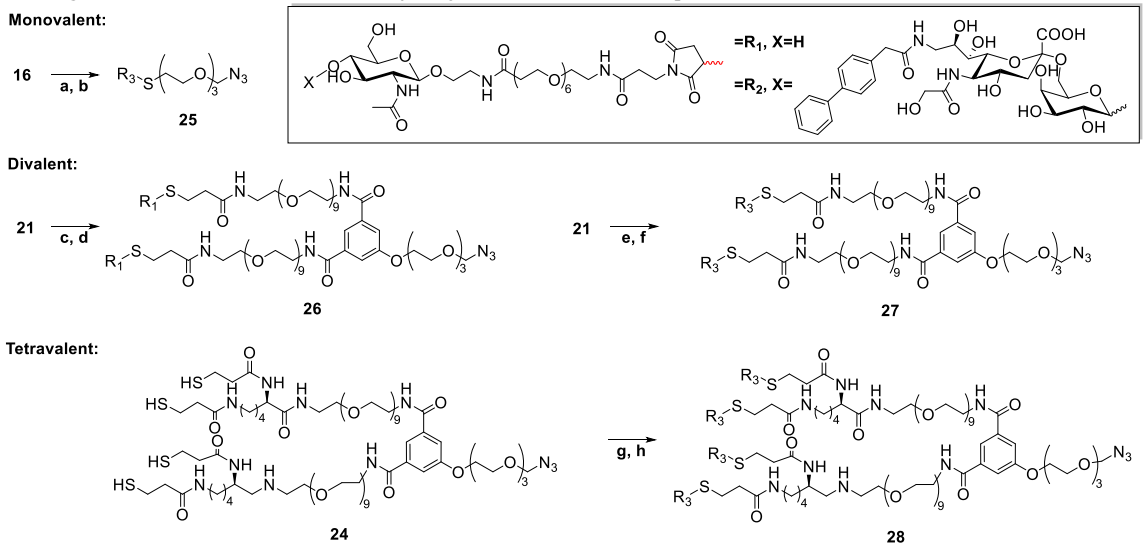

Reagents and Conditions: a) N_3-PEG_3-SH, DMSO, R.T., 5h **d)** NaOH (pH= 9-10), H_2O, 37°C, 15h, 85% over two steps **c)** I) **g)** NHS-PEG_6-Maleimide, triethylamine, DMSO, R.T., 4h, 90%, II) Compound **21,** DMSO, R.T., 6h **d)** NaOH (pH= 9-10), H_2O, 37°C, 15h, 85% over two steps **e)** Compound **16,** DMSO, R.T., 24h **f)** NaOH (pH= 9-10), H_2O, 37°C, 15h, 90% over two step **g)** Compound **16,** DMSO, R.T., 24h **h)** NaOH (pH= 9-10), H_2O, 37°C, 15h, 97% over two steps

The need for this ring opening hydrolysis of the clicked product is two-fold and can be seen in scheme 6. First, the original Michael addition is reversible. This means that over time, the scaffold can start losing the CD22 ligands by elimination. This loss of payload is even more likely *in vivo*, as different thiol moieties found here can displace the linker and attach to the ligand.[14–16] One of the most likely candidates for this in vivo is glutathione (GSH), which is found in intracellular concentrations of around 1-10 mM[17]. Ring opening under slightly alkaline conditions prevents these side reactions and makes the conjugation irreversible thereby forming stable conjugates.

Scheme 6. *Maleimide-thiol click chemistry and the ring opening stabilization.*

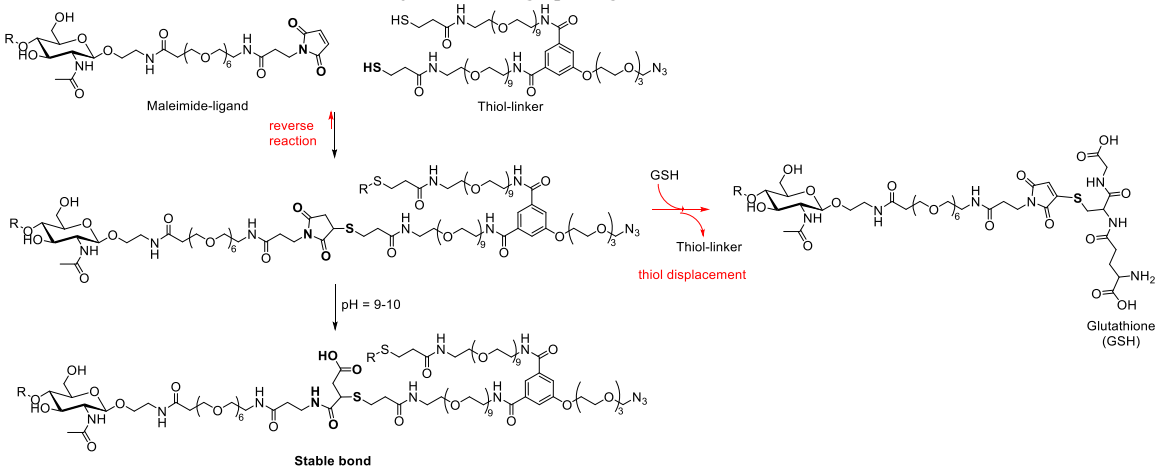

7.6 AFFINITIES (K_D) OF MULTIVALENT LIGANDS

To determine the effect of the multivalency on binding a single CD22 receptor in solution, microscalethermophoresis (MST) was used to measure the EC_{50} of the ligands for the receptor. For the monovalent ligand, no binding was observed, meaning that the K_D > 25 µM which was the cut-off for the assay used. For the divalent and tetravalent ligand, an EC_{50} of 440 nM and 190 nM was measured respectively. Figure 4 shows the binding curve of the di- and tetravalent ligand. In accordance with previously reported data, this thus depicts a major improvement over the monovalent ligand. What is notable, is that in previous assays this interaction was probed as a multivalent-multivalent interaction using SPR.[11,12] This experiment shows that the affinity gain is not only due to double binding but might also in part be due to other effects such as rebinding events.

Figure 4. *Microscale thermophoresis binding curves that were used to calculate the EC_{50} of the di and tetravalent ligands.*

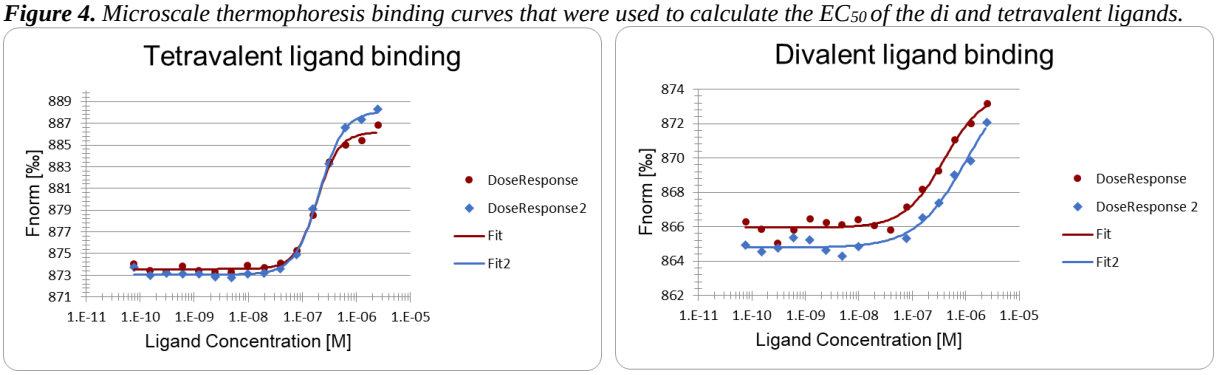

7.7 MODIFICATION OF OVALBUMIN

To obtain the desired modification of Ovalbumin with the mCD22 ligands, it was first modified with a BCN-capped linker to allow for copper-free click chemistry. To find the optimal reaction conditions, ovalbumin was reacted with different equivalents of bicyclononyne N-hydroxy succinimide (BCN-NHS) and the number of BCN groups attached was assessed using mass spectrometry. Figure 5 shows the modification level obtained when adding different equivalents of BCN-NHS.

Figure 5. *Equivalents of BCN-NHS added, and the modification level obtained as a distribution of species found by ESI-TOF.*

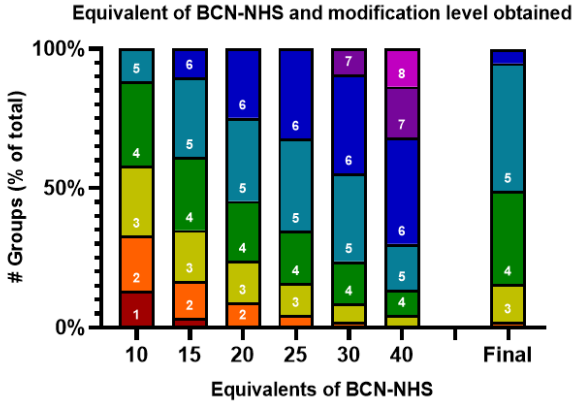

At 25 equivalents, most of the material was modified with 3-6 ligands, with only a very minor part having 2 ligands or less. This is desirable because these lower modified ovalbumin species and especially any unreacted ovalbumin might trigger a B-cell response. Increasing the equivalents even further mostly increases the average ligand number, but for this study it was decided that an average of 4 ligands or more was sufficient. The reason for this is that using the tetravalent ligand, this would already give 16 ligands per ovalbumin, which means it is very highly decorated making up almost half of the final complex by weight. On the right, a column can be seen of the final material obtained using the large-scale preparation and 25 equivalents of glycan. Although slightly different from the pilot scale, having a narrower distribution, almost no material with 2 ligands or less was seen, and the average modification level is above 4, meaning the predetermined requirements were met. Next, the BCN modified ovalbumin was reacted with the azido-ligands by simply mixing them together in buffer and allowing them to react. Figure 6 shows the complexes made and their appearance by SDS-PAGE gel.

Figure 6. *Schematic representation of the conjugates synthesized and their appearance by SDS page.*

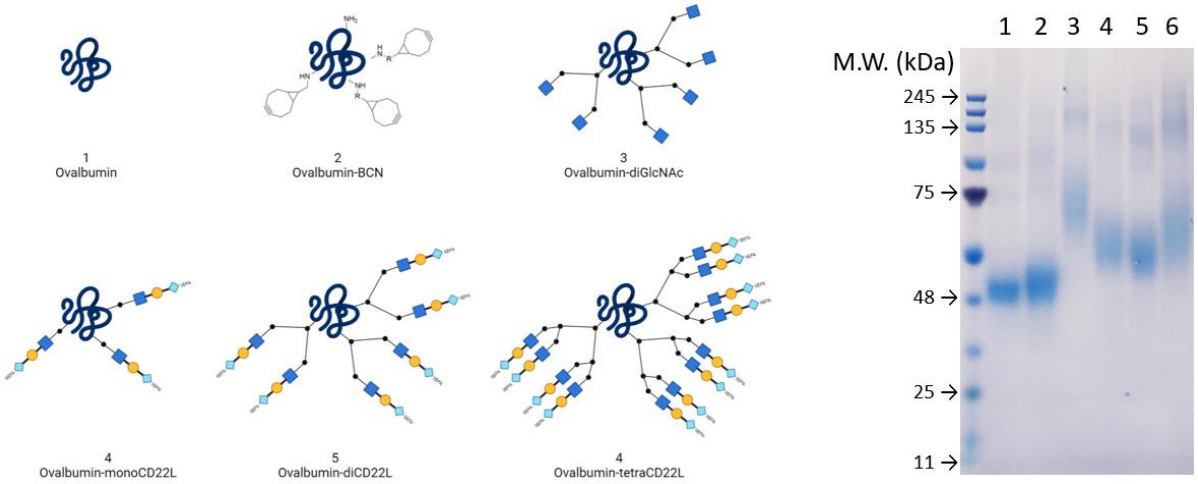

It should be noted that SDS-PAGE cannot give an accurate representation of the mass of the final conjugates. The mobility through the gel is based on both the shape of the final conjugate as well as the charge. Both are likely influenced by the modifications, as the linker might not denature into the same shape as the peptide chain does, and the charge normally obtained through the SDS is changed as the ligands can displace the SDS. Furthermore, the neuraminic acids themselves carry a negative charge. Therefore, two different methods are used to determine the modification level: absorbance and mass spectrometry.

Absorbance can be used, as the linker has an absorbance maximum of λ_{max} = 253 nm likely stemming from the biphenylacetamide group, while the ovalbumin has an absorbance maximum of λ_{max} = 280 nm. The extinction coefficients were measured for ovalbumin and the ligand, giving A_{253} = 13 300 $M^{-1}cm^{-1}$ & A_{280} = 30 500 $M^{-1}cm^{-1}$ and A_{253} = 11 500 $M^{-1}cm^{-1}$ & A_{280} = 2 700 $M^{-1}cm^{-1}$, respectively. This difference in absorbance of more than 10-fold at A_{280} means that knowing the extinction coefficients and measuring the absorbance of a sample at both wavelengths, the concentration of both the ligand and the ovalbumin can be determined.

The second method is based on mass spectrometry. Although this method can determine the exact masses of the species present, it is not strictly quantitative in nature as the final signal intensity is a product of not just the quantity present but also ionization efficiency. Most likely, the number of ligands is therefore somewhat underestimated as higher modification levels resulted in decreased signal. As the GlcNAc and BCN groups have no absorbance, their conjugates were characterized by mass spectrometry to get an estimation of the modification level. The monovalent CD22 conjugate was also characterized by mass spectrometry, to show that the modification level appeared similar for it and the control divalent GlcNAc conjugate. The divalent CD22 and tetravalent CD22 conjugates did not give a reliable signal by either MALDI or ESI. Table 1 shows the conjugates obtained and the calculated modification level.

Table 1. *Conjugates obtained and the characteristics by absorbance and mass spectrometry.*

	Absorbance				Mass spectrometry	
Conjugate	**Ovalbumin (mM)**	**Ligand (mM)**	**#ligands**	**#linkers**	**M/z**	**#modifications (method)**
OVA	81.8	3*	0.03*	0	44458	0 (ESI/MALDI)
OVA-BCN	-	-	-	-	46449	4.0 (ESI)
OVA-diGlcNAc	-	-	-	-	58049	4.0 (MALDI)
OVA-monoCD22	85.2	399	4.7	4.7	51843	3.5 (MALDI)
OVA-diCD22	89.2	832	9.3	4.7	-	-
OVA-tetraCD22	97.3	1570	16.1	4.2	-	-

As can be seen, all conjugates appear to be in the 4-5 ligands attached range as desired, considering that mass spectrometry indeed appears to give a lower modification level for the same compound as can be seen for the mono-CD22 ligand.

7.8 EC_{50} OF CONJUGATES FOR SPLENIC B-CELLS

To assess the accessibility and avidity of the ligands when presented on Ovalbumin, their ability to bind murine splenic B-cells and their endocytosis was determined using FACS. Splenocytes were extracted from murine spleens and a dilution series of the fluorescently labelled conjugates was added. All compounds were labelled with identical amounts of Alexa Fluor 647 (AF647) per OVA by reacting the compound with increasing amounts of AF647-NHS until the desired labelling level was obtained. The B-cells were gated on using forward/side scatter, B220 & CD19 double positive, and the conjugate fluorescence was measured. Background fluorescence was determined using B-cells extracted from $CD22^{-/-}$ mice. The experiment was performed at 4°C and 37 °C, as endocytosis is halted at 4°C which allows for the differentiation of the two phenomena. Figure 7 shows the B-cell binding and B-cell endocytosis of the Ovalbumin conjugates.

Figure 7. *B-cell binding and endocytosis of the conjugates modified with different types of CD22 ligands.*

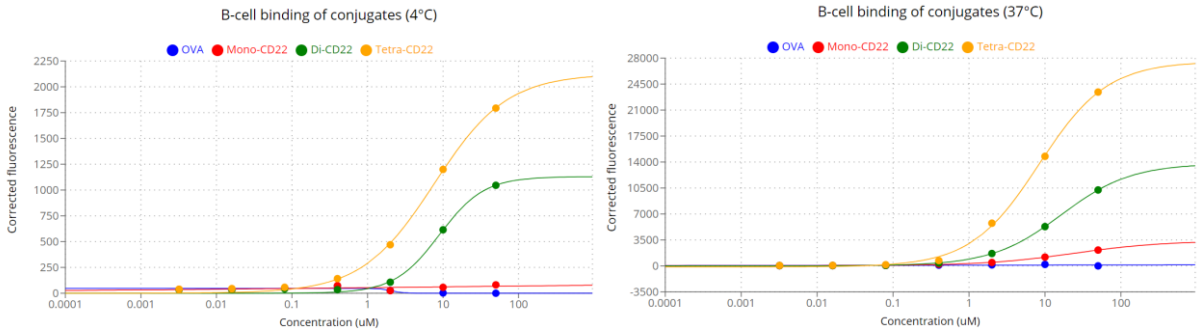

As can be seen, the EC_{50} of the di- and tetravalent conjugates seems to be identical at 16 and 8 µM respectively taking the double number of ligands into account. However, much more of the conjugate seems to be attached to the cells as evidenced by the higher fluorescence reading. Moreover, the monovalent ligands seem to poorly bind to the B-cells at all. This observation implies that the multivalent ligands are both accessible and functional. When looking at the experiment allowing endocytosis, there seems to be about a 10-fold increase in ligand associated per cell, indicating that endocytosis is indeed taking place. Again, the tetravalent ligand seems to be highly effective, but this time the monovalent ligands appears to show some endocytosis as well indicating that this ligand is likely accessible and functional but less potent.

7.9 IN VIVO STUDIES

7.9.1 First dose study

To investigate the optimal dose for supressing the B-cell mediated IgG1 antibody production, the IgG1 titers against OVA and the monovalent ligand conjugate were measured weekly giving three either 100, 50 or 10 µg injections spaced one week apart. Figure 7 shows the dosing and bleeding scheme.

Figure 7. *First dose study timeline*

All doses were tested in Balb/c mice and the 50 µg dose was also tested in C57BL/6. The endotoxin level of the administered solutions was measured to ensure that they were similar between groups. The reason for this is that the receptor for endotoxins, TLR4, is known to enhance BCR activation and may thus counteract any CD22 mediated suppression.[18] Table 2 summarizes the study groups.

Table 2. *Table of first dose study groups*

Injected material	Dose	Injection route	Strain	Endotoxin level
OVA	100 µg	S.C.	Balb/c	13.8 EU/mL
OVA	50 µg	S.C.	Balb/c	6.9 EU/mL
OVA	10 µg	S.C.	Balb/c	1.4 EU/mL
OVA	50 µg	S.C.	C57BL/6	6.9 EU/mL
OVA-CD22	100 µg	S.C.	Balb/c	13.2 EU/mL
OVA-CD22	50 µg	S.C.	Balb/c	6.6 EU/mL
OVA-CD22	10 µg	S.C.	Balb/c	1.3 EU/mL
OVA-CD22	50 µg	S.C.	C57BL/6	6.6 EU/mL

During this study, one error was made while giving the injections. On day 8, the OVA-CD22 groups marked in red receiving 100 µg and 50 µg received a dose of OVA instead of OVA-CD22. Because of this, the results of these groups are unreliable. However, in this scenario some suppression is still to be expected. For all groups, antibody levels against OVA were measured. Using an internal standard on the ELISA plate consisting of a dilution series of commercial anti-OVA IgG1, these could be correlated to an exact value in ng/mL. For the group receiving the monovalent conjugate, antibody levels against the conjugate were also determined. As no conjugate-standard antibody was available, these values could not be expressed in ng/mL. For this, the titer was calculated as the first dilution giving 2*average of negative control + 2*standard deviation of negative control. Figure 8 shows the antibody levels against OVA in ng/mL on day 14 and 21, figure 9 shows the anti-injectable titers on day 14 and 21 (N=5).

Figure 8. *Anti-OVA IgG1 on day 14 and 21*

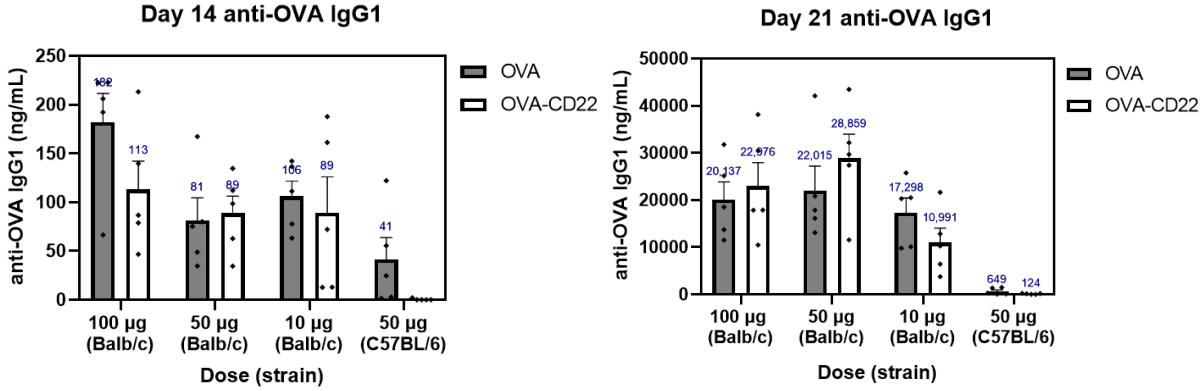

At first glance, it seems like the suppression is ineffective in all groups but the C57BL/6 mice. This was a surprising result, as previous studies seemed to indicate that the monovalent ligand would give some suppression in all groups. In the C57BL/6 mice, very low titers are developed for both the control and the monovalent conjugate. Next, we investigated the total antibody level against the substance that was injected by coated the ELISA plate with that substance. In the case of the mice receiving OVA, the plate was coated with OVA. In the case of mice receiving OVA-CD22, the plate was coated with OVA-CD22. Figure 9 shows the results based on this anti-injectable IgG1 titer. Unfortunately, the suppression in the C57BL/6 groups seems to disappear entirely here, meaning that antibodies are likely being formed against the linker and/or ligand.

Figure 9. *Anti-Injectable IgG1 on day 14 and 21*

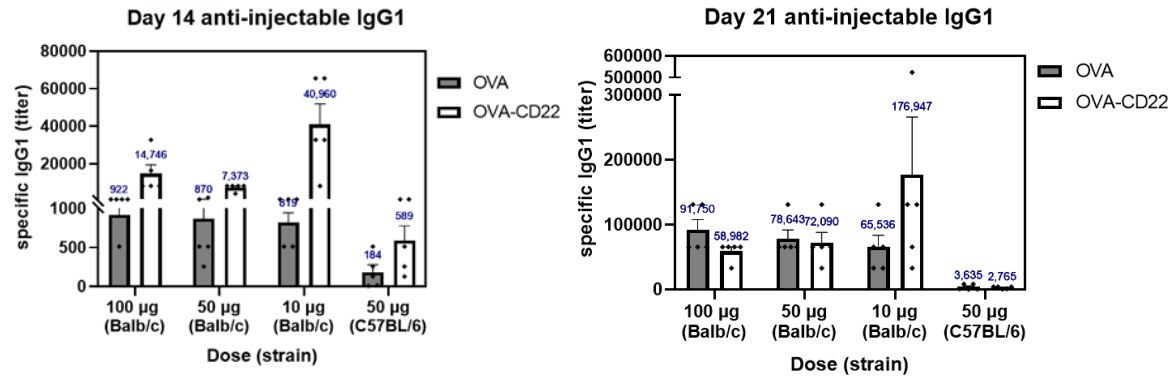

It was hypothesized that the lack of full suppression could be due to the presence of endotoxins. As mentioned before, endotoxins can stimulate and activate B-cells and enhance activation mediated by the BCR. Moreover, it was of course expected that increasing the valency of the ligand could have the desired effect. To ensure that the positive control (OVA) was effective at inducing an immune repose without any endotoxins in the preparation, it was decided to perform a second dose study.

7.9.2 Second dose study

In this study, the effects of dose, injection route and endotoxin levels on the anti-OVA IgG1 production were measured. Three 10 or 100 µg doses of endotoxin-containing or endotoxin-free OVA were given either subcutaneous (S.C.) or intravenous (I.V.). Next, the IgG1 antibody levels were measured every 7 days for 5 weeks. Figure 10 shows the dosing scheme and table 3 shows an overview of the study groups.

Figure 10. *Second dose study timeline*

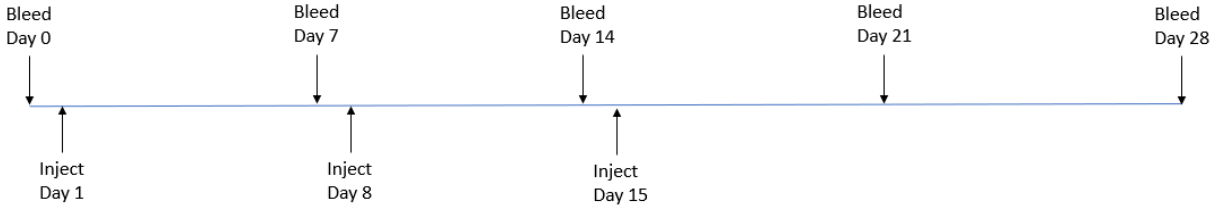

Table 3. *Table of second study groups*

Injected material	Dose	Injection route	Strain	Endotoxin level
Regular OVA	100 µg	S.C.	Balb/c	23 EU/mL
Regular OVA	10 µg	S.C.	Balb/c	2.3 EU/mL
Regular OVA	100 µg	I.V.	Balb/c	23 EU/mL
Regular OVA	10 µg	I.V.	Balb/c	2.3 EU/mL
LPS-free OVA	100 µg	S.C.	Balb/c	<0.1 EU/mL
LPS-free OVA	10 µg	S.C.	Balb/c	<0.1 EU/mL
LPS-free OVA	100 µg	I.V.	Balb/c	<0.1 EU/mL
LPS-free OVA	10 µg	I.V.	Balb/c	<0.1 EU/mL

Figure 11 shows the antibody levels on the final two weeks of the study. Despite this being a study with low power (N=3), a few trends become apparent. First, the antibody levels seem to reach their maximum at day 21 with a subcutaneous injection of endotoxin-containing ovalbumin. However, with endotoxin-free ovalbumin, the levels are consistently higher at day 28 over day 21. Thus, in the next study the antibody levels will be measured until day 28. Moreover, of all the endotoxin free groups, the 10 µg S.C. groups appears to give the best antibody production. Therefore, this dose and injection route will be chosen as the route for assessing suppression.

Figure 11. *Anti-OVA IgG1 on day 21 and 28*

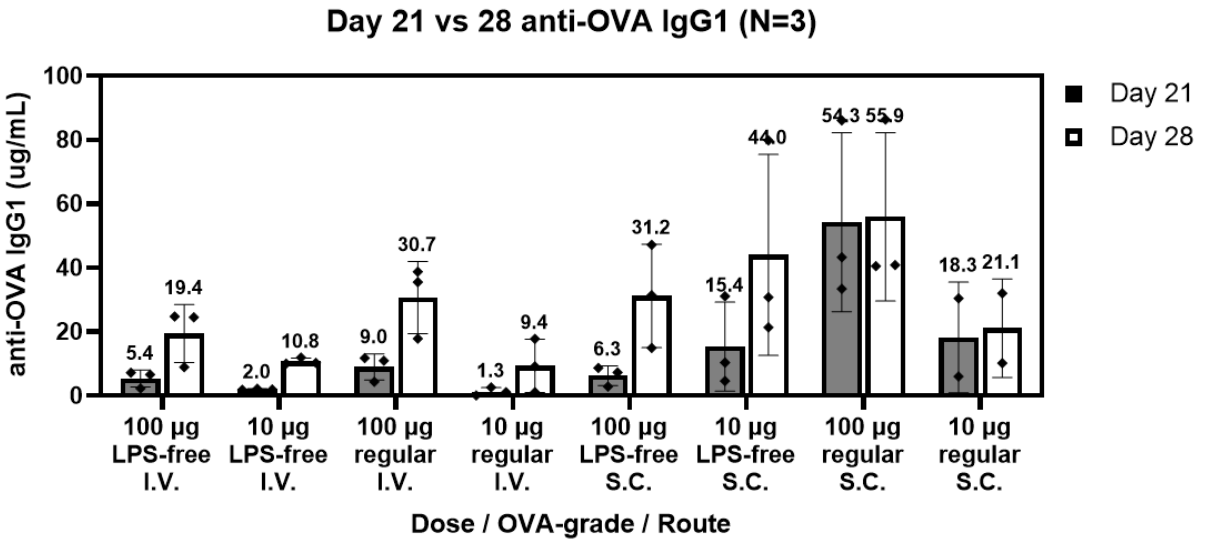

7.9.3 Multivalent ligands

To investigate if the multivalent ligands can give the desired suppression, and if the endotoxin free preparations do indeed perform better, a third in vivo study was done. Figure 12 shows the injection and bleeding scheme, which is identical to the previous study design.

Figure 12. *Study timeline*

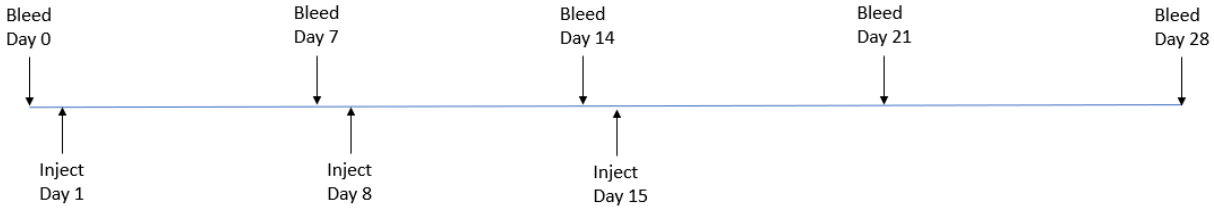

Figure 13 shows the anti-OVA IgG1 and anti-injectable IgG1 over time for the 5 groups. As can be seen, unmodified OVA gives the highest anti-OVA IgG1. The second control group, OVA modified with the divalent linker and GlcNAc groups, appears to be slightly lower than the ovalbumin. In contrast with the first *in vivo* study, the monovalent ligand does seem to show suppression of anti-OVA IgG1 antibodies. Therefore, eliminating endotoxin might indeed lead to better CD22 mediated suppression. This result is however greatly outperformed by the divalent and tetravalent ligand which seem to show a more than 10x suppression. Therefore, one might conclude that the multivalent ligands are also working. There is a robust reduction of anti-OVA IgG1.

Unfortunately, the suppression of antibodies appears to be limited to anti-OVA antibodies. When looking at antibodies against the substance that is being injected by coating the ELISA plate for each group with that substance, it appears to be identical for all OVA conjugates, regardless of the modification present. This indicates that although OVA antibodies are supressed, antibodies are now being generated against the linker and/or ligand. This implies that the the original idea has not worked fully as B-cells are still being activated. This could be due to multiple factors relating to the way these ligands are presented, which are discussed in chapter 8.

Figure 13. *Anti-OVA IgG1 and anti-injectable IgG1 over time for the different conjugates.*

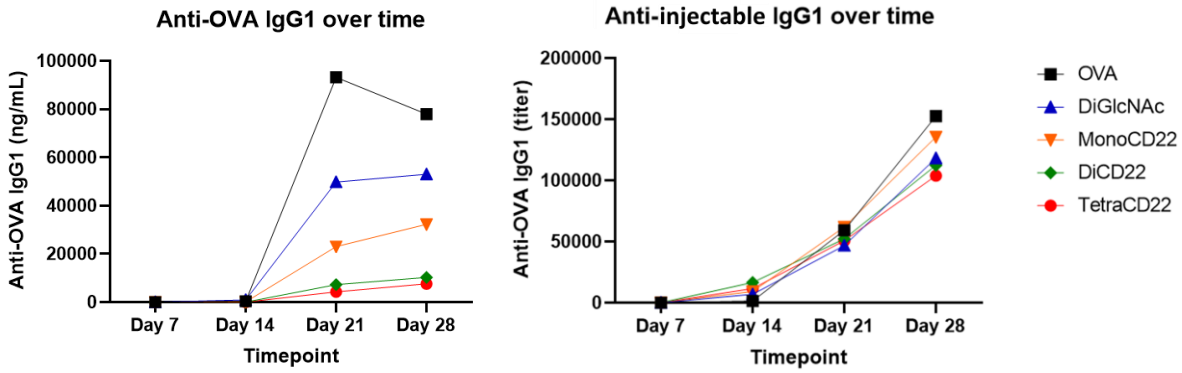

8 SUMMARY & OUTLOOK

To summarize, the designed multivalent CD22 ligands were synthesized successfully. A large-scale synthetic route for preparing 5- and 9-position modified sialic acid was developed and used to synthesize multigram quantities of this common intermediate. Novel di- and tetravalent scaffolds were developed based on existing literature and these were synthesized on 50-200 mg scales. The conjugation of these ligands to the model antigen Ovalbumin (OVA) was optimized and the resulting conjugates were characterized using absorbance and ESI/MALDI-TOF. Conjugates were obtained carrying four to five mono-, di- or tetravalent CD22 ligands.

The conjugates were studied *in vivo* to assess their capability of suppressing anti-OVA IgG1 antibody formation. In this regard, the monovalent ligand showed minor suppression, while the di- and tetravalent ligand showed an over 10-fold reduction in anti-OVA IgG1 production. Therefore, supressing the formation of OVA directed antibodies was successful. However, when examining the total antibody against the conjugate that was injected, there was no change in the antibody production. This likely indicates that some parts of scaffold and linker are immunogenic, and antibodies are being generated against those parts instead of the OVA.

8.1 ANALYSE ANTIBODY EPITOPES

To find the cause behind immunogenicity of groups on the OVA, the exact parts that are immunogenic should be identified. Multiple groups that are part of the scaffold are known to be immunogenic in mice and humans and these might be cause of the observed unwanted immunogenicity. If these parts are known, they could be changed to less immunogenic alternatives which might give the ligand a chance to perform better.

One important variable that could be tested, is to investigate if the murine CD22 ligand itself is immunogenic and whether any antibodies are directed against it. This does not have to be the case, as the antibodies seen could also be directed against the linker only. This could be examined by attaching the ligand to a different protein such as bovine serum albumin (BSA) on a different linker and use this conjugate to perform the ELISA using the blood from the mice that receive the OVA conjugate with ligand and current linker. If any antibodies are directed against the ligand, these specifically should show up. In this case, it would be very hard to continue the project, and a new high affinity ligand should be found.

One part of the scaffold that is known to be quite immunogenic are the polyethylene glycol (PEG) linkers. These are known to illicit anti-PEG antibodies and this effect is known to be aggravated when presented on proteins.[19] This is a known problem in drug development, and many patients have pre-existing anti-PEG antibodies due to their widespread occurrence in healthcare and cosmetic products.[20] Although no alternative to PEG has currently made it into the clinic, much effort has already been put into developing alternatives and it is expected that viable alternatives will be found in the future.[21] One of the linkers often proposed, are carbohydrate based linkers.

8.2 SWITCH TO NATURAL SCAFFOLDS

One possibility for removing the possibly immunogenic PEG linkers is the use of naturally occurring bi- and/or tetra-antennary N-glycans. These could also multimerize the mCD22 ligand and have been shown to give an excellent affinity increase as well.[11] To attach these without any linker, they could be reacted with the surface exposed lysine's directly by converting the terminal glucosamine into the oxazoline. Combining these oxazoline glycans with a proteins has been shown to cause nonenzymatic glycation of the protein with lysine residues.[22]

Since this strategy does depend on good excess of the oxazoline and the efficacy may vary per protein due to the relatively low reactivity of the oxazoline group, the anomeric hydroxyl could also be converted into the azide using the commercially available reagent 2-azido-1,3-dimethylimidazolinium hexafluorophosphate.[23] This would allow for the use of click chemistry with a BCN group as with the original strategy. The BCN-NHS used should in that instance also not contain any peg spacer, as this could introduce immunogenicity as well.

8.3 EMPLOY MIXED LIGANDS

Another possibility to enhance the B-cell suppression would be to use a combination of high affinity ligands, or to use ligands that can bind multiple SigLec receptors such as Siglec-G as well. Siglec-G is another inhibitory Siglec receptor that is found on the B-cells surface, and it has been shown to induce B-cell tolerance to BCR activation independent of CD22.[24] By binding both receptors, the tolerogenic response may thus be enhanced.

A clue that suggests that direct glycosylation of a protein is capable to induce B-cell tolerance was published earlier this year. Here, Erlebacher *et al.* showed that ovalbumin glycosylated by trophoblasts, the outer cells of the placenta that is formed from the foetus, can induce B-cell dependent tolerance in the mother.[25] In other words, in vivo OVA is able to be glycosylated in such a way that B-cell suppression is achieved. Therefore, our strategy should be viable as this is the same effect as we try to achieve here. In their experiments, they showed that a foetal membrane bound OVA which is shed into the maternal bloodstream does not illicit an immune response, despite the antigenic disparity between foetus and mother. Moreover, this form of glycosylated OVA conveys tolerance as these mice do not develop an immune response upon challenge with regular OVA contrary to unpregnant mice. Remarkably, this seems to be due to the presence of only a single natural N-glycan, as ovalbumin has only one glycosylation site and the molecular weight by SDS page appears to be quite low.

These glycans are likely heterogeneous, and thus to mimic this natural phenomenon their structure would need to be unravelled first and the effective glycans identified. However, these glycans may be very complex in their synthesis. Therefore, high affinity ligands may still prove to be simplest route to achieve the desired suppression if the protein of interest is to be glycosylated *in vitro*. However, in the above-mentioned paper they showed that Lyn-/- mice showed a much greater reduction in the development of the tolerance than CD22-/- mice did. This could be explained by the fact that Lyn is responsible for the CD22 as well as Siglec-G mediated suppression. Therefore, to mimic the natural situation in which suppression is achieved, high affinity ligands of both CD22 and Siglec-G (which is known) could be added onto the OVA to reach a maximal synergistic suppressive effect.

9 METHODS

9.1 GENERAL METHODS

For all syntheses, synthetic grade chemicals were used. Technical grade solvents were used unless specified otherwise. The reaction progress was monitored via TLC. The TLC plates used were Silicagel 60 F254TLC plates. Column chromatography was performed with SiliaFlash® P60 (40-63 µm) silica. Molecular sieves were generic brand 4 Å molecular sieves. The eluent denoted in the methods is the solvent mixture in which the compound eluded. ^{1}H and ^{13}C NMR spectra were recorded on a 400 MHz Brucker or 600 MHz Brucker NMR spectrometer.

(1) 1,4,5,6-tetra-O-acetyl- N-acetyl-glucosamine

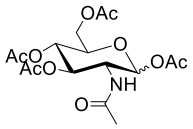

1

To a suspension of GlcNAc (5.12 g, 23 mmol) in pyridine (30 mL) was added acetic anhydride (50 mL) and the mixture was stirred at room temperature for 4 h during which all solid dissolved. Next, the reaction mixture was concentrated *in vacuo*, azeotroping twice with toluene (2 x 50 mL). Next, the residue was dissolved in DCM (25 mL) and washed with aqueous HCL (25 mL, 1M), $NaHCO_3$ (25 mL, sat.), brine (25 mL) and dried over magnesium sulphate. Concentration *in vacuo* gave compound **1** as a white foam (9.0 g, quant.). ^{1}H NMR was in accordance with previously reported data.[26]

(2) 1-(N-Cbz-2-aminoethyl)-4,5,6-tri-O-acetyl-N-acetyl-β-D-glucosamine

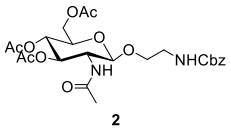

2

To a stirred solution of compound **1** (9.0g, 23 mmol) in dry DCE (4.5 mL) was added TMSOTf (4.5 mL, 25.1 mmol) and the mixture was stirred at 45°C overnight under inert atmosphere. Next, the mixture was neutralized with triethylamine (7.5 mL) and stored at -20°C for 6 weeks. The mixture was purified using column chromatography (EtOAc:Hex 3:2, 0.5% Et_3N) which afforded compound the intermediate as a viscous orange oil (4.78 g, 87%).

To a stirred solution of the intermediate (4.78 g, 20 mmol) in DCM (50 mL) were added molecular sieves (4A) and the mixture was stirred at room temperature for 15 minutes under inert atmosphere. Next, TMSOTf (1.5 mL, 6 mmol) was added, and the mixture was stirred at room temperature for 15h and then for 3 hours at 40°C. Next, the reactions was quenched with triethylamine (3 mL) and filtered and the filtrate was concentrated *in vacuo*. Purification using flash chromatography (0:1 Hexane:EtOAc) afforded compound **2** (8.21 g, 78%, β isomer only) as a white foam. ^{1}H NMR was in accordance with previously reported data.[27]

(3) 1-(N-Cbz-2-aminoethyl)-N-acetyl-β-D-glucosamine

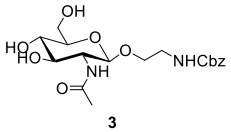

3

To a solution of compound **2** (8.21g, 15.7 mmol) in methanol (30 mL) was added sodium methoxide (325mg, 4.7 mmol) and the mixture was stirred at room temperature overnight. Next, the mixture was quenched using Amberlite H^+ until neutral pH and filtered. Concentration of the filtrate *in vacuo* afforded compound **3** (5.86 g, 94%) as an off-white solid. ^{1}H NMR was in accordance with previously reported data.[27]

(4) N-Cbz-2-aminoethyl [β-D-galactopyranosyl]-(1→4)-2-deoxy-2-aminoacetyl-β-D-glucopyranoside or N-Cbz-2-aminoethyl-β-LacNAc

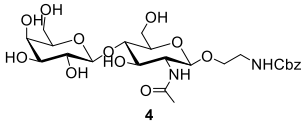

4

To a solution of compound **3** (119 mg, 0.3 mmol) in buffer (2.5 mL, 100 mM Tris, pH=7.5, 10 mM $MnCl_2$) was added UDP-Glc (336 mg, 0.6 mmol) and LgtB-GalE (600 µL) solution and the mixture was incubated at 37°C overnight. Next, the mixture was purified using P-2 size exclusion and Spek-Pak C18 (1:5 MeOH:H_2O). Lyophilization of the final material afforded compound **4** (115mg, 69%) as a white solid. ^{1}H NMR (600 MHz, D_2O) δ 7.36 (dq, J = 15.7, 7.6 Hz, 5H, Ar-H), 5.05 (m, 2H, linker CH_2), 4.40 (m, 2H, H-1 GlcNAc + H-1 Gal), 3.72 (m, 20H), 3.46 (m, 2H), 3.24 (m, 2H, linker CH_2), 1.89 (s, 3H, NHAc GlcNAc).

(5) 1-(2-aminoethyl)-N-acetyl-β-D-glucosamine

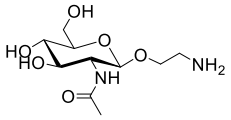

5

To a solution of compound **4** (80 mg, 0.2 mmol) in H_2O (2 mL) was added Pd/C (80mg, dry, 10% Pd) and a drop of acetic acid and the mixture was placed under hydrogen atmosphere (balloon) and stirred at room temperature for 48 hours. The mixture was filtered through a syringe filter (0.2 µM) washing twice with methanol (2 mL). The filtrate was concentrated *in vacuo* to remove methanol and lyophilized which afforded compound **5** (63 mg, quant) as a white solid. ^{1}H NMR was in accordance with previously reported data.[27]

(7) 2,4,7,8,9-penta-O-acetyl-sialic acid methyl ester

Sialic acid (30g, 97.1 mmol) was dissolved in methanol (400 mL). To this, amberlite-H^+ (approx. 20 mL) was added and this mixture was stirred at room temperature for 2 days. Next, the slightly opaque solution was filtered, and concentrated in vacuo. This afforded sialic acid methyl ester as a white powder, which was used without further characterization.

Sialic acid methyl ester (max. 97.1 mmol) obtained in the previous step was dissolved in pyridine (120 mL). To this, 4-N,N-dimethylamino pyridine (1.44g, 11.7 mmol) was added and the mixture was cooled to 0°C using an ice bath. Acetic anhydride (90 mL) was added slowly, and the mixture was stirred on ice for 15 minutes. The ice bath was removed, and the mixture was stirred at room temperature for 5 hours. Next, the mixture was concentrated in vacuo to a thick syrup. This was redissolved in 150 mL of toluene and concentrated again 4 times to remove leftover acetic anhydride and pyridine. The remaining off-white foam was stored at room temperature overnight. Next, the residue was dissolved in 600 mL of EtOAc and washed with 200 mL of 1N HCl, H_2O, saturated $NaHCO_3$ and brine consecutively. The organic layer was then dried over $MgSO_4$ for 15 minutes, filtered, and the filtrate was concentrated in vacuo. This afforded compound **7** (48.7 g, 94% over two steps) as a white foam. ^{1}H NMR was in accordance with previously reported data.[28]

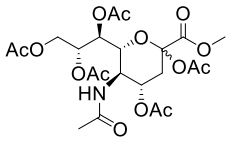

7

(8) 2-desoxy-2-S-(p-tolylthio)-sialic acid methyl ester

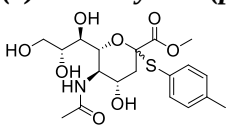

8

Compound **7** (48.7g, 91.3 mmol) and p-thiocresol (22.7g, 183 mmol) were dissolved in DCM (150 mL). To this, BF_3▪Et_2O (16.9 mL, 137 mmol) was added slowly over the course of 5 minutes. The mixture was then stirred at room temperature for 48 hours. Next, saturated $NaHCO_3$ solution (300 mL) was added slowly over the course of 10 minutes and the mixture was stirred for 30 minutes until no more bubbling was observed. The biphasic mixture was transferred to a separatory funnel and the organic layer was extracted. Next, this layer was washed with saturated $NaHCO_3$ solution (100 mL) and brine (200 mL) and subsequently dried over Mg_2SO_4 for 15 minutes. The solids were filtered off, and the filtrate was concentrated *in vacuo*. Purification using flash chromatography (0:1 Hexane:EtOAc) afforded the intermediate compound as a white foam.

This intermediate (max 91.3 mmol) obtained in the previous step was dissolved in methanol (185 mL). Sodium methoxide solution was added (18.25 mL, 0.5M) and the mixture was stirred at room temperature for 3 hours. Next, Amberlite H^+ was added until pH<7, and the mixture was filtered and concentrated *in vacuo*. This afforded compound **8** as a white foam (35.7g, 91% over two steps). ^{1}H NMR was in accordance with previously reported data.[29]

(9) 2-desoxy-2-S-(p-tolylthio)-9-desoxy-9-azido-sialic acid methyl ester

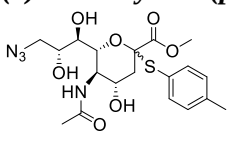

9

Compound **8** (35.7g, 83.1 mmol) was azeotropically dried using anhydrous pyridine (100 mL). Next, it was dissolved in anhydrous pyridine (820 mL) and the solution was put under inert atmosphere (nitrogen) and cooled to 0°C. Under strong stirring, a solution of tosyl choride (20.6g) in pyridine (50 mL) was added dropwise over the course of 1 hour. The mixture was left to react at 0°C for 2

hours, after which the ice was allowed to slowly melt reacting the mixture for an additional 15 hours. The mixture was quenched with methanol (50 mL) and concentrated *in vacuo*. Flash chromatography (0:9:1 hexane:EtOAc:methanol) afforded the intermediate compound as a white foam (33.6g, 69%).

To as stirred solution of the intermediate compound (32.1g, 55mol) in acetone:water (9:1, 500 mL), sodium azide (35.7g, 550 mmol) was added. The flask was fitted with a condenser and the mixture was refluxed at 80°C for 48 hours. The reaction mixture was concentrated in vacuo, redissolved in EtOAc and filtered through a silica plug. Concentration *in vacuo* afforded compound **9** as a white foam (16.6g, 65%). ^{1}H NMR was in accordance with previously reported data.[9]

(10) 2-desoxy-2-S-(p-tolylthio)-4,7,8-tri-O-acetyl-5-N-desactyl-5-N-(t-butyloxycarbonyl)-9-desoxy-9-azido-sialic acid methyl ester

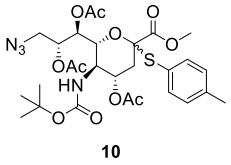

10

To a stirred solution of compound **9** (13.0g, 28.6 mmol) in pyridine (75 mL) was added acetic anhydride (50 mL) and the mixture was stirred for 15 hours at room temperature. Next, the mixture was concentrated in vacuo, azeotroping the residue 3x with toluene (150 mL). This afforded the intermediate compound as a white solid which was used without further purification.

To a stirred solution of the intermediate compound (max 28.6 mmol) and DMAP (1.74g, 14.3 mmol) in THF (250 mL) was added Boc_2O (33 mL, 143 mmol) and the mixture was refluxed at 60°C for 15h. Next, a second portion of Boc_2O (16 mL, 72 mmol) was added and the mixture was refluxed at 60°C for 8h. The solution was allowed to cool to room temperature and was used without further purification

To the solution (max 28.6 mmol) in THF obtained above was added methanol (125 mL) and K_2CO_3 (9.86g, 71.5 mmol) and the mixture was vigorously stirred at room temperature for 72h. As well as forming the desired product, this also resulted in the suspected partial deacetylation of one or multiple OAc groups as evidenced by TLC. The mixture was concentrated in vacuo at 15°C and resuspended in DCM (300 mL). Next, the mixture was filtered, and the filtrate concentrated in vacuo to obtain a deep orange solid containing a mixture of products.

The obtained solid was then re-acetylated by dissolving in pyridine (75 mL) and acetic anhydride (50 mL) and stirring the mixture for 15h at room temperature. This resulted in full conversion into a single product as seen by TLC. Next, the mixture was concentrated in vacuo, azeotroping the residue 3x with toluene (150 mL). Flash chromatography (EtOAc:Hex, 1:3) afforded compound **10** as a white foam (12.5g, 68%). ^{1}H NMR (400 MHz, $CDCl_3$, β-anomer) δ 7.32 (d, J = 8.1 Hz, 2H, Ar-H), 7.21 (d, J = 7.8 Hz, 2H, Ar-H), 5.55 (t, J = 2.2 Hz, 1H, Sia-H7), 5.30 (m, 1H, Sia-H8) 4.85 (d, J = 9.4 Hz, 1H, Sia-H4), 4.54 (dd, J = 10.6, 2.6 Hz, 1H, Sia-H5), 4.41 (m, 1H, NH), 4.14 (q, J = 7.2 Hz, 1H, EtOAc impurity), 3.81 (m, 1H, Sia-H6), 3.69 (m, 4H, C(=O)-O-CH_3 + Sia-H9$_\alpha$), 3.34 (dd, J = 13.5, 9.2 Hz, 1H, Sia-H9$_\beta$), 2.71 (dd, J = 13.8, 4.9 Hz, 1H, + Sia-H3$_\alpha$), 2.37 (s, 3H, CH_3-Ar), 2.09 (m, 10H, 3x OAc + Sia-H3$_\beta$), 1.41 (d, J = 8.0 Hz, 9H, tert-Butyl), 1.28 (t, J = 7.1 Hz, 3H, EtOAc impurity).

(11) 2-desoxy-2-S-(p-tolylthio)-4,7,8-tri-O-acetyl-5-N-glycoyl-9-desoxy-9-azido-neuraminic acid methyl ester

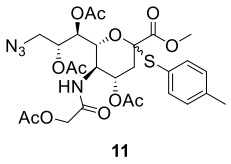

11

To a solution of compound **10** (2.55g, 4.0 mmol) in DCM (50 mL) was added TFA (50 mL) and the mixture was stirred at room temperature for 1 hour. Next, the mixture was concentrated in vacuo, azeotroping the residue with methanol (3x50 mL) and diethyl ether (2x50 mL). This afforded the intermediate as a white foam.

This intermediate was redissolved in DCM (25 mL) and triethylamine as added (5.6 mL, 40 mmol). The mixture was stirred for 15 minutes, and then under strong stirring acetoxyacetyl chloride (0.52 mL, 4.8 mmol) was added dropwise. After 1 hour the mixture was diluted with DCM (200 mL), washed with 1M HCl (200 mL) and sat. $NaHCO_3$ (200 mL) and dried over magnesium sulphate. The

obtained suspension was filtered and concentrated in vacuo to afford compound **11** as a white foam (2.55g, quant.). ^{1}H NMR was in accordance with previously reported data.[30]

(13) Sodium 5-N-(hydroxyacetyl)-9-desoxy-9-azido-neuraminate

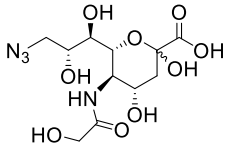

13

To a solution of compound **11** (500 mg, 784µmol) in methanol (1.5 mL) was added sodium methoxide solution (0.5M, 0.15 mL) and the mixture was stirred at room temperature overnight. Next, the mixture was diluted with methanol (10 mL) and sodium hydroxide solution (10 mL, 0.4 M) and stirred for 5 hours. The pH was adjusted to pH 7-8 using Amberlite H^+ and the mixture was filtered to remove the Amberlite resin. The filtrate was concentrated *in vacuo* at 4 °C. Purification using flash chromatography (1:1 DCM:MeOH) afforded the intermediate as a white foam (quant).

To a solution of the intermediate (784µmol) in phosphate buffer (100 mL, 50mM, pH=7.4) was added elemental iodine (200mg, 790µmol) and the mixture was stirred at room temperature for 24h. Next, the brown solution was transferred to a separatory funnel and washed with hexane until completely clear (3x150 mL). The resulting aqueous layer was concentrated *in vacuo*. Purification using P-2 size exclusion and Sep-Pak C18 (1:1 MeOH:H_2O) and subsequent lyophilization afforded compound **13** as a white foam (quant). ^{1}H NMR was in accordance with previously reported data.[31]

(14) Sodium [5-N-(hydroxyacetyl)-9-desoxy-9-azido-α-D-neuraminate]-(2→3)-N-Cbz-2-aminoethyl-β-LacNAc

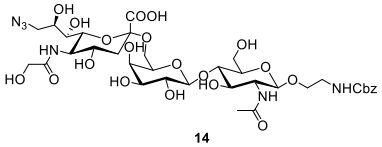

14

To a solution of compound **13** (285 µmol), compound **4** (133mg, 238µmol) and CTP (230mg, 475µmol) in buffer (10 mL, 100mM Tris pH=9, 50mM $MgCl_2$) was added NmCSS (100µL) and the mixture was incubated for 3h at 37°C. Next, NmCSS (100µL) and Pd2,6ST (300µL) were added and the mixture was incubated for 4h at 37°C. Next, Pd2,6ST (300µL) was added and the mixture was incubated overnight at 37°C. The resulting solution was centrifuged (3000g) and the supernatant lyophilized. Purification using P-2 size exclusion and Sep-Pak C18 (1:1 MeOH:H_2O) and subsequent lyophilization afforded compound **14** as a fluffy white solid (82mg, 77%). ^{1}H NMR (600 MHz, D_2O) δ 7.36 (dq, J = 16.4, 7.7 Hz, 5H, Ar-H), 5.05 (m, 2H, CH_2 Cbz), 4.46 (d, J = 8 Hz, 1H, H-1 GlcNAc), 4.36 (d, J = 7.9 Hz, 1H, H-1 Gal), 4.04 (s, 2H, CH_2 NeuGc), 3.61 (m, 23H), 3.24 (m, 2H, linker CH_2), 2.60 (dd, J = 12.4, 4.6 Hz, 1H, H-3$_\alpha$ NeuGc), 1.92 (s, 3H, CH_3 Ac GlcNAc), 1.64 (t, J = 12.1 Hz, 1H, H-3$_\beta$ NeuGc).

(15) Sodium [5-N-(hydroxyacetyl)-9-desoxy-9-(biphenylacetamido)-α-D-neuraminate]-(2→3)-2-aminoethyl-β-LacNAc

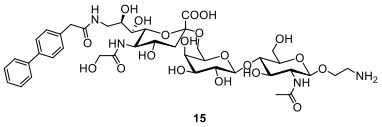

15

To a solution of compound **14** (82mg, 92µmol) in MeOH:H_2O (1.8 mL : 0.2 mL) was added a solution of PPh_3 (96mg, 368µmol) in THF:H_2O (1.0 mL : 0.5 mL) and the mixture was stirred for 24h at room temperature. The mixture was concentrated *in vacuo* to remove all non-aqueous solvent, diluted with H_2O (30 mL) and washed with EtOAc (3x 50 mL). Lyophilization afforded the intermediate as a white solid (quant.).

In DCM (10 mL) was dissolved BPA (636 mg, 3.0 mmol), DCC (680 mg, 3.3 mmol) and NHS (362 mg, 3.15 mmol). To this, DIPEA (50 µL, 0.3 mmol) was added and the mixture was stirred 5h at room temperature. The reaction mixture was filtered washing with DCM (2x 5 mL) and the filtrate concentrated *in vacuo.* This afforded crude BPA-NHS (800 mg) as an off-white solid.

To a solution of the obtained intermediate (92 µmol) in H_2O:THF (4 mL : 1 mL) was added BPA-NHS crude (171 mg, 554 µmol) and DIPEA (40 µL, 230µmol) and the mixture was incubated for 3h at room temperature. The mixture was neutralized with Amberlite H^+, filtered and concentrated in vacuo to give the intermediate as a white solid (45mg, 53%)

To a solution of this intermediate (45mg, 49µmol) in H_2O (1 mL) was added Pd/C (50mg, 10%, dry) and the solution was placed under hydrogen atmosphere (balloon) and stirred at room temperature overnight. Next, the mixture was filtered over celite (454). Lyophilization of the filtrate afforded compound **15** as a white solid (40mg, 88%). ^{1}H NMR (600 MHz, D_2O) δ 7.65 (m, 4H, Ar-H), 7.46 (m, 2H, Ar-H), 7.36 (m, 3H, Ar-H), 4.47 (d, J = 8.2 Hz, 1H, H-1 GlcNAc), 4.34 (d, J = 7.9 Hz, 1H, H-1 Gal), 3.70 (m, 25H), 3.35 (dd, J = 9.0, 1.6 Hz, 1H), 3.26 (m, 1H), 3.12 (m, 2H, linker CH_2), 2.59 (dd, J = 12.4, 4.6 Hz, 1H, H-3$_\alpha$ NeuGc), 1.96 (s, 3H, NHAc GlcNAc), 1.62 (t, J = 12.2 Hz, 1H, H-3$_\beta$ NeuGc).

(16) Sodium [5-N-(hydroxyacetyl)-9-desoxy-9-(biphenylacetamido)-α-D-neuraminate]-(2→3)-N-(Mal-PEG$_6$-amido)-2-aminoethyl-β-LacNAc

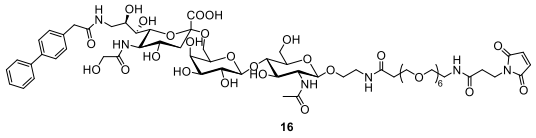

16

To a solution of compound XX (40mg, 43µmol) in anhydrous DMSO (300µL) was added NHS-dPEG$_6$-Mal (27mg, 45µmol) and triethylamine (6µL, 43µmol) and the mixture was incubated at 37°C for 6 hours. Next, the mixture was lyophilized and redissolved in H_2O + 0.1% TFA (1 mL). Purification of this solution using HPLC (C18, 0-50% ACN:H_2O) gave compound XX as a white solid (33mg, 52%). ^{1}H NMR (600 MHz, D_2O) δ 7.64 (m, 4H. Ar-H), 7.46 (td, J = 7.4, 1.2 Hz, 2H, Ar-H), 7.37 (m, 3H, Ar-H), 6.76 (t, J = 0.9 Hz, 2H, HC=CH maleimide), 4.43 (dd, J = 8.3, 1.2 Hz, 1H, H-1 GlcNAc), 4.34 (dd, J = 7.9, 1.1 Hz, 1H, H-1 Gal), 3.60 (m, 65H), 2.58 (dd, J = 12.3, 4.5 Hz, 1H, H-3$_\alpha$ NeuGc), 1.94 (q, J = 1.0 Hz, 3H, CH_3 Ac GlcNAc), 1.68 (t, J = 12.2 Hz, 1H, H-3$_\beta$ NeuGc).

(17) 1-Tosyl-PEG$_3$-N$_3$

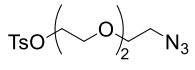

17

To a solution of HO-PEG$_3$-Cl (5.09g, 30 mmol) in DMF (60 mL) was added sodium azide (2.93g, 45 mmol) and the mixture was stirred at 100°C overnight. Next, the mixture was concentrated *in vacuo* and the remaining residue redissolved in DCM (40 mL) and water (40 mL). The organic phase was extracted and washed with water (3x 40 mL) and brine (20 mL). The organic phase was dried over Mg_2SO_4, filtered and concentrated in vacuo to give the intermediate as a colourless oil.

To a solution of the intermediate (30 mmol) in DCM (50 mL) on ice was added triethylamine (12.5 mL, 90 mmol) and the mixture was stirred for 15 minutes. Next, a solution of tosyl chloride (7.125g, 37.5 mmol) in DCM (50 mL) was added and the mixture was allowed to warm up to room temperature and stirred overnight. The reaction mixture was concentrated *in vacuo* and purification using flash chromatography (0-60% EtOAc in hexanes) which afforded compound **17** as a viscous clear oil (4.460g, 45% over two steps). ^{1}H NMR (400 MHz, CDCl3) δ 7.82 (m, 2H), 7.36 (m, 2H), 4.19 (m, 2H), 3.72 (m, 2H), 3.66 (m, 2H), 3.62 (s, 4H), 3.39 (dd, J = 5.6, 4.5 Hz, 2H), 2.47 (d, J = 0.8 Hz, 3H).

(18) 5-(2-(2-(2-azidoethoxy)ethoxy)ethoxy)isophthalate

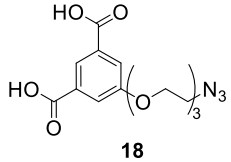

18

To a solution of compound **17** (2.5g, 7.6 mmol) in acetonitrile (40 mL) was added dimethyl 5-hydroxyisophtalic acid (1.33g, 6.3 mmol) and caesium carbonate (3.0g, 9.5 mmol) and the mixture was heated until reflux and stirred overnight. The next day, the mixture was filtered and the filtrated concentrated in vacuo to obtain crude compound XX (2.39g).

This crude was redissolved in methanol (20 mL), potassium hydroxide was added (3.36g, 60 mmol) and the mixture was stirred at room temperature overnight. Next, the mixture was concentrated in vacuo and the residue redissolved in H_2O (200 mL) to obtain a clear solution. To this solution, concentrated hydrochloric acid was added dropwise until pH<2. The white precipitate that formed was filtered and dried in a dessicator to obtain compound **18** (1.68g, 66% over two steps). ^{1}H NMR (600 MHz, MeOD) δ 8.27 (t, J = 1.5 Hz, 1H), 7.81 (d, J = 1.4 Hz, 2H), 4.26 (m, 2H), 3.92 (m, 2H), 3.72 (m, 6H), 3.38 (m, 2H), 3.31 (s, 12H) HRMS (ESI-TOF) Calc for $C_{14}H_{17}N_3O_7$ $[M-H]^-$ 338.0988, found 338.1039

(19) bis-(26-t-Boc-amido-nona(ethoxy))-5-(2-(2-(2-azidoethoxy)ethoxy)ethoxy)isophthalate

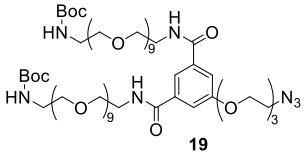

19

To a solution of compound **18** (mg, 7.5 mmol) in THF (5 mL) was added NH_2-PEG_9-NHBoc (1g, 18 mmol), EDCl (684mg, 30 mmol) and DIPEA (290 µL) and the mixture was stirred at room temperature for 48 hours. The reaction mixture was concentrated in vacuo and the residue purified using flash chromatography to afford compound **19** as an orange oil (523mg, 49%). ^{1}H NMR (600 MHz, $CDCl_3$) δ 7.90 (s, 1H, Ar-H), 7.61 (d, J = 1.4 Hz, 2H, Ar-H), 4.24 (m, 2H), 3.90 (m, 2H), 3.64 (m, 92H), 3.41 (dd, J = 5.6, 4.6 Hz, 2H), 3.32 (d, J = 5.8 Hz, 4H), 2.00 (s, 6H), 1.27 (s, 6H) HRMS (ESI-TOF) Calc for $C_{64}H_{117}N_7O_{27}$ $[M+H]^-$ 1416.8076, found 1416.8059

(20) bis-(26-amino-nona(ethoxy))-5-(2-(2-(2-azidoethoxy)ethoxy)ethoxy)isophthalate di-trifluoroacetate

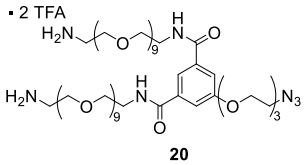

20

To a solution of compound **19** (180mg, 127µmol) in DCM (20 mL) was added TFA (20 mL) and the mixture was stirred at room temperature for 2 hours. The mixture was concentrated in vacuo and the residue purified using a C18 seppack to give compound **20** as a light brown oil (180mg, 98%) 1H NMR (600 MHz, CDCl3) δ 7.92 (p, J = 1.5 Hz, 1H), 7.60 (m, 2H), 4.28 (p, J = 2.7 Hz, 2H), 3.92 (dt, J = 6.2, 2.7 Hz, 2H), 3.67 (m, 88H), 3.39 (d, J = 6.2 Hz, 2H), 3.19 (s, 4H) ; HRMS (ESI-TOF) Calc for $C_{54}H_{101}N_7O_{23}$ $[M+H]^-$ 1216.7027, found 1216.6934

(21) bis-(N-(thiopropionyl)-26-amido-nona(ethoxy))-5-(2-(2-(2-azidoethoxy)ethoxy)ethoxy)isophthalate

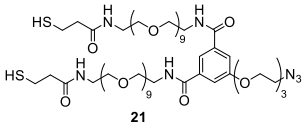

21

In DCM (10 mL) was dissolved S-acetyl-thiopropionic acid (444mg, 3.0 mmol), DCC (680mg, 3.3 mmol) and NHS (362mg, 3.15 mmol). To this, DIPEA (50µL, 0.3 mmol) was added and the mixture was stirred 5h at room temperature. The reaction mixture was filtered washing with DCM (2x 5 mL) and the filtrate concentrated *in vacuo.* This afforded crude S-acetyl-thiopropionic acid NHS ester (675mg) as a white solid.

To a solution of compound **20** (120mg, 99µmol) in DCM (1 mL) was added acetylthiopropionic acid-NHS crude (97mg) and Et_3N (35µL, 248 µmol) and the mixture was incubated for 5h at 37°C. The mixture was concentrated *in vacuo* and the obtained residue redissolved in MeOH (2 mL) to which NaOMe (0.2 mL, 0.5M) was added dropwise over the course of a few minutes until pH=13. Next, the mixture was quickly neutralized using Amberlite H^+ and filtered. The filtrate was concentrated *in vacuo* and purified using a Seppack C8 (3:1 MeOH:H_2O) which afforded compound **21** as a viscous clear liquid (112mg, 81%). ^{1}H NMR (600 MHz, MeOD) δ 7.92 (q, J = 1.6 Hz, 1H), 7.60 (d, J = 1.5 Hz, 2H), 4.28 (m, 2H), 3.92 (m, 2H), 3.64 (m, 88H), 3.39 (q, J = 4.9 Hz, 6H), 2.76 (tt, J = 6.8, 1.1 Hz, 4H), 2.52 (t, J = 6.9 Hz, 4H).

(22) bis-(26-(1,5-di-N-Boc-amido-pentyl-carboxamide)-nona(ethoxy))-5-(2-(2-(2-azidoethoxy)ethoxy)ethoxy)isophthalate

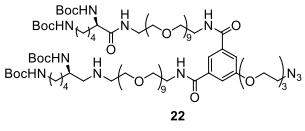

22

To a solution of **20** (180mg, 124µmol) in THF (10 mL) was added DIPEA (220µL, 1.27 mmol) and the mixture was stirred at room temperature for 15 minutes. Next, Boc-Lys(Boc)-OSu (274mg, 635µmol) was added and the mixture was stirred at room temperature for 15 hours. Flash chromatography (10% MeOH in DCM) afforded compound **22** as a clear oil (130mg, 55%) ^{1}H NMR (600 MHz, MeOD) δ 7.92 (t, J = 1.5 Hz, 1H), 7.60 (d, J = 1.4 Hz, 2H), 4.28 (m, 2H), 4.00 (d, J = 7.2 Hz, 2H), 3.92 (m, 2H), 3.75 (m, 2H), 3.65 (m, 88H), 3.55 (t, J = 5.5 Hz, 4H), 3.40 (m, 6H), 3.04 (m, 4H), 1.73 (s, 2H), 1.61 (m, 2H), 1.45 (d, J = 7.2 Hz, 52H) ; HRMS (ESI-TOF) Calc for $C_{86}H_{157}N_{11}O_{33}$ $[M-H]^-$ 1872.0945, found 1872.1153

(23) bis-(26-(1,5-di-aminopentyl-carboxamide)-nona(ethoxy))-5-(2-(2-(2-azidoethoxy)ethoxy)ethoxy)isophthalate tetra-trifluoroacetate

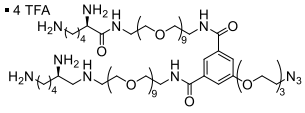

23

To a solution of **22** (128mg, 68µmol) in DCM (2 mL) was added TFA (2 mL) and the mixture was stirred at room temperature for 3 hours. The mixture was concentrated in vacuo and the residue purified using a C18 seppack to give compound **23** as a clear oil (130mg, 100%). ^{1}H NMR (600 MHz, MeOD) δ 7.92 (q, J = 1.4 Hz, 1H), 7.60 (d, J = 1.5 Hz, 2H), 4.28 (m, 2H), 3.92 (m, 2H), 3.75 (m, 2H), 3.63 (m, 88H), 3.39 (q, J = 5.0 Hz, 6H), 2.76 (t, J = 6.9 Hz, 4H), 2.52 (t, J = 6.9 Hz, 4H) ; HRMS (ESI-TOF) Calc for $C_{66}H_{125}N_{11}O_{25}$ $[M+FA]^-$ 1516.8825, found 1516.9040

(24) bis-(26-(1,5-di-N-thiopropionyl-amido-pentyl-carboxamide)-nona(ethoxy))-5-(2-(2-(2-azidoethoxy)ethoxy)ethoxy)isophthalate

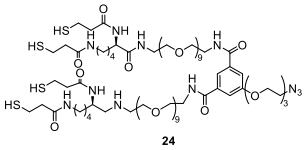

24

To a solution of compound **23** (133mg, 68µmol) in DCM (1 mL) was added acetylthiopropionic acid-NHS crude (133mg) and Et_3N (347µL, 340 µmol) and the mixture was incubated for 5h at 37°C. The mixture was concentrated *in vacuo* and the obtained residue redissolved in MeOH (2 mL) to which NaOMe (0.2 mL, 0.5M) was added dropwise over the course of a few minutes until pH=13. Next, the mixture was quickly neutralized using Amberlite H^+ and filtered. The filtrate was concentrated *in vacuo* and purified using a Seppack C8 (3:1 MeOH:H_2O) which afforded compound **24** as a viscous clear oil (87mg, 70%). ^{1}H NMR (600 MHz, MeOD) δ 7.92 (q, J = 1.5 Hz, 1H), 7.60 (d, J = 1.5 Hz, 2H), 4.30 (m, 4H), 3.92 (m, 2H), 3.65 (m, 88H), 3.39 (m, 6H), 3.21 (t, J = 7.0 Hz, 4H), 2.76 (dt, J = 9.0, 6.8 Hz, 8H), 2.58 (td, J = 6.8, 2.4 Hz, 4H), 2.49 (t, J = 6.8 Hz, 4H), 1.82 (ddt, J = 13.6, 9.9, 5.9 Hz, 2H), 1.67 (dp, J = 13.9, 4.6 Hz, 4H), 1.55 (m, 4H), 1.43 (m, 4H).

(25) Monovalent-CD22L-N_3

To a stirred solution of compound **16** (6.0mg, 4µmol) in DMSO (100µL) was added N_3-PEG_3-SH (1.9mg, 8 µmol) and the mixture was stirred at room temperature for 5 hours. Next, the mixture was lyophilized and redissolved in dilute sodium hydroxide (200µL, pH=9.0) and the mixture was incubated for 15h at 37°C. Purification of this solution using HPLC (C18, 0-50% ACN:H_2O + 0.1% TFA), neutralization with sodium hydroxide of the fractions containing product, lyophilization and P4 desalting gave compound **25** as a white solid (5.5mg, 79%). ^{1}H NMR and assignment of characteristic peaks can be found in appendix 11.2

(26) Divalent-GlcNAc-N_3

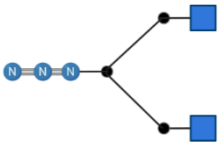

To a solution of compound **5** (40 mg, 125 µmol) in anhydrous DMSO (2 mL) was added NHS-PEG_6-Maleimide (112.5 mg, 18 7µmol) and triethylamine (20 µL, 125 µmol) and the mixture was stirred at room temperature for 4 hours. Next, the solution was lyophilized and the obtained residue purified using a Sep-Pak C8 (2:1 MeOH:H_2O) which afforded GlcNAc-Maleimide intermediate as a white solid (84 mg, 90%) which was used without further purification. ^{1}H NMR can be found in appendix 11.2.

To a stirred solution of GlcNAc-Maleimide intermediate (84mg, 60µmol) in DMSO (500µL) was added compound **21** (11.8mg, 15.8 µmol) and Et_3N until slightly basic and the mixture was stirred at room temperature for 6 hours. Next, the mixture was diluted with water (5 mL) which gave a pH of around 9 and the mixture was incubated for 15h at 37°C. Purification using HPLC (C18, 0-50% ACN:H_2O + 0.1% TFA) and lyophilization gave compound **26** as a white solid (36mg, 85%). ^{1}H NMR and assignment of characteristic peaks can be found in appendix 11.2

(27) Divalent-CD22L-N_3

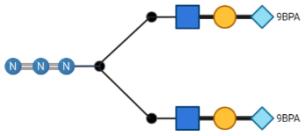

To a stirred solution of compound **16** (8.0mg, 5.4µmol) in DMSO (100µL) was added compound **21** (3.8mg, 2.72 µmol) in DMSO (38 µL) and Et_3N (1 µL) and the mixture was stirred at room temperature for 48 hours. Next, the mixture was lyophilized and redissolved in dilute sodium hydroxide (200µL, pH=9.0) and the mixture was incubated for 15h at 37°C. Purification of this solution using HPLC (C18, 0-50% ACN:H_2O + 0.1% TFA), neutralization with sodium hydroxide of the fractions containing product, lyophilization and P4 desalting gave compound **27** as a white solid (2.45µmol by UV, 90%). ^{1}H NMR and assignment of characteristic peaks can be found in appendix 11.2 ; HRMS (ESI-TOF) Calc for $C_{185}H_{295}N_{19}O_{87}S_2$ $[M+H_2O]^+$ 4255.8713, found 4255.66 (deconvoluted)

(28) Tetravalent-CD22L-N_3

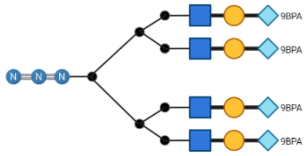

To a stirred solution of compound **16** (16.0mg, 10.9 µmol) in DMSO (100µL) was added compound **24** (2.3mg, 1.26 µmol) in DMSO (38 µL) and Et_3N (1.5 µL) and the mixture was stirred at room temperature for 48 hours. Next, the mixture was lyophilized and redissolved in dilute sodium hydroxide (200µL, pH=9.0) and the mixture was incubated for 15h at 37°C. Purification of this solution using HPLC (C18, 0-50% ACN:H_2O + 0.1% TFA), neutralization with sodium hydroxide of the fractions containing product, lyophilization and P4 desalting gave compound **28** as a white solid (1.22µmol by UV, 97%). ^{1}H NMR and assignment of characteristic peaks can be found in appendix 11.2 ; HRMS (ESI-TOF) Calc for $C_{326}H_{509}N_{35}O_{153}S_4$ $[M+Na]^+$ 7497.8640, found 7497.52 (deconvoluted)

(29) Monovalent-CD22L-AF647

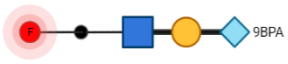

To a solution of **25** (0.25mg, 0.15 µmol) in DMSO (15µL) was added BCN-AF647 (0.68mg, 0.60µmol) in DMSO (13.6µL) and the mixture was incubated at 37°C for 15 hours. Purification over P4 size exclusion twice in H_2O gave compound **29** as a blue solution which was characterized by UV-VIS.

(30) Divalent-GlcNAc-AF647

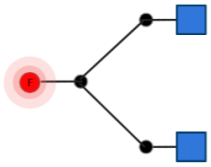

To a solution of **26** (0.25mg, 0.15 µmol) in DMSO (15µL) was added BCN-AF647 (0.68mg, 0.60µmol) in DMSO (13.6µL) and the mixture was incubated at 37°C for 15 hours. Purification over P4 size exclusion twice in H_2O gave compound **30** as a blue solution which was characterized by UV-VIS.

(31) Divalent-CD22L-AF647

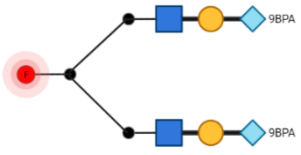

To a solution of **27** (0.25mg, 0.15 µmol) in DMSO (15µL) was added BCN-AF647 (0.68mg, 0.60µmol) in DMSO (13.6µL) and the mixture was incubated at 37°C for 15 hours. Purification over P4 size exclusion twice in H_2O gave compound **31** as a blue solution which was characterized by UV-VIS.

(32) Tetravalent-CD22L-AF647

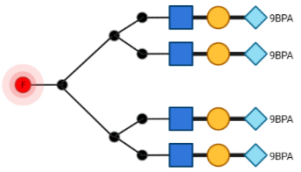

To a solution of **28** (0.25mg, 0.15 µmol) in DMSO (15µL) was added BCN-AF647 (0.68mg, 0.60µmol) in DMSO (13.6µL) and the mixture was incubated at 37°C for 15 hours. Purification over P4 size exclusion twice in H_2O gave compound **32** as a blue solution which was characterized by UV-VIS.

(33) Ovalbumin-BCN

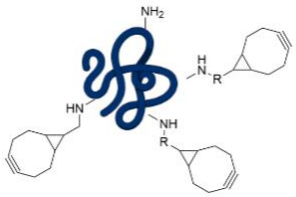

To a solution of LPS-free vacigrade® Ovalbumin (20mg, 0.47 µmol) in PBS (1 mL) was added BCN-PEG_6-NHS (6.3mg, 11.75µmol) in DMSO (63µL) and the mixture was incubated at 25°C for 2.5 hours, then 4°C for 15 hours. Purification over G-100 size exclusion in PBS gave BCN-Ovalbumin **33** (quant) with an estimated modification level of 4.8 by ESI-MS.

(34) Ovalbumin-Monovalent-CD22L

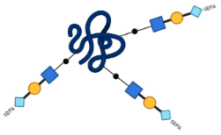

To a solution of Ovalbumin-BCN **33** (53 nmol) in PBS (300µL) was added conjugate **25** (1.05 µmol) in DMSO (105µL) and the mixture was incubated at 25°C for 3 hours, then 4°C for 15 hours. Purification over G-100 size exclusion in PBS gave conjugate **34** (quant) as a solution which was characterized by UV-VIS.

(35) Ovalbumin-Divalent-GlcNAc

To a solution of Ovalbumin-BCN **33** (53 nmol) in PBS (300µL) was added conjugate **26** (1.05 µmol) in DMSO (105µL) and the mixture was incubated at 25°C for 3 hours, then 4°C for 15 hours. Purification over G-100 size exclusion in PBS gave conjugate **35** (quant) as a solution which was characterized by UV-VIS.

(36) Ovalbumin-Divalent-CD22L

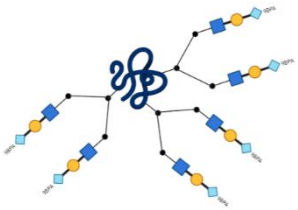

To a solution of Ovalbumin-BCN **33** (53 nmol) in PBS (300µL) was added conjugate **27** (1.05 µmol) in DMSO (105µL) and the mixture was incubated at 25°C for 3 hours, then 4°C for 15 hours. Purification over G-100 size exclusion in PBS gave conjugate **36** (quant) as a solution which was characterized by UV-VIS.

(37) Ovalbumin-Tetravalent-CD22L

To a solution of Ovalbumin-BCN **33** (53 nmol) in PBS (300µL) was added conjugate **28** (1.05 µmol) in DMSO (105µL) and the mixture was incubated at 25°C for 3 hours, then 4°C for 15 hours. Purification over G-100 size exclusion in PBS gave conjugate **37** (quant) as a solution which was characterized by UV-VIS.

(38) Ovalbumin-AF647

To a solution of Ovalbumin (7.0 nmol) in PBS (87µL) was added AF647-NHS (20 µg) in DMSO (20µL) and the mixture was incubated at 25°C for 3 hours, then 4°C for 15 hours. The compound was purified over G-100 size exclusion and concentrated using spin filters (10 kDa). To the obtained solution (100µL) was added AF647-NHS (100 µg) in DMSO (10µL) and the mixture was incubated at 25°C for 3 hours, then 4°C for 15 hours. Purification over G-100 size exclusion in PBS gave conjugate **38** as a blue solution which was characterized by UV-VIS.

(39) Ovalbumin-Monovalent-CD22L-AF647

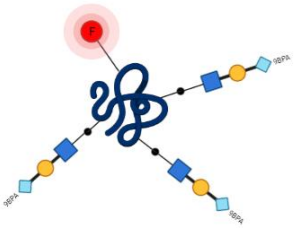

To a solution of Ovalbumin (7.0 nmol) in PBS (81µL) was added AF647-NHS (20 µg) in DMSO (20µL) and the mixture was incubated at 25°C for 3 hours, then 4°C for 15 hours The compound was purified over G-100 size exclusion and concentrated using spin filters (10 kDa). To the obtained solution (100µL) was added AF647-NHS (100 µg) in DMSO (10µL) and the mixture was incubated at 25°C for 3 hours, then 4°C for 15 hours. Purification over G-100 size exclusion in PBS gave conjugate **39** as a blue solution which was characterized by UV-VIS.

(40) Ovalbumin-Divalent-GlcNAc-AF647

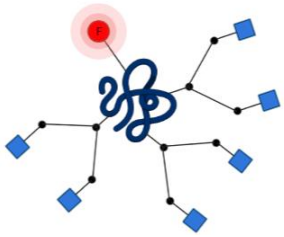

To a solution of Ovalbumin (7.0 nmol) in PBS (95µL) was added AF647-NHS (20 µg) in DMSO (20µL) and the mixture was incubated at 25°C for 3 hours, then 4°C for 15 hours. The compound was purified over G-100 size exclusion and concentrated using spin filters (10 kDa). To the obtained solution (100µL) was added AF647-NHS (100 µg) in DMSO (10µL) and the mixture was incubated at 25°C for 3 hours, then 4°C for 15 hours. Purification over G-100 size exclusion in PBS gave conjugate **40** as a blue solution which was characterized by UV-VIS.

(41) Ovalbumin-Divalent-CD22L-AF647

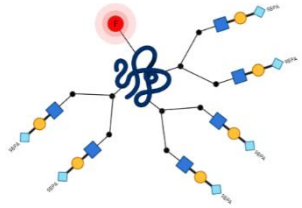

To a solution of Ovalbumin (7.0 nmol) in PBS (77µL) was added AF647-NHS (20 µg) in DMSO (20µL) and the mixture was incubated at 25°C for 3 hours, then 4°C for 15 hours. The compound was purified over G-100 size exclusion and concentrated using spin filters (10 kDa). To the obtained solution (100µL) was added AF647-NHS (100 µg) in DMSO (10µL) and the mixture was incubated at 25°C for 3 hours, then 4°C for 15 hours. The compound was purified over G-100 size exclusion and concentrated using spin filters (10 kDa). To the obtained solution (100µL) was added AF647-NHS (500 µg) in DMSO (50µL) and the mixture was incubated at 25°C for 3 hours, then 4°C for 15 hours. Purification over G-100 size exclusion in PBS gave conjugate **41** as a blue solution which was characterized by UV-VIS.

(42) Ovalbumin-Tetravalent-CD22L-AF647

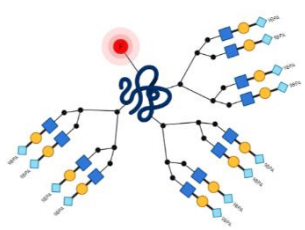

To a solution of Ovalbumin (7.0 nmol) in PBS (71µL) was added AF647-NHS (20 µg) in DMSO (20µL) and the mixture was incubated at 25°C for 3 hours, then 4°C for 15 hours. The compound was purified over G-100 size exclusion and concentrated using spin filters (10 kDa). To the obtained solution (100µL) was added AF647-NHS (100 µg) in DMSO (10µL) and the mixture was incubated at 25°C for 3 hours, then 4°C for 15 hours. The compound was purified over G-100 size exclusion and concentrated using spin filters (10 kDa). To the obtained solution (100µL) was added AF647-NHS (1000 µg) in DMSO (100µL) and the mixture was incubated at 25°C for 3 hours, then 4°C for 15 hours. Purification over G-100 size exclusion in PBS gave conjugate **42** as a blue solution which was characterized by UV-VIS.

9.2 DETERMINATION OF EXTINCTION COEFFICIENT

Ovalbumin (10.31 mg) was dissolved in water (1 mL). This solution was used to prepare a twofold dilution series from 0.241 mM to 1.88 µM which was measured in quintuplicate for absorbance at 253, 260 and 280 nm.

Compound **16** (2.00 mg) was dissolved in H_2O (100 uL). Isopropyl alcohol (30.5 µL, 0.40 µmol) was added to water (970 µL) and mixed vigorously. Next, this solution (10 µL) was added to water (990

µL) to give a solution of 4.00 mM isopropyl alcohol. Next, the compound 16 solution (50µL) and the isopropyl alcohol solution (50µL) were added to 450 µL of D_2O and measured by ^1H NMR. Integrals recorded were 8.00 (aromatic region), 1.00 (H-3 sialic acid), 0.96 (isopropyl alcohol). This gave a concentration of 22.7 mM of the original compound **16** solution. This solution was used to prepare a two-fold dilution series from 0.987 mM to 7.72 µM which was measure in quintuplicate for absorbance at 253, 260 and 280 nm.

Compound **XX** (20.00 mg) was dissolved in water (1 mL). This solution was used to prepare a twofold dilution series from 0.683 mM to 5.34 µM which was measure in quintuplicate for absorbance at 253, 260 and 280 nm.

The extinction coefficients were determined using linear regression using y=ax

9.3 EC_{50} DETERMINATION FOR CD22 IN SOLUTION

To determine the affinity of the multivalent ligands for CD22 in solution, Microscale Thermophoresis (MST) using the NanoTemper Monolith was used. First, solutions of the fluorescently labelled ligands (800 nM) in binding buffer (PBS + 0.05% TWEEN-20) were prepared. Before each experiment, the solutions were freshly diluted in binding buffer to 80nM. A solution of mCD22 (BAE33829.1) in binding buffer (5 µM) was prepared, aliquoted into single use portions and snap frozen in liquid nitrogen. The aliquots were stored at -80°C and thawed on ice before use. The above solutions were used in accordance with the instructions provided by the Monolith.

9.4 EC_{50} DETERMINATION BY B-CELL BINDING

The spleen was removed from the mice and stored in ice cold RPMI (1X RPMI 1640 + L-glutamine + Penicillin-Streptamycin 100-100 U/ml + 0.3mg/mL Glutamine + 10% heat inactivated FBS). The spleens were mechanically digested through a 40 µm cell strainer to remove cell aggregates and centrifuged to collect the cells (350 g, 5 min, 4°C). The erythrocytes were lysed with lysis buffer (82.6 g/L NH_4Cl, 0.27 g/L EDTA, 10 g/L $KHCO_3$) at room temperature for 3-4 minutes, and quickly quenched with an equal volume of RPMI and centrifuged to collect the cells (350 g, 5 min, 4°C). The cells were resuspended in RPMI and the final volume adjusted to give a concentration of 37.5 x 10^6 cells / mL, and 1.5 x 10^6 cells were added to each well of a 96 round-bottom well plate. The conjugates or dilutions were added to the wells and the plate was incubated at 4°C or 37°C for 1h. The plate was centrifuged (350 g, 5 min, 4°C) and the liquid discard. The cells were washed once with ice cold DPBS (200µL), centrifuged again (350 g, 5 min, 4°C) and the liquid discarded. Zombie-UV solution (40µL, prepared according to manual) was added to the cells and the plate was incubate at 4°C for 30 minutes. Ice cold FACS buffer (150µL, HBSS + 2% FBS + 2.5 mM EDTA + 25 mM HEPES + 0.05% NaN_3) was added and incubated for 5 minutes at 4°C to quench the dye. The plate was centrifuged (350 g, 5 min, 4°C) and the liquid discarded. Fc-Block solution (50µL, 1:100 in FACS buffer) was added to the cells and they were incubated at 4°C for 10 minutes. The plate was centrifuged (350 g, 5 min, 4°C) and the liquid discarded. Antibody solution (50 µL, 1:200 B220-PE and 1:400 CD19-FITC in FACS buffer) was added to the cells and they were incubated at 4°C for 10 minutes. The plate was centrifuged (350 g, 5 min, 4°C) and the liquid discarded. The cells were resuspended in ice cold FACS buffer (150µL) and measured with a ZETA YETI flow cytometer.

9.5 SPECIFIC IG-G1 SERUM ELISA

A high binding 384-well flat bottom ELISA plate (Nunc Maxi-sorb) was coated with coating solution (40µL, 7.5 µg/mL OVA or Conjugate in PBS pH=7.4), covered with parafilm and stored at 4°C overnight. The solution was discarded, and the plate washed 5 times by full emersion in PBS-T (PBS + 0.1% Tween-20). The plate was blocked for 2 h at RT with blocking buffer (100µL, PBS-T + 1% BSA) on a rotating platform (45 rpm) while covered with parafilm to prevent evaporation. The

solution was discarded, and the plate dried by spinning the plate upside down on some tissue paper at 1200 rpm for 1 minute. Blocking buffer (60µL) was added to the top wells and blocking buffer (40µL) to all others. Serum sample (20µL) OR freshy diluted 1000 ng/mL mouse IgG1 standard (20µL, positive control) OR mouse serum from day 0 (20µL, negative control) was added to the top wells. Top rows were diluted using 2-fold serial dilutions downwards (40 µL into 40 µL) and the last 40 µL was discarded from the bottom row. The plate was incubated at RT for 1h on a rotating platform (45 rpm) and covered with parafilm to prevent evaporation. The liquid was discarded, the plate washed 5 times by full emersion in PBS-T and the plate dried by spinning the plate upside down on some tissue paper at 1200 rpm for 1 minute. Freshly diluted HRP-conjugated goat anti-mouse IgG1 (40 µL, 1:2,000 dilution in blocking buffer) was added to the plate. The plate was incubated at RT for 1h on a rotating platform (45 rpm) and covered with parafilm to prevent evaporation. The liquid was discarded, the plate washed 5 times by full emersion in PBS-T and the plate dried by spinning the plate upside down on some tissue paper at 1200 rpm for 1 minute. TMB substrate (50µL) was added to all wells and incubated at RT in the dark for 10 min or until good color development. The plate was quenched with H_2SO_4 (50µL) and the absorbance measured (450 nm) with a BioTek plate reader immediately.

10 REFERENCES

1. Hodgson, J. Refreshing the biologic pipeline 2020. *Nat. Biotechnol.* **39**, 135–143 (2021).
2. Makurvet, F. D. Biologics vs. small molecules: Drug costs and patient access. *Med. Drug Discov.* **9**, 100075 (2021).
3. Ascendia Pharma. Biologics vs. Small Molecule Drugs: Which Are Better? https://ascendiapharma.com/2021/10/27/biologics-vs-small-molecule-drugs/ (2021).
4. Vaisman-Mentesh, A., Gutierrez-Gonzalez, M., DeKosky, B. J. & Wine, Y. The Molecular Mechanisms That Underlie the Immune Biology of Anti-drug Antibody Formation Following Treatment With Monoclonal Antibodies. *Front. Immunol.* **11**, 1951 (2020).
5. Warren, C. M., Jiang, J. & Gupta, R. S. Epidemiology and Burden of Food Allergy. *Curr. Allergy Asthma Rep.* **20**, 6 (2020).
6. Sobhani, N. *et al.* CTLA-4 in Regulatory T Cells for Cancer Immunotherapy. *Cancers (Basel).* **13**, (2021).
7. Yuning Wang, M. G. Ushering the New Era in Anti-Drug Antibody Assays with Next Generation Protein Sequencing. *June 30* https://www.rapidnovor.com/anti-drug-antibody-assays-with-next-generation-protein-sequencing/ (2021).
8. Enterina, J. R., Jung, J. & Macauley, M. S. Coordinated roles for glycans in regulating the inhibitory function of CD22 on B cells. *Biomed. J.* **42**, 218–232 (2019).
9. Rillahan, C. D., Schwartz, E., McBride, R., Fokin, V. V & Paulson, J. C. Click and pick: identification of sialoside analogues for siglec-based cell targeting. *Angew. Chem. Int. Ed. Engl.* **51**, 11014–11018 (2012).
10. Collins, B. E. *et al.* High-affinity ligand probes of CD22 overcome the threshold set by cis ligands to allow for binding, endocytosis, and killing of B cells. *J. Immunol.* **177**, 2994–3003 (2006).
11. Peng, W. & Paulson, J. C. CD22 Ligands on a Natural N-Glycan Scaffold Efficiently Deliver Toxins to B-Lymphoma Cells. *J. Am. Chem. Soc.* **139**, 12450–12458 (2017).
12. Harumoto, T. *et al.* Enhancement of Gene Knockdown on CD22-Expressing Cells by Chemically Modified Glycan Ligand–siRNA Conjugates. *ACS Chem. Biol.* **17**, 292–298 (2022).
13. Rillahan, C. D. *et al.* Disubstituted Sialic Acid Ligands Targeting Siglecs CD33 and CD22 Associated with Myeloid Leukaemias and B Cell Lymphomas. *Chem. Sci.* **5**, 2398–2406 (2014).
14. Fontaine, S. D., Reid, R., Robinson, L., Ashley, G. W. & Santi, D. V. Long-term stabilization of maleimide-thiol conjugates. *Bioconjug. Chem.* **26**, 145–152 (2015).
15. Lahnsteiner, M. *et al.* Improving the Stability of Maleimide-Thiol Conjugation for Drug Targeting. *Chemistry* **26**, 15867–15870 (2020).
16. Tumey, L. N. *et al.* Mild Method for Succinimide Hydrolysis on ADCs: Impact on ADC Potency, Stability, Exposure, and Efficacy. *Bioconjug. Chem.* **25**, 1871–1880 (2014).
17. Forman, H. J., Zhang, H. & Rinna, A. Glutathione: overview of its protective roles, measurement, and biosynthesis. *Mol. Aspects Med.* **30**, 1–12 (2009).
18. Pone, E. J. *et al.* BCR-signalling synergizes with TLR-signalling for induction of AID and immunoglobulin class-switching through the non-canonical NF-κB pathway. *Nat. Commun.* **3**, 767 (2012).

19. Wan, X. *et al.* Effect of protein immunogenicity and PEG size and branching on the anti-PEG immune response to PEGylated proteins. *Process Biochem.* **52**, 183–191 (2017).

20. Chen, B.-M., Cheng, T.-L. & Roffler, S. R. Polyethylene Glycol Immunogenicity: Theoretical, Clinical, and Practical Aspects of Anti-Polyethylene Glycol Antibodies. *ACS Nano* **15**, 14022–14048 (2021).

21. Hoang Thi, T. T. *et al.* The Importance of Poly(ethylene glycol) Alternatives for Overcoming PEG Immunogenicity in Drug Delivery and Bioconjugation. *Polymers (Basel).* **12**, (2020).

22. Li, C. & Wang, L.-X. Chemoenzymatic Methods for the Synthesis of Glycoproteins. *Chem. Rev.* **118**, 8359–8413 (2018).

23. Lim, D., Brimble, M. A., Kowalczyk, R., Watson, A. J. A. & Fairbanks, A. J. Protecting-group-free one-pot synthesis of glycoconjugates directly from reducing sugars. *Angew. Chem. Int. Ed. Engl.* **53**, 11907–11911 (2014).

24. Pfrengle, F., Macauley, M. S., Kawasaki, N. & Paulson, J. C. Copresentation of antigen and ligands of Siglec-G induces B cell tolerance independent of CD22. *J. Immunol.* **191**, 1724–1731 (2013).

25. Rizzuto, G. *et al.* Establishment of fetomaternal tolerance through glycan-mediated B cell suppression. *Nature* **603**, 497–502 (2022).

26. Seitz, A. *et al.* Site-Selective Acylation of Pyranosides with Oligopeptide Catalysts. *J. Org. Chem.* **86**, 3907–3922 (2021).

27. Šardzík, R. *et al.* Preparation of aminoethyl glycosides for glycoconjugation. *Beilstein J. Org. Chem.* **6**, 699–703 (2010).

28. Tsai, Y.-F. *et al.* The total synthesis of a ganglioside Hp-s1 analogue possessing neuritogenic activity by chemoselective activation glycosylation. *Org. Biomol. Chem.* **10**, 931–934 (2012).

29. Lin, H. *et al.* Rhamnose modified bovine serum albumin as a carrier protein promotes the immune response against sTn antigen. *Chem. Commun.* **56**, 13959–13962 (2020).

30. Abdu-Allah, H. H. M. *et al.* Potent small molecule mouse CD22-inhibitors: Exploring the interaction of the residue at C-2 of sialic acid scaffold. *Bioorg. Med. Chem. Lett.* **19**, 5573–5575 (2009).

31. Cheng, B. *et al.* 9-Azido Analogues of Three Sialic Acid Forms for Metabolic Remodeling of Cell-Surface Sialoglycans. *ACS Chem. Biol.* **14**, 2141–2147 (2019).

11 SUPPLEMENTAL INFORMATION

11.1 EXTINCTION COEFFICIENT

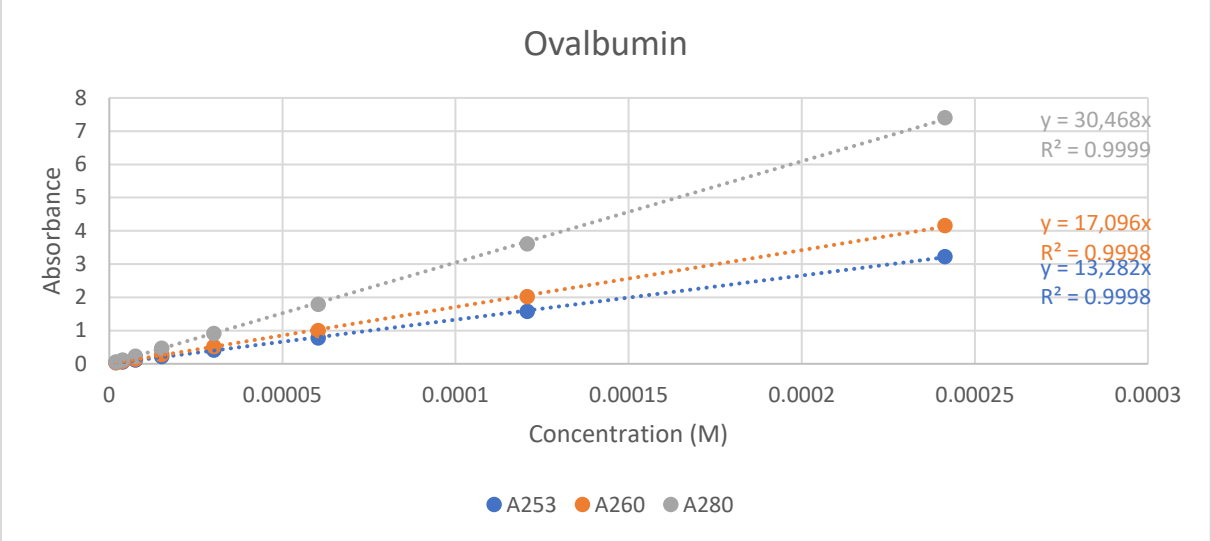

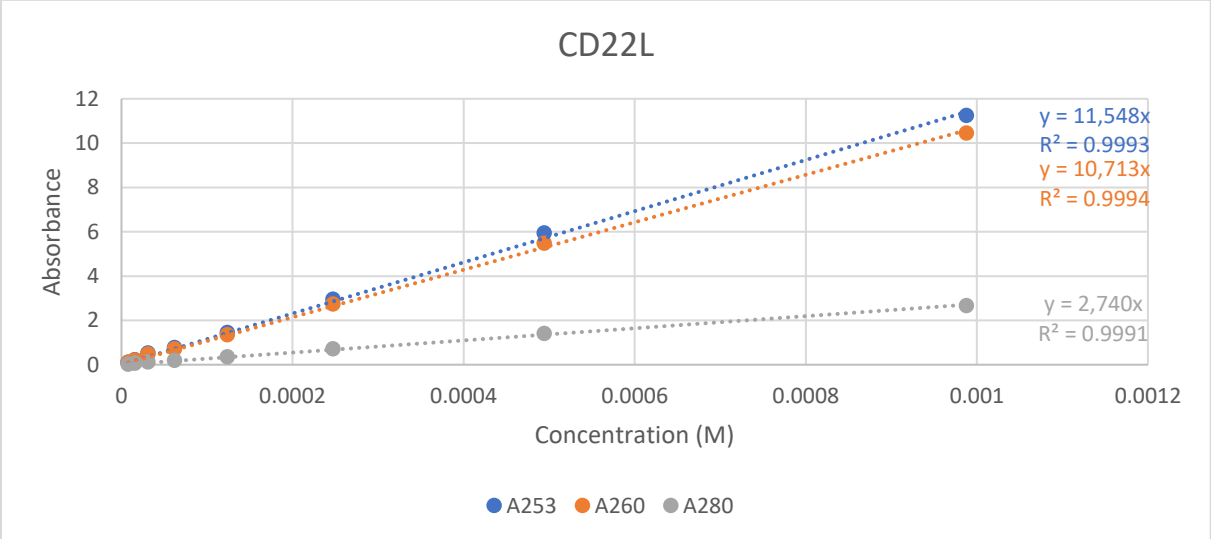

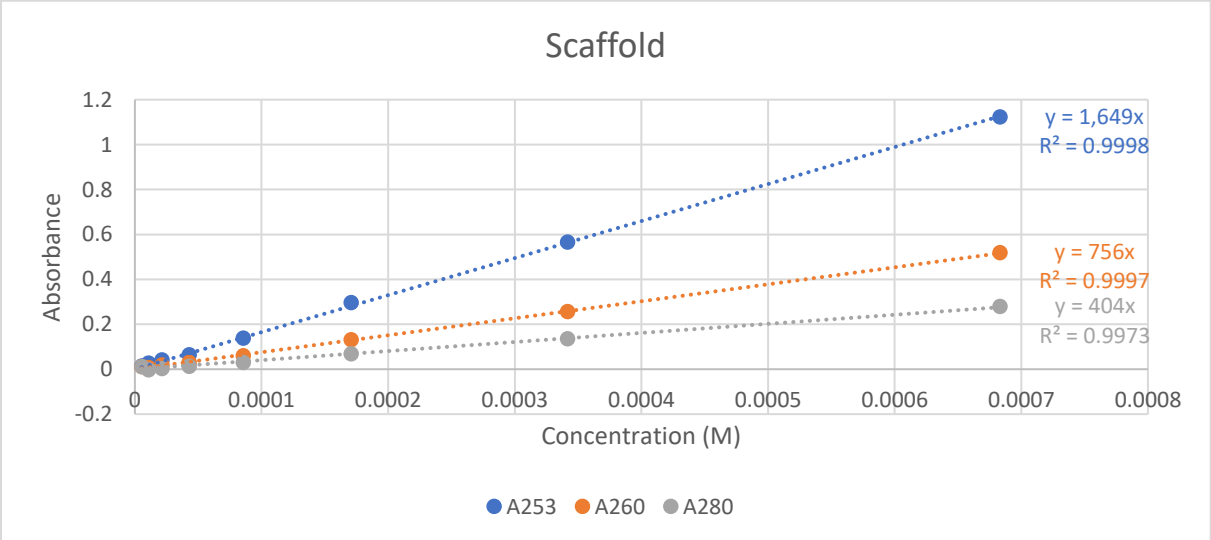

11.2 NMR SPECTRA

(1) 1,4,5,6-tetra-O-acetyl- N-acetyl-glucosamine

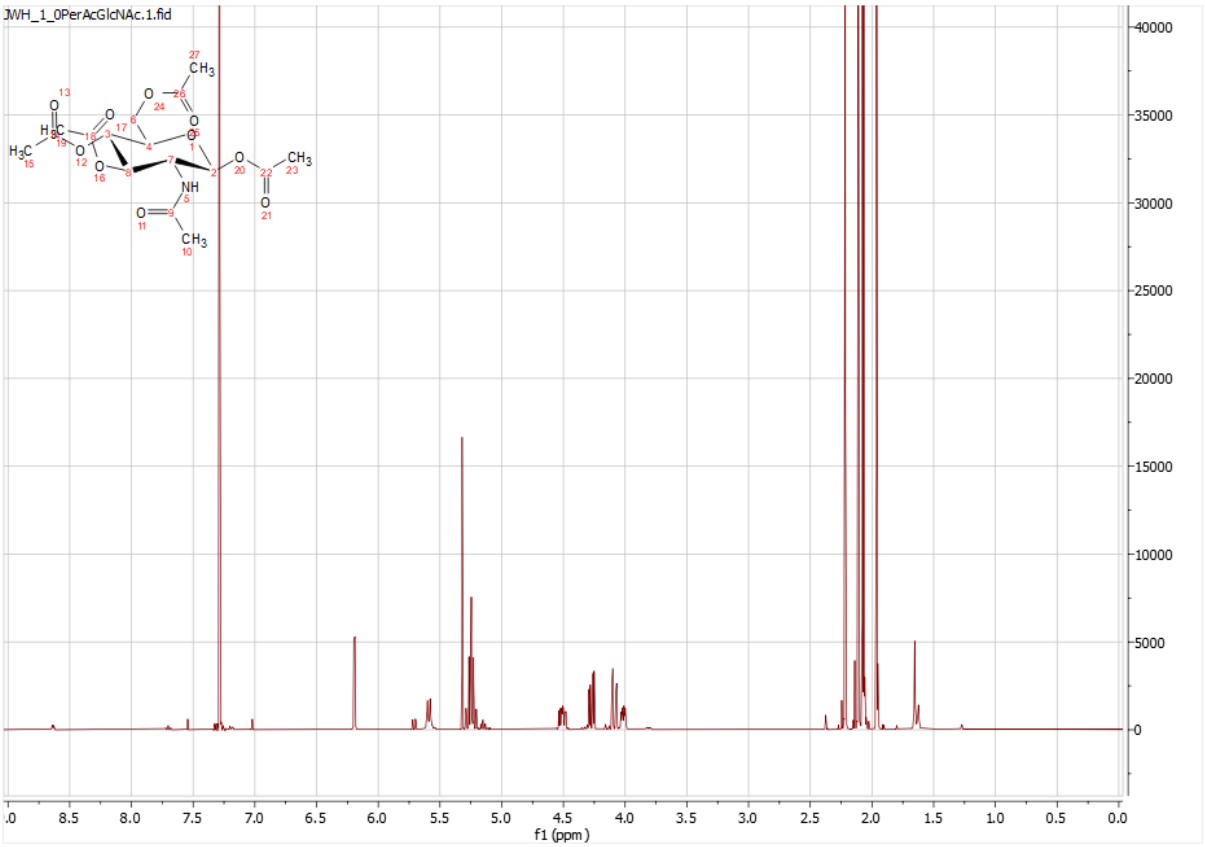

(3) 1-(N-Cbz-2-aminoethyl)-N-acetyl-β-D-glucosamine

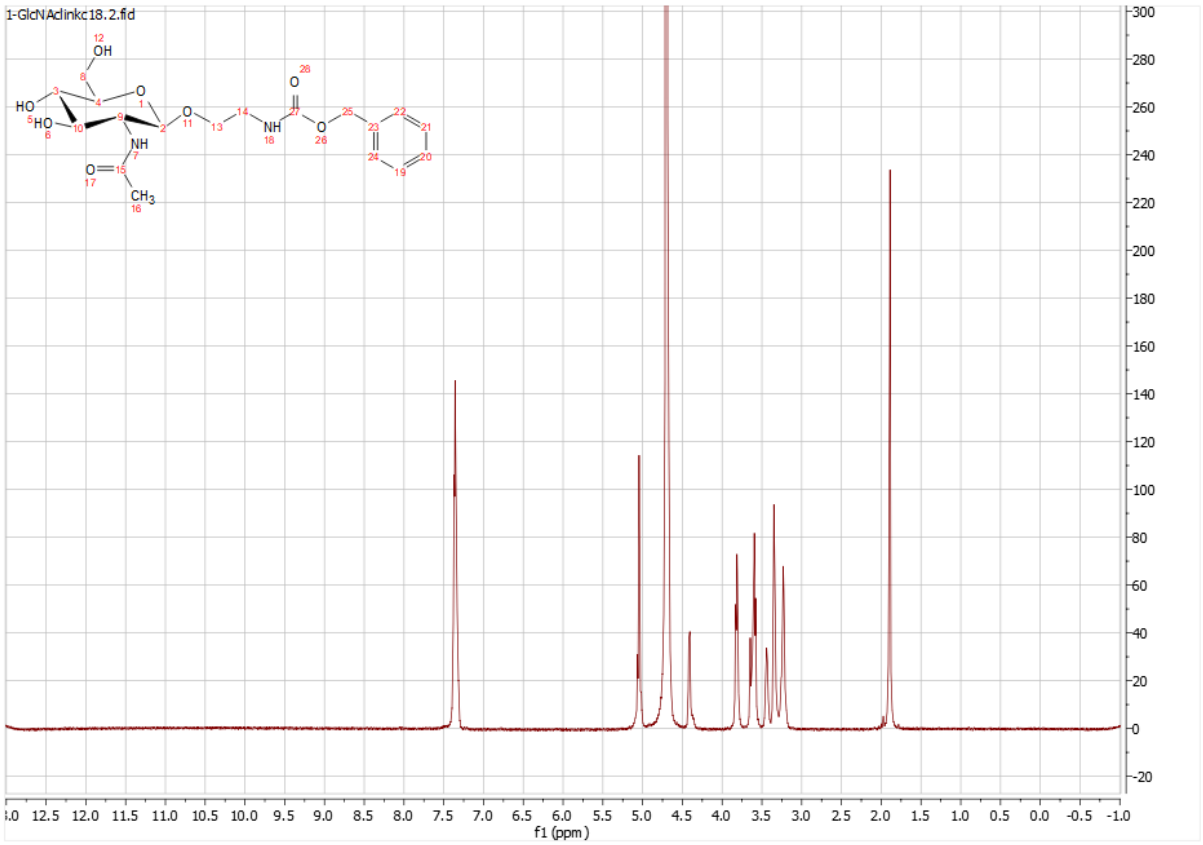

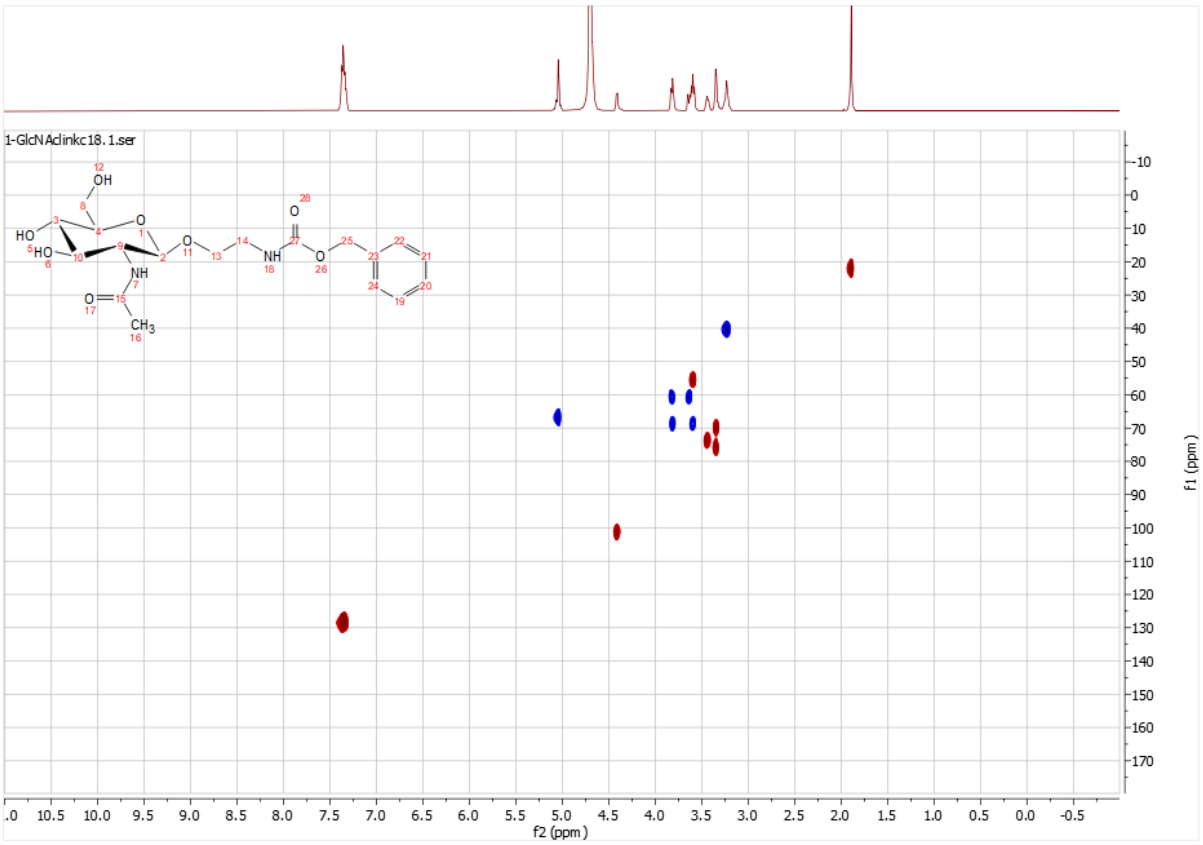

(4) N-Cbz-2-aminoethyl [ß-D-galactopyranosyl]-(1→4)-2-deoxy-2-aminoacetyl-ß-D-glucopyranoside or N-Cbz-2-aminoethyl-ß-LacNAc

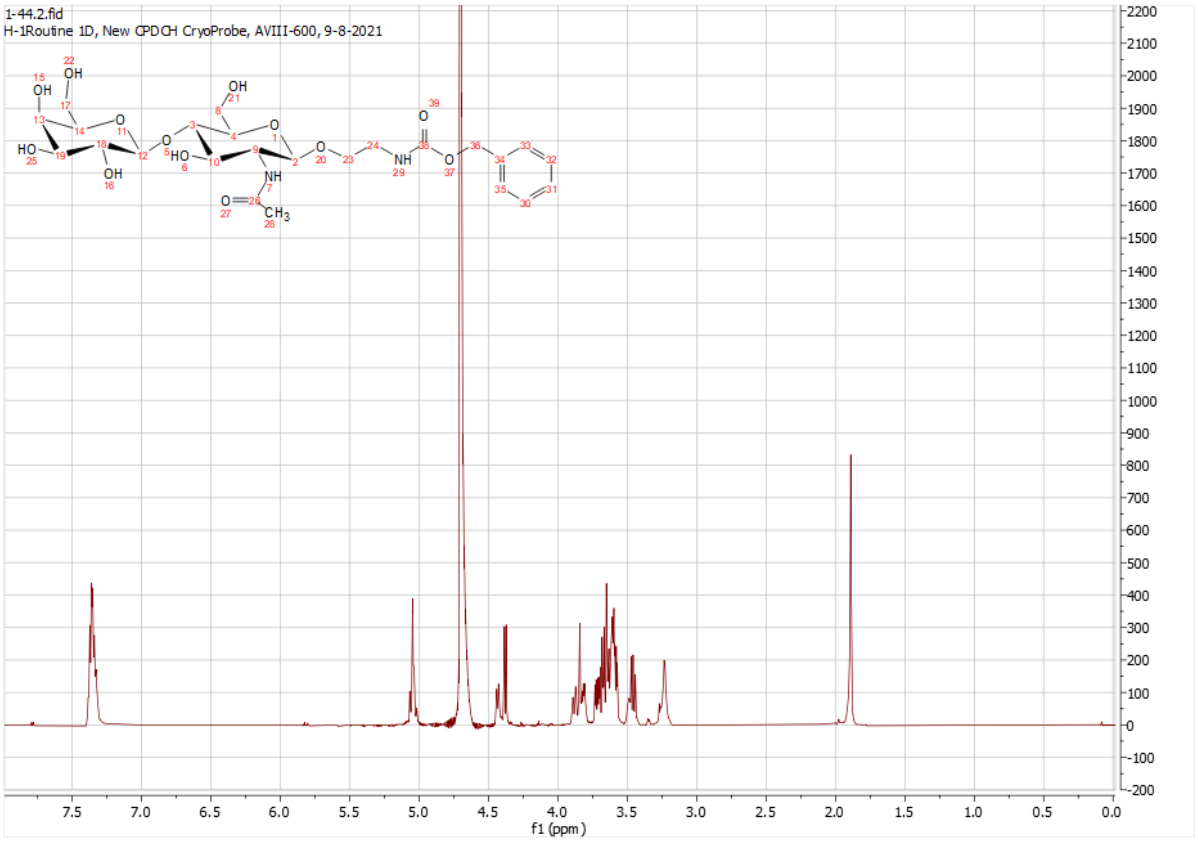

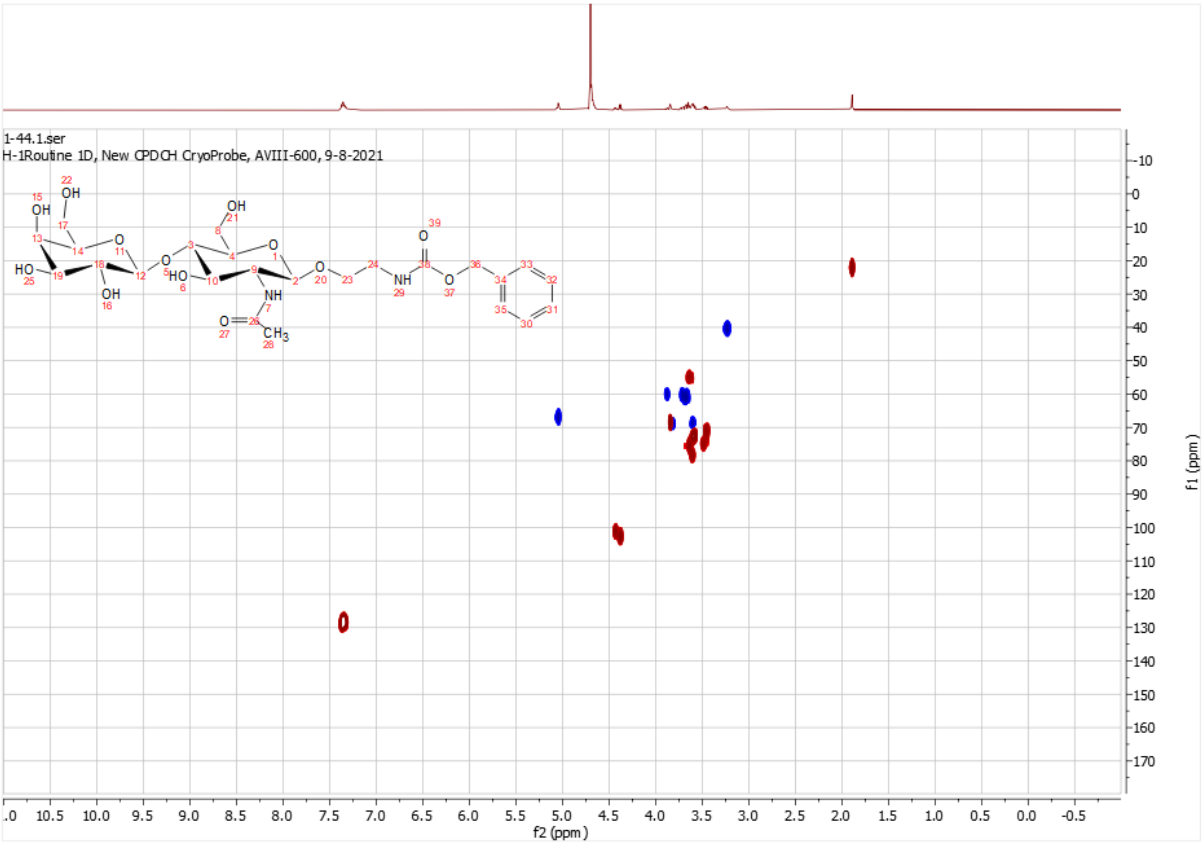

(5) 1-(2-aminoethyl)-N-acetyl-β-D-glucosamine

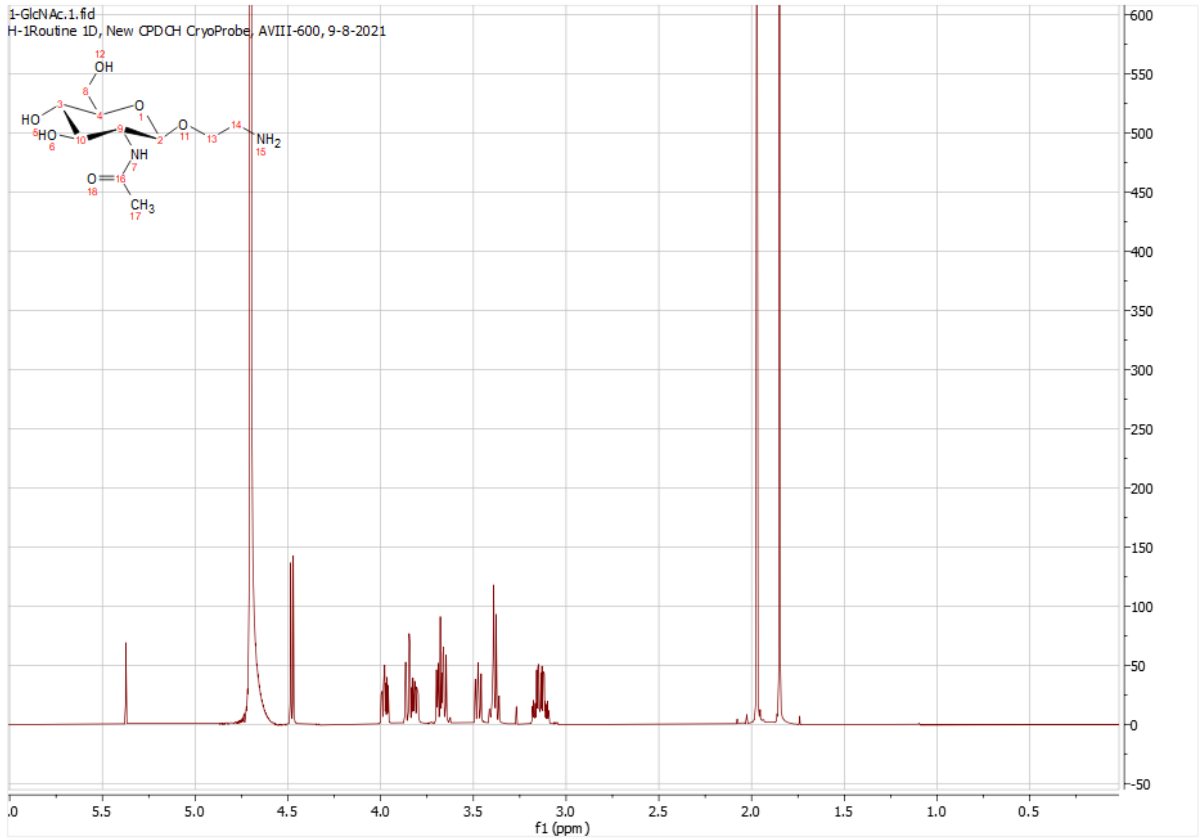

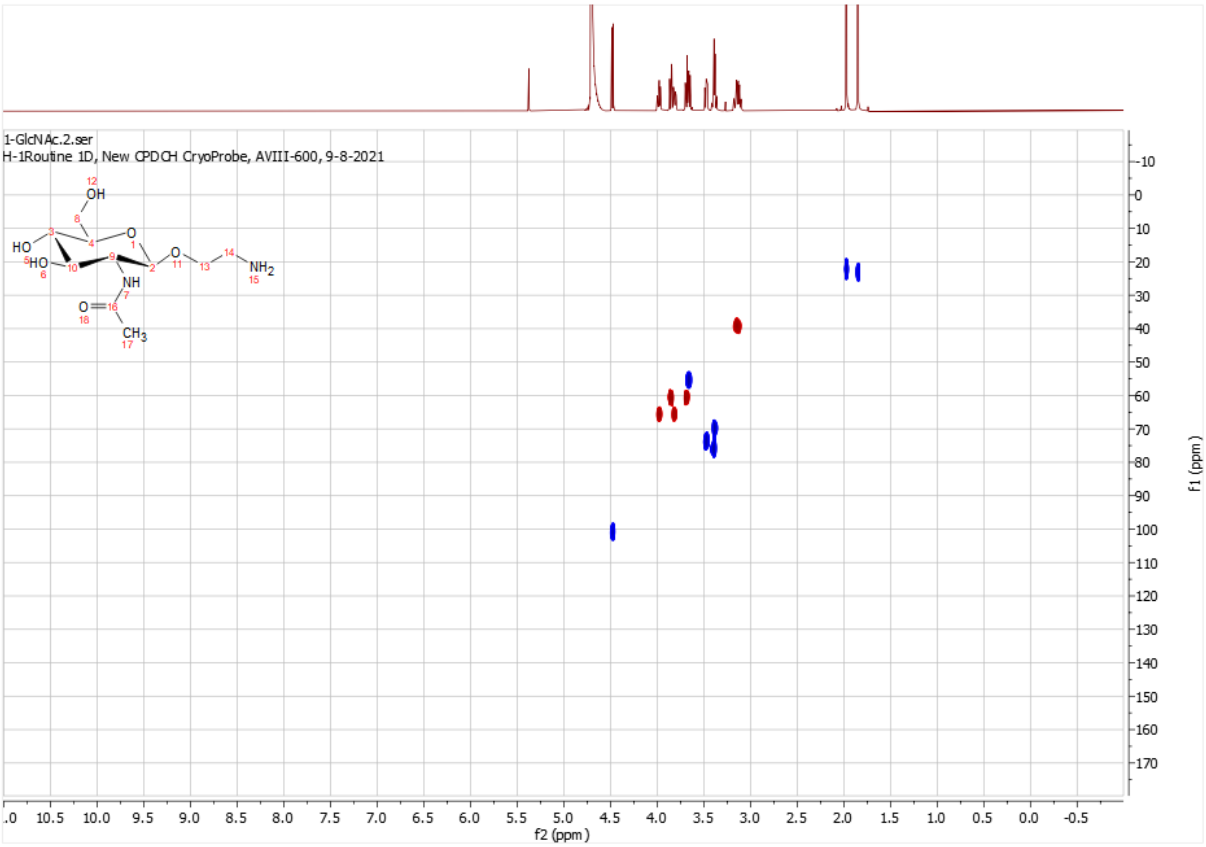

(8) 2-desoxy-2-S-(p-tolylthio)-sialic acid methyl ester

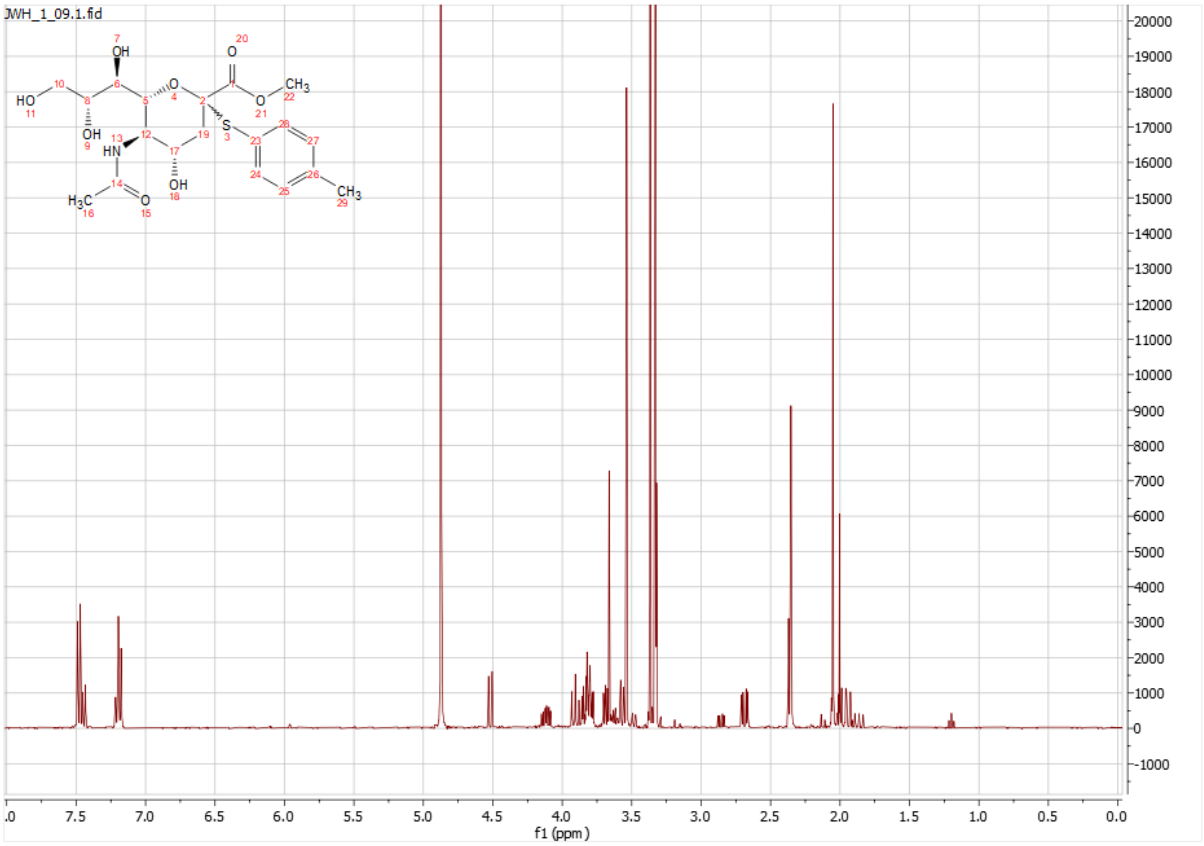

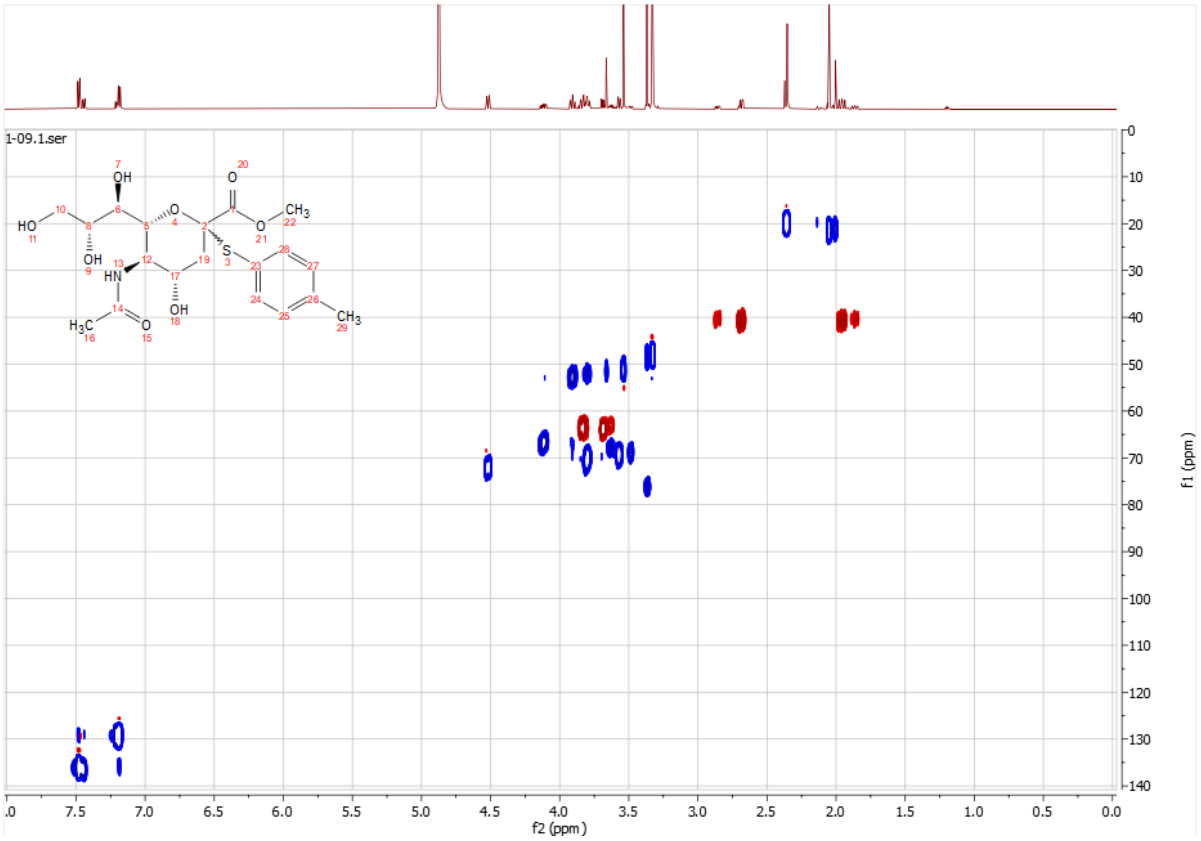

(9) 2-desoxy-2-S-(p-tolylthio)-9-desoxy-9-azido-sialic acid methyl ester

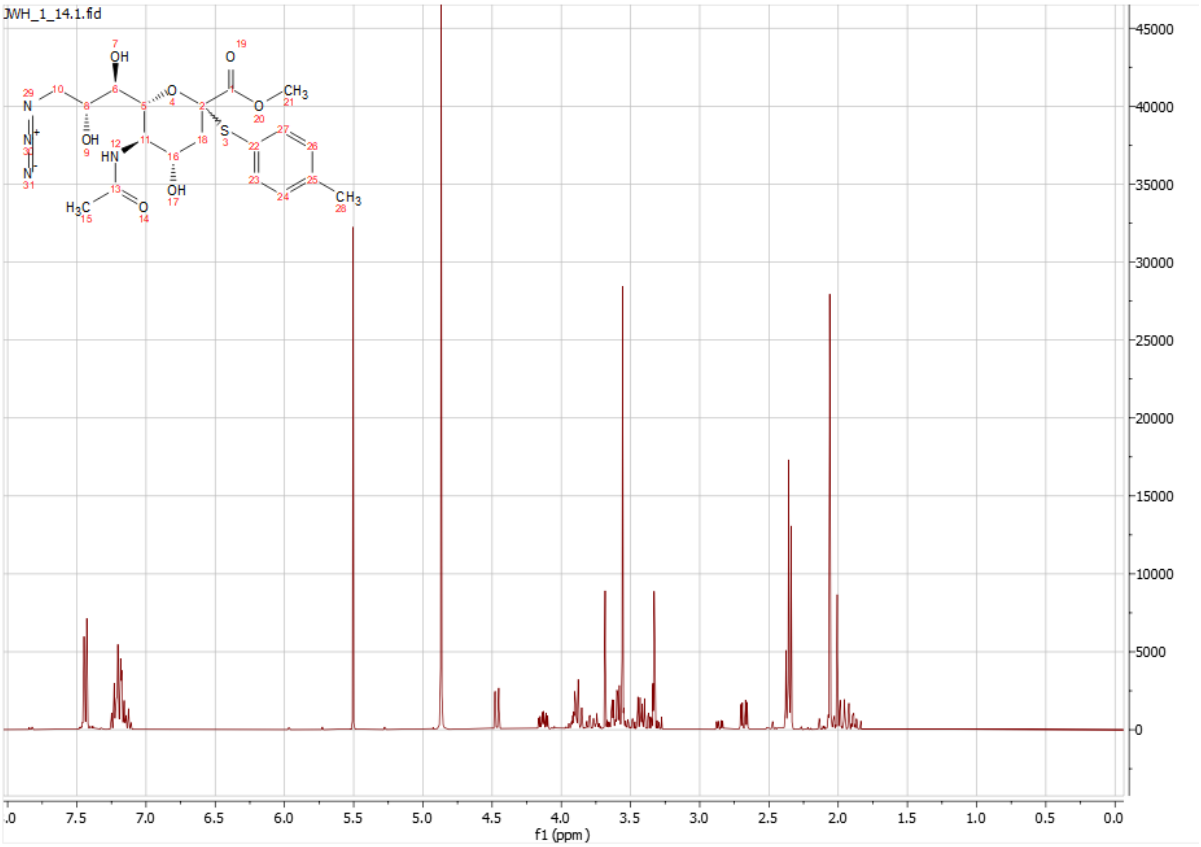

(10) 2-desoxy-2-S-(p-tolylthio)-4,7,8-tri-O-acetyl-5-N-desactyl-5-N-(t-butyloxycarbonyl)-9-desoxy-9-azido-sialic acid methyl ester

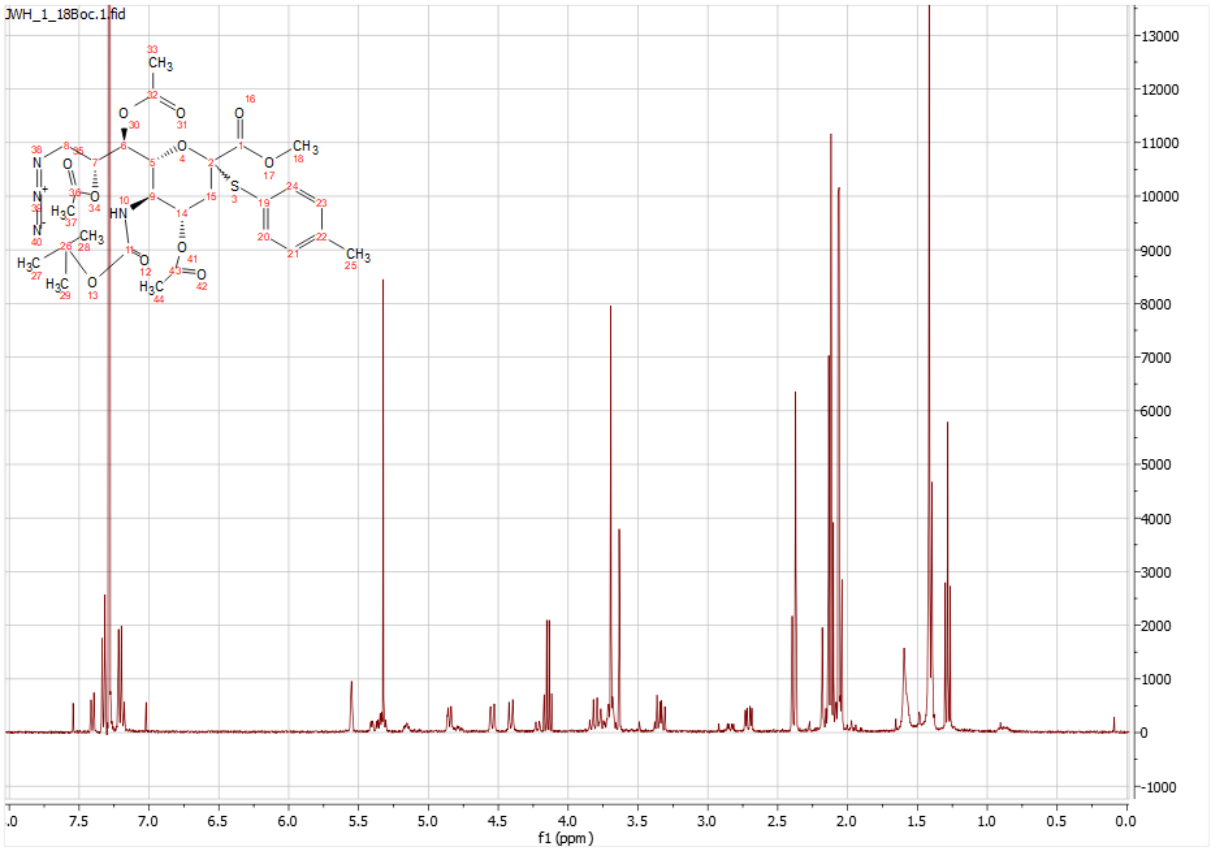

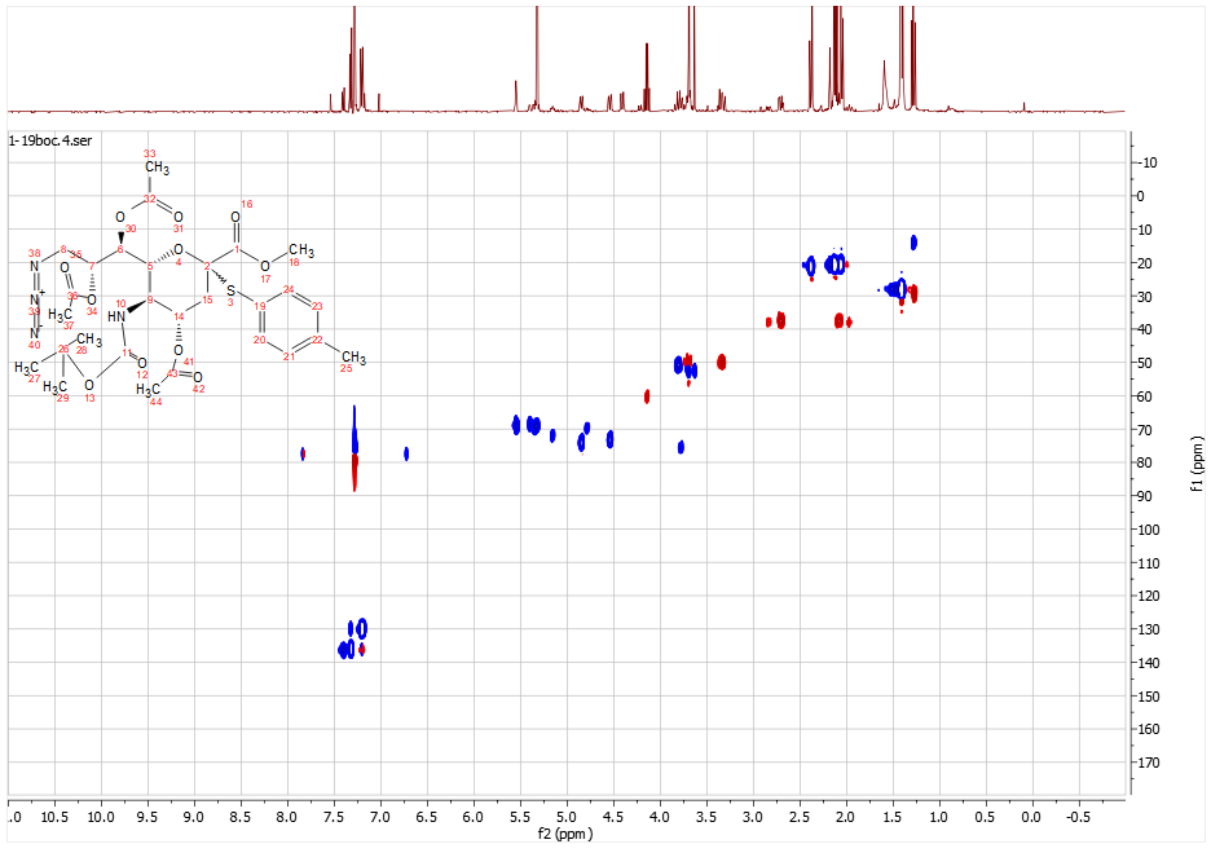

(11) 2-desoxy-2-S-(p-tolylthio)-4,7,8-tri-O-acetyl-5-N-glycoyl-9-desoxy-9-azido-neuraminic acid methyl ester

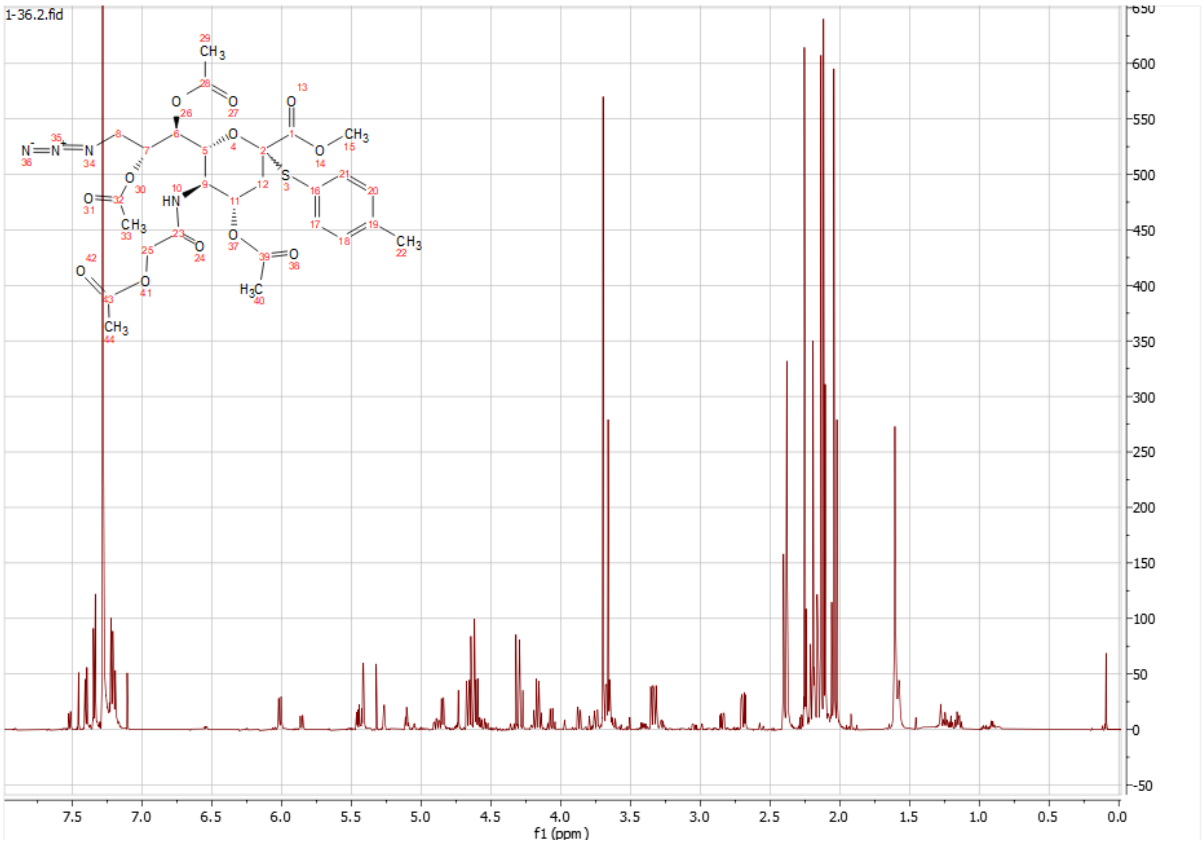

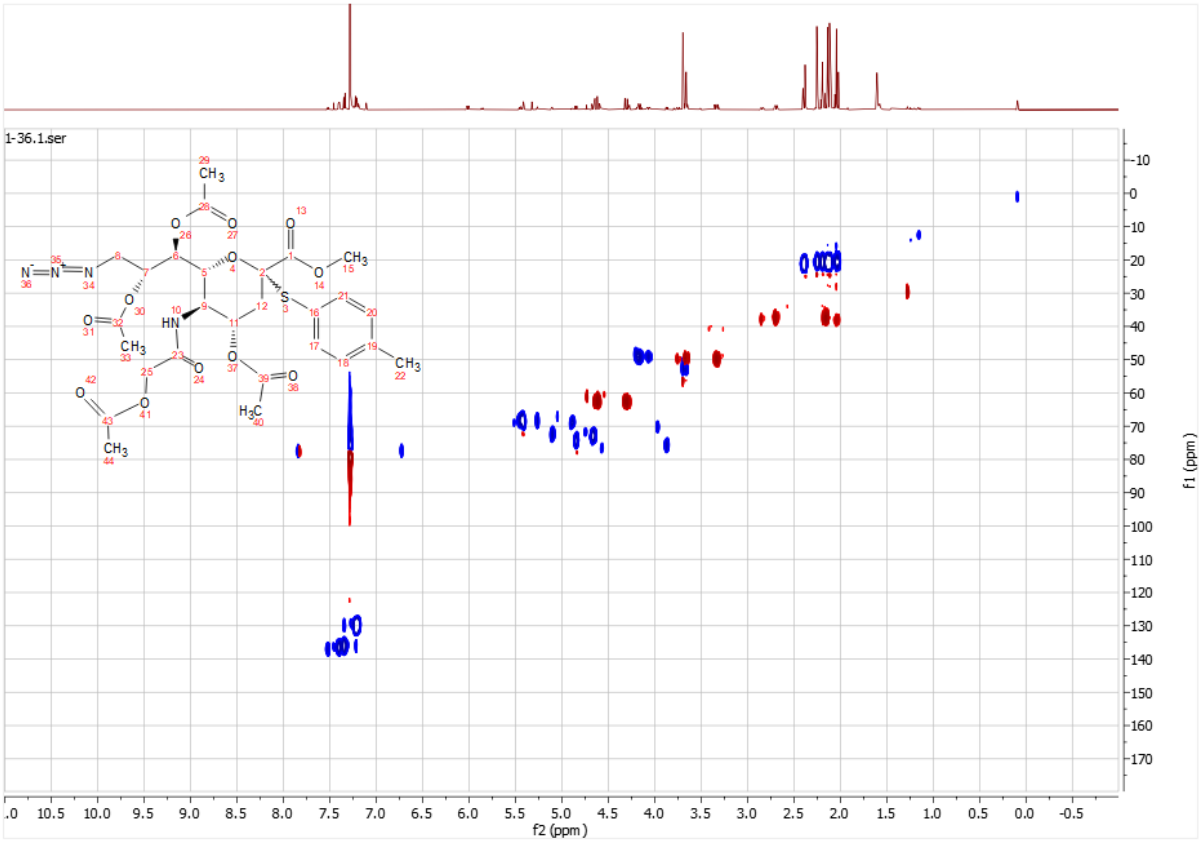

(12) Sodium 2-desoxy-2-S-(p-tolylthio)-5-N-desactyl-5-N-glycoyl-9-desoxy-9-azido-neuraminate

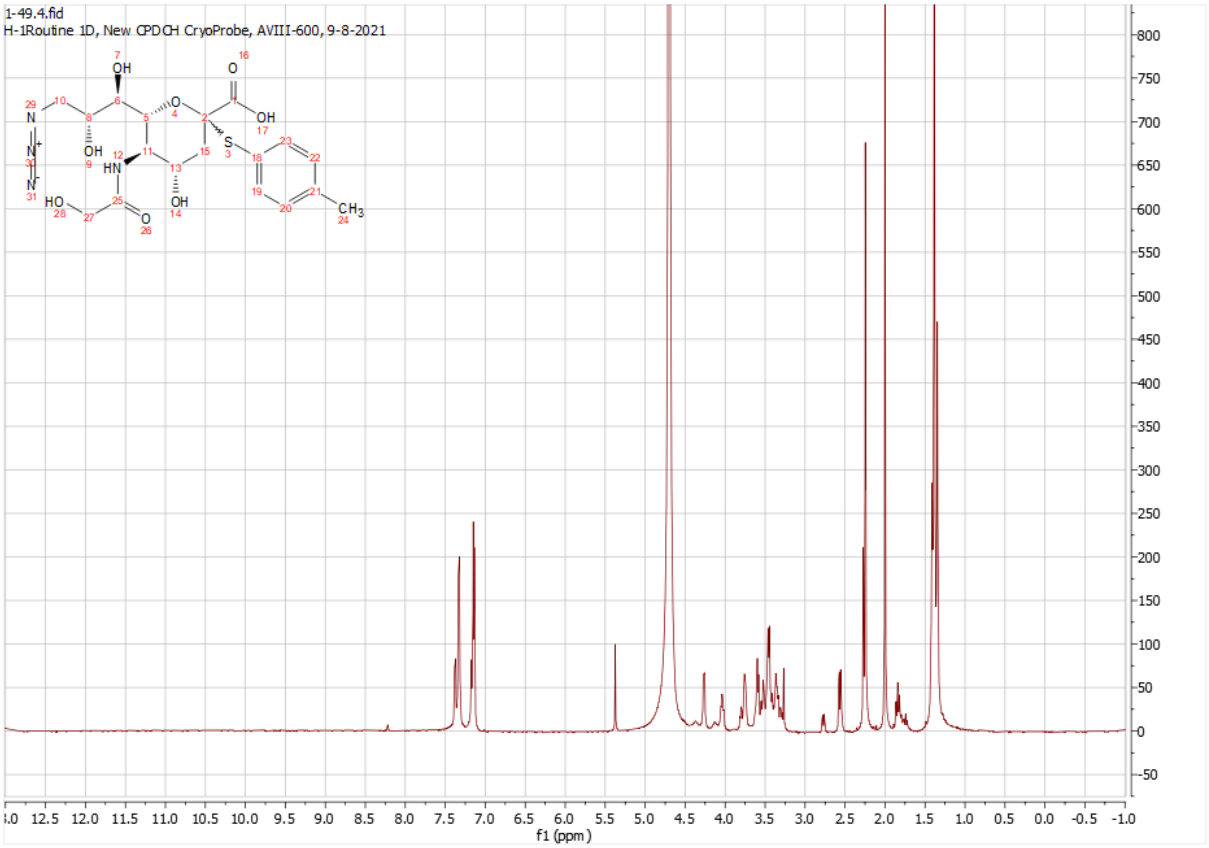

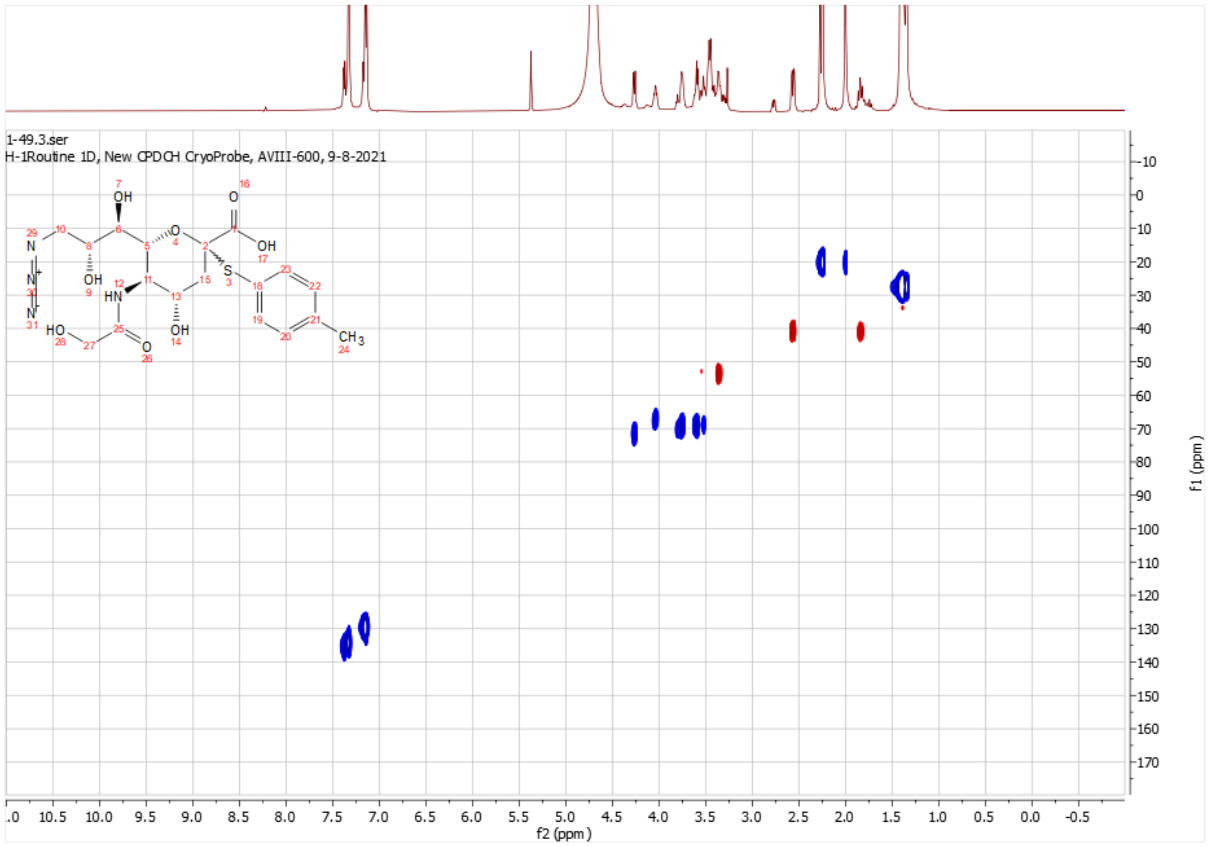

(13) Sodium 5-N-(hydroxyacetyl)-9-desoxy-9-azido-neuraminate

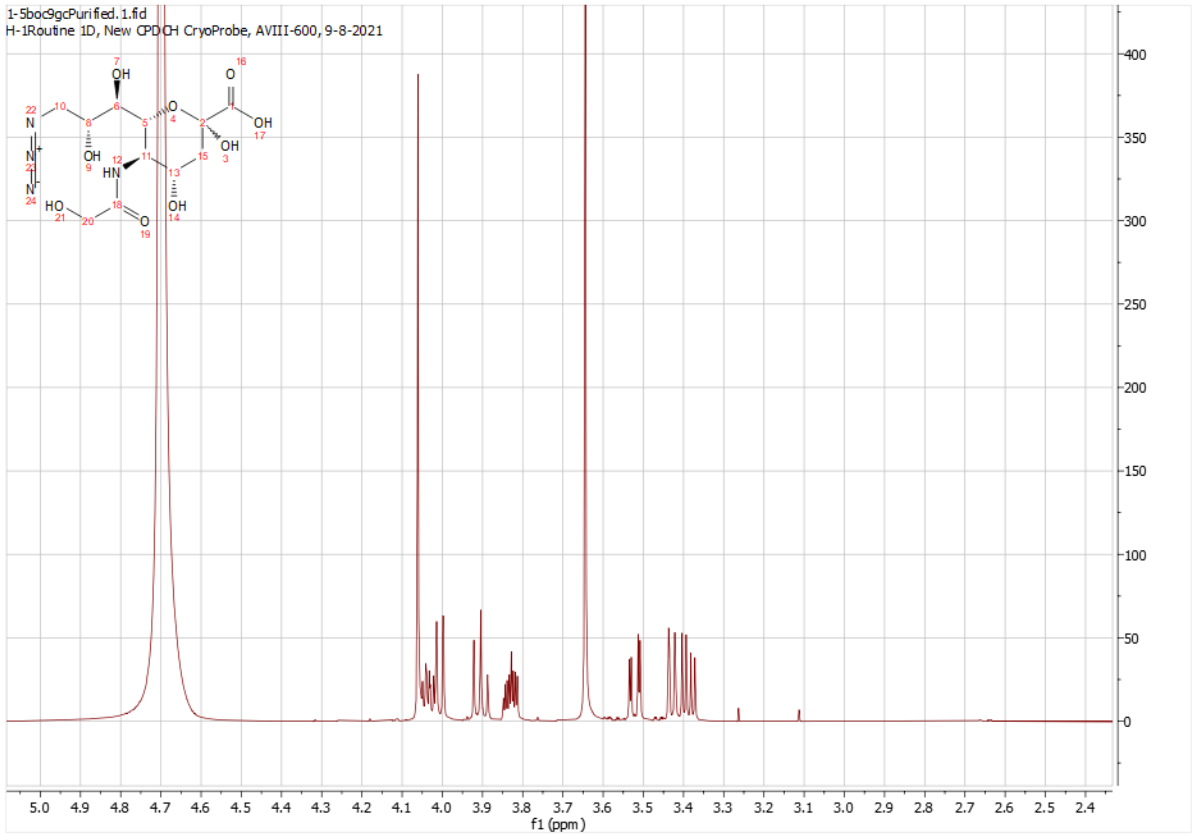

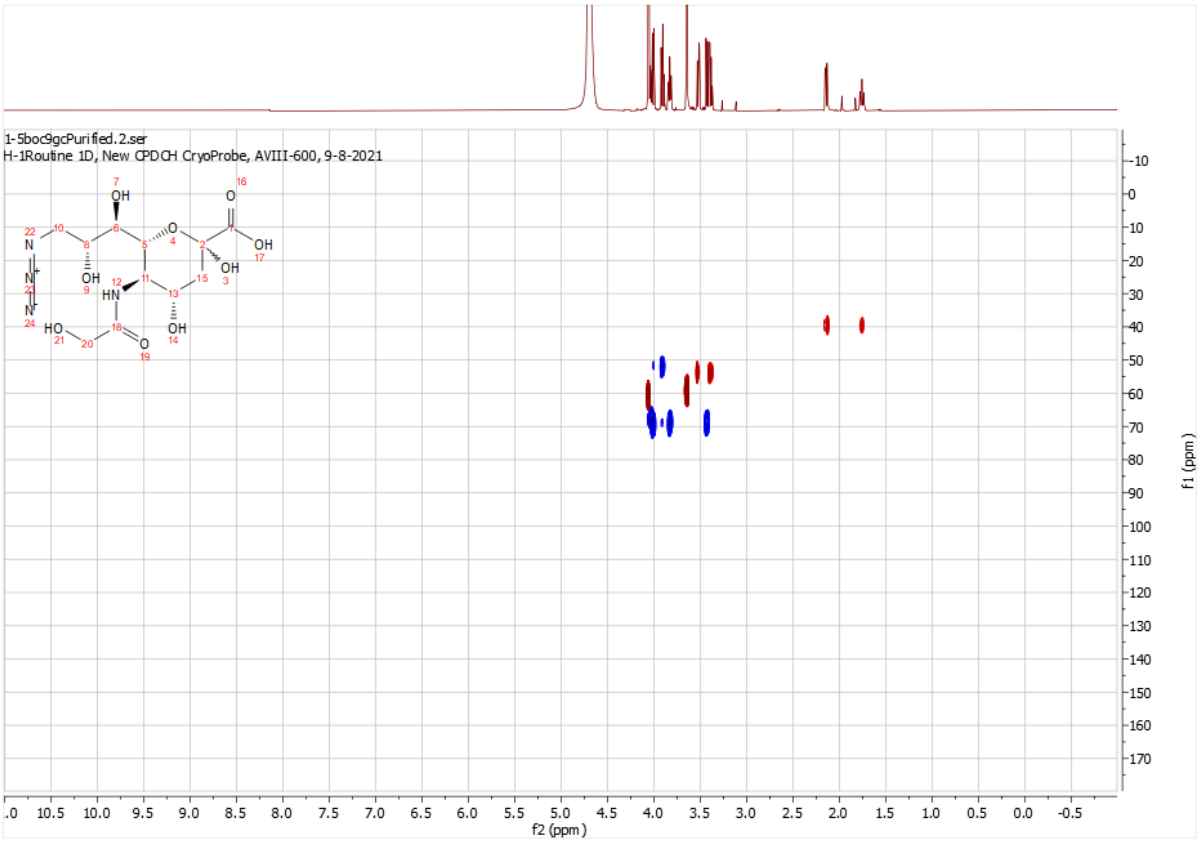

(14) Sodium [5-N-(hydroxyacetyl)-9-desoxy-9-azido-α-D-neuraminate]-(2→3)-N-Cbz-2-aminoethyl-β-LacNAc

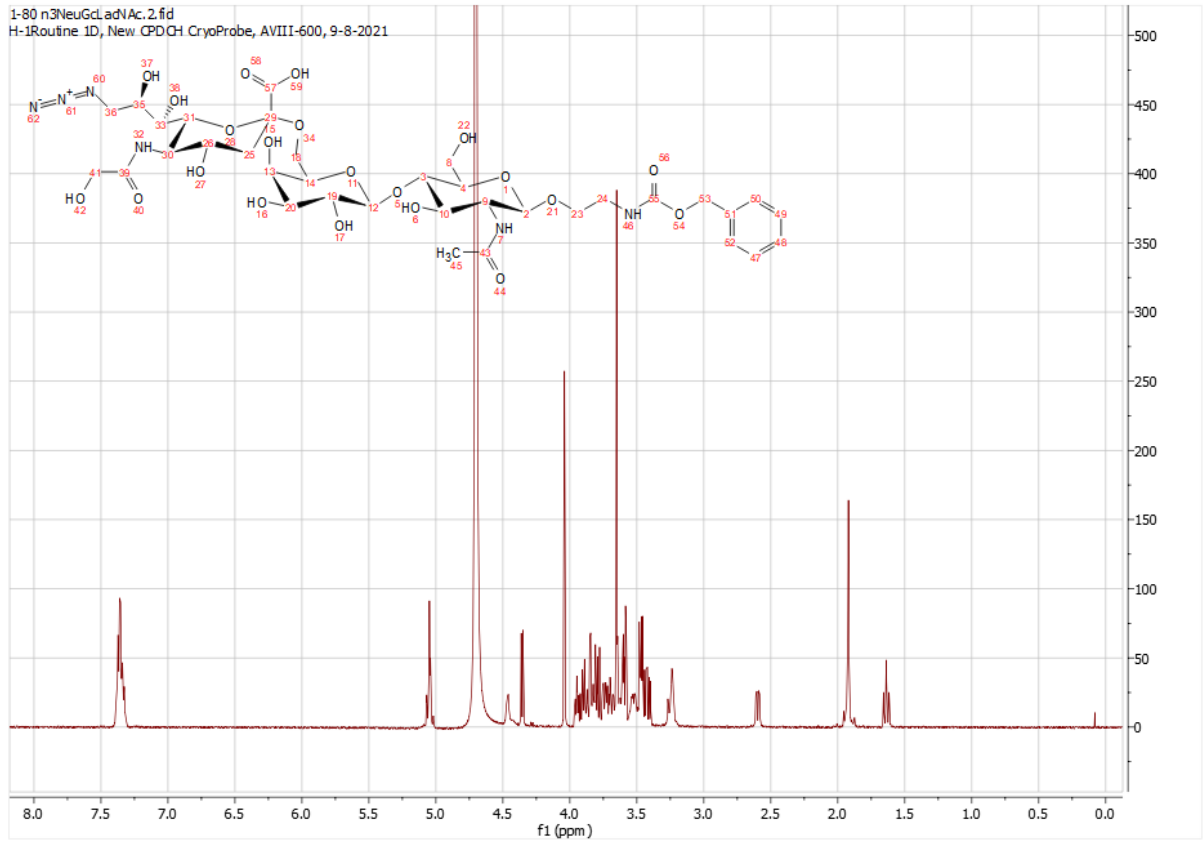

(15) Sodium [5-N-(hydroxyacetyl)-9-desoxy-9-(biphenylacetamido)-α-D-neuraminate]-(2→3)-2-aminoethyl-β-LacNAc

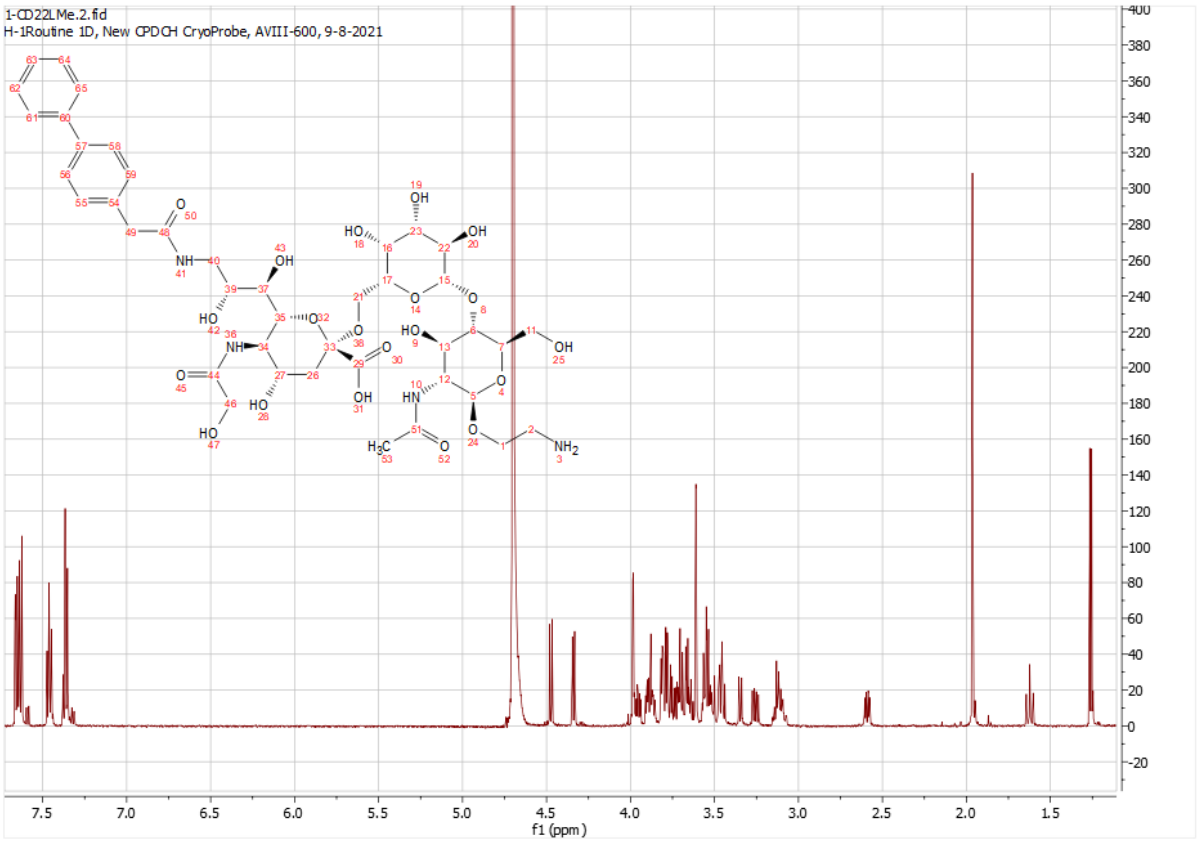

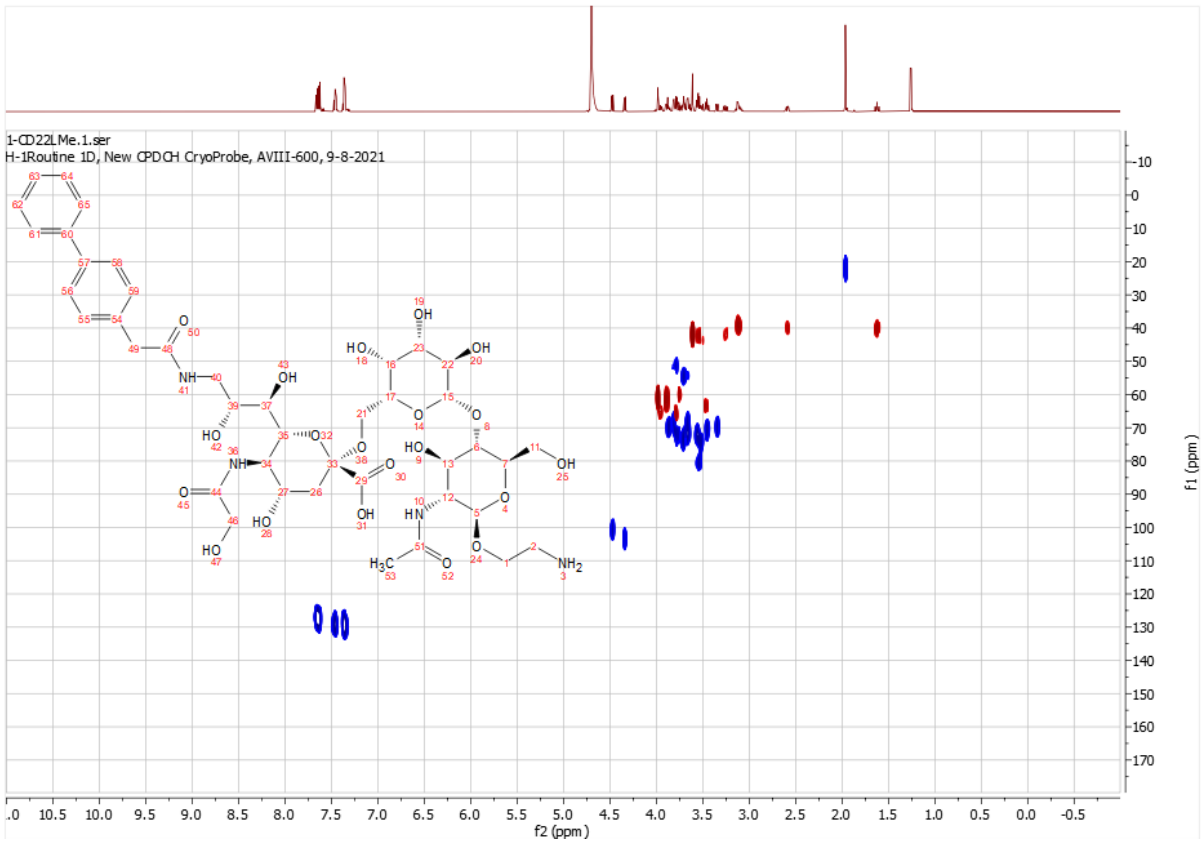

(16) Sodium [5-N-(hydroxyacetyl)-9-desoxy-9-(biphenylacetamido)-α-D-neuraminate]-(2→3)-N-(Mal-PEG$_6$-amido)-2-aminoethyl-β-LacNAc

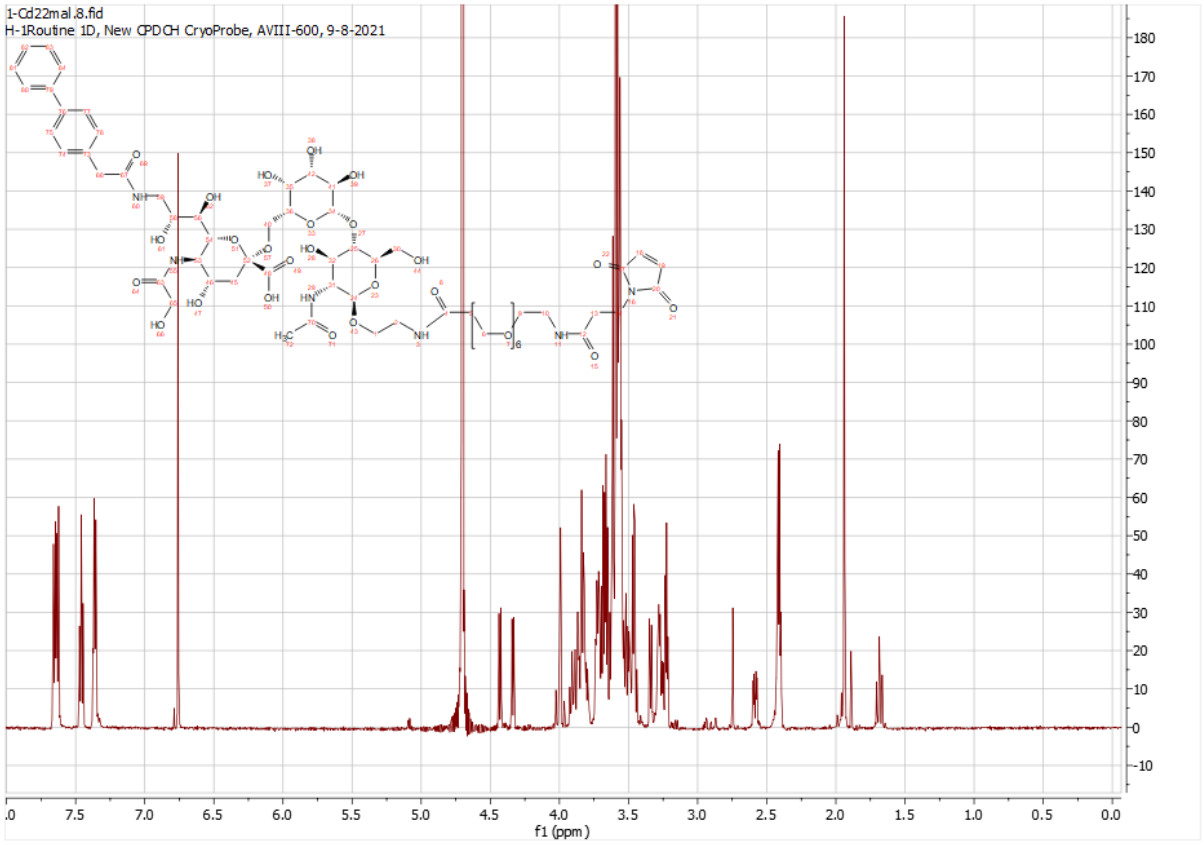

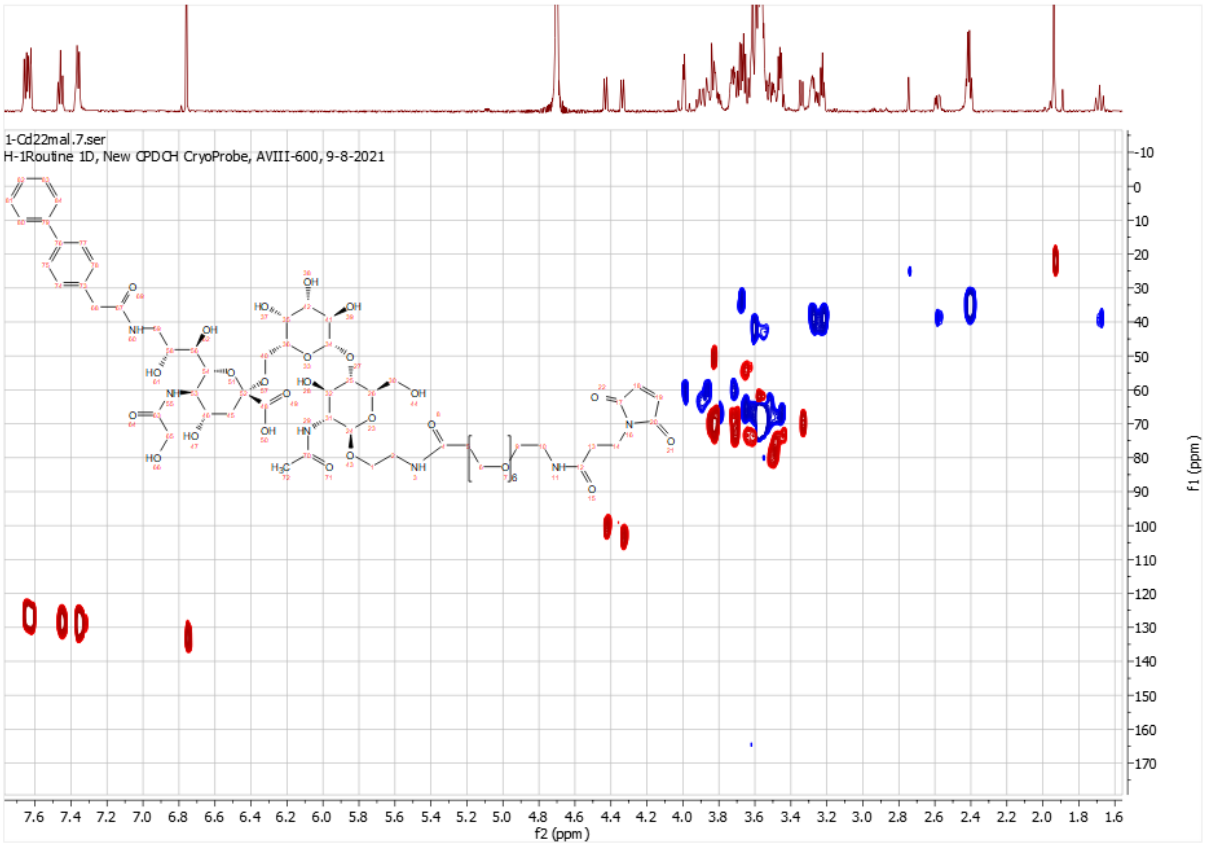

(17) 1-Tosyl-PEG$_3$-N$_3$

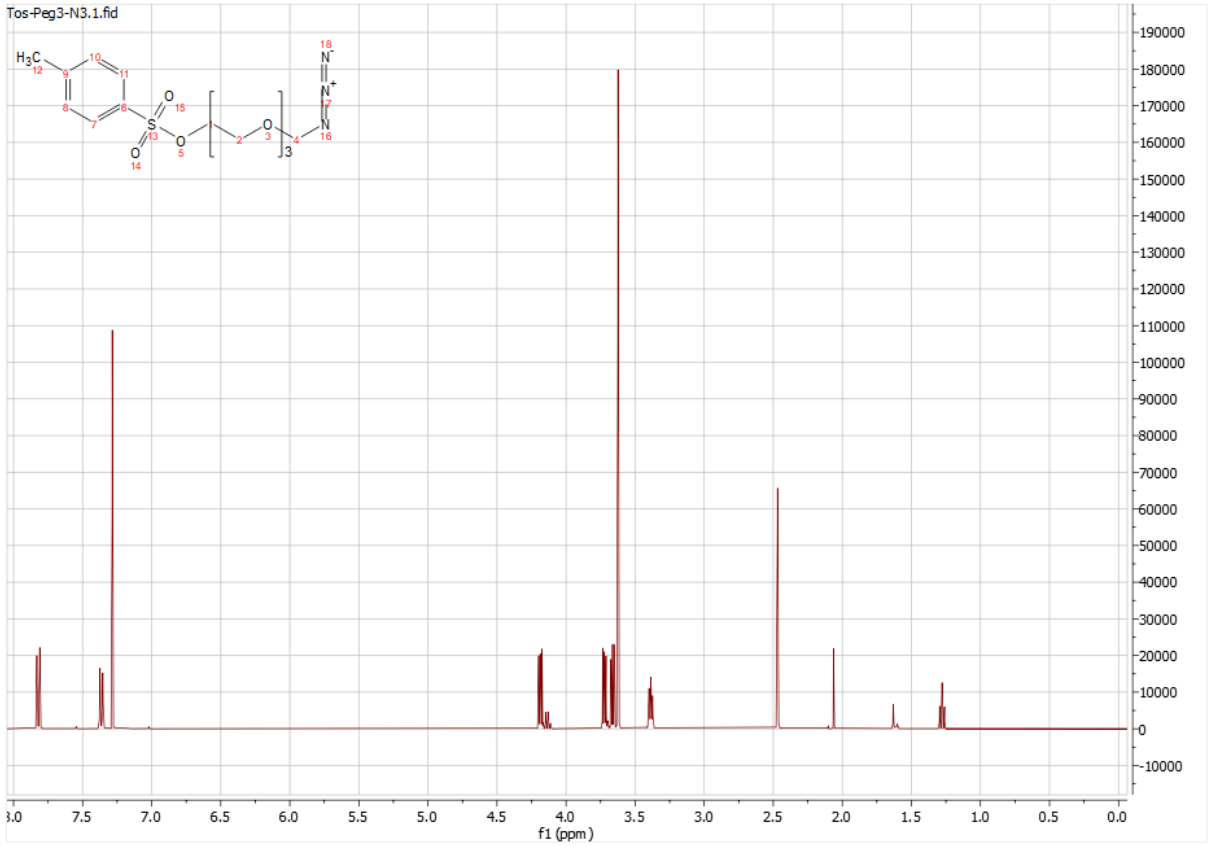

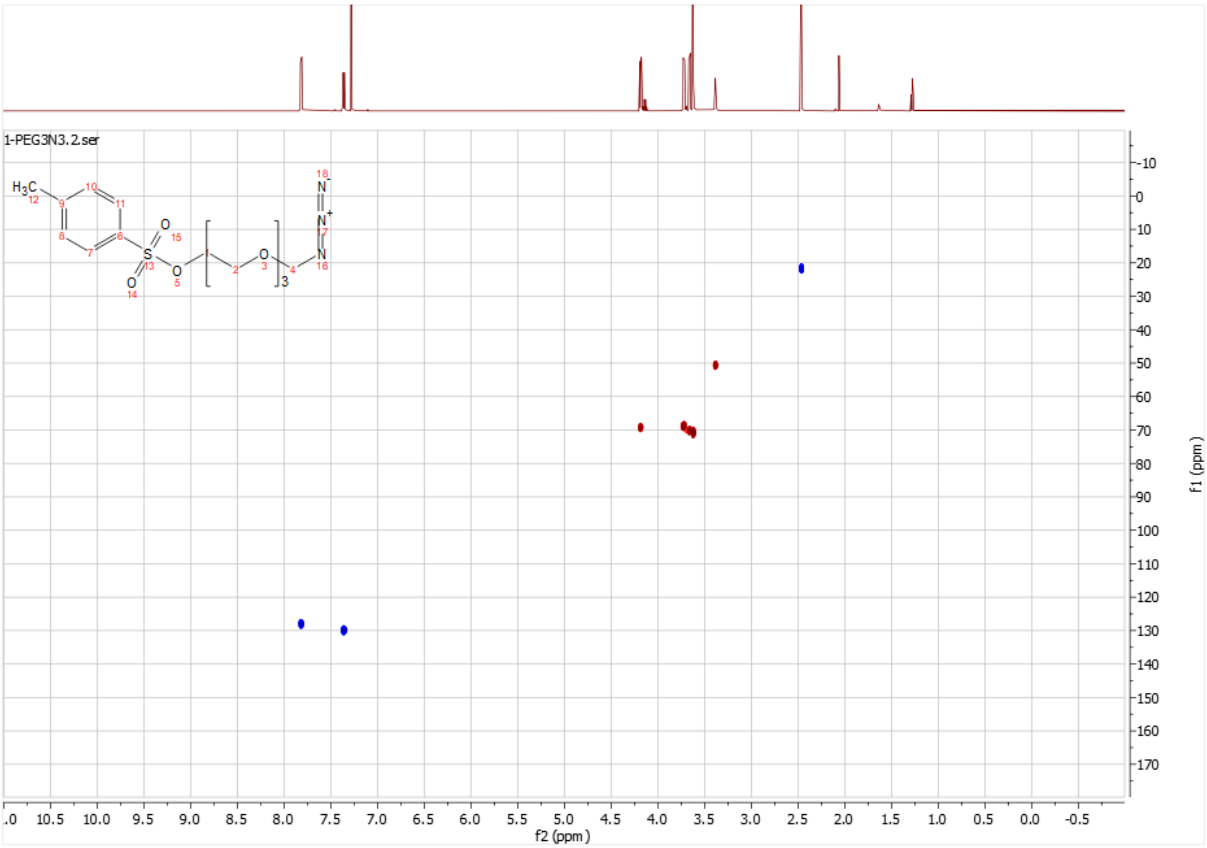

(18) 5-(2-(2-(2-azidoethoxy)ethoxy)ethoxy)isophthalate

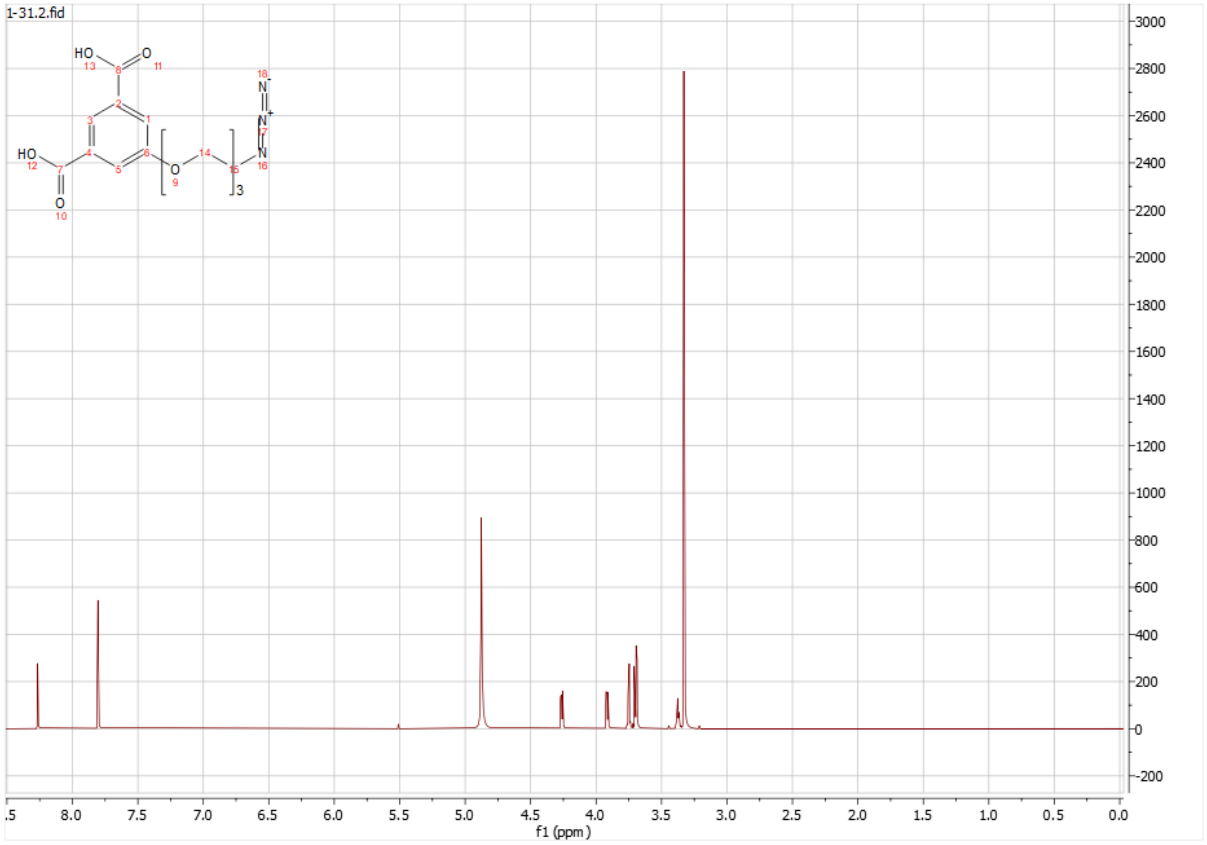

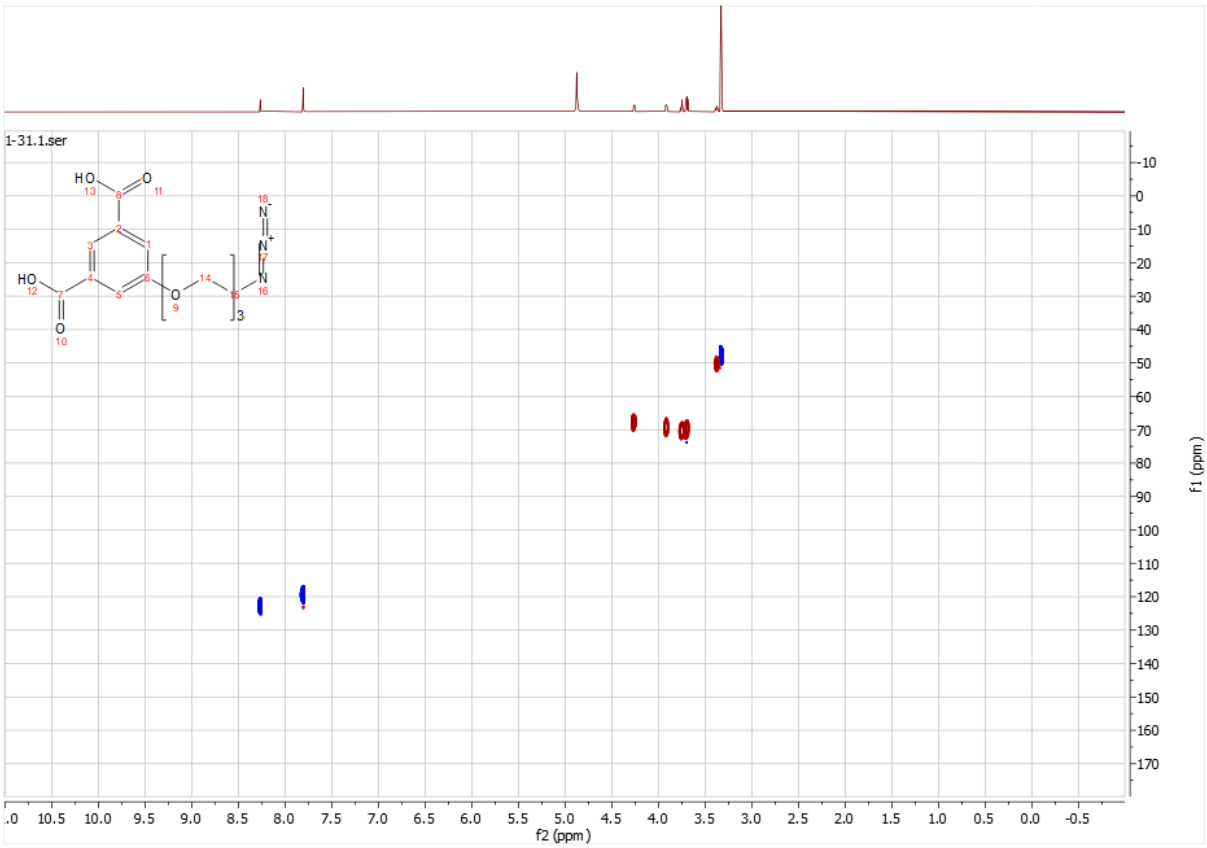

(19) bis-(26-t-Boc-amido-nona(ethoxy))-5-(2-(2-(2-azidoethoxy)ethoxy)ethoxy)isophthalate

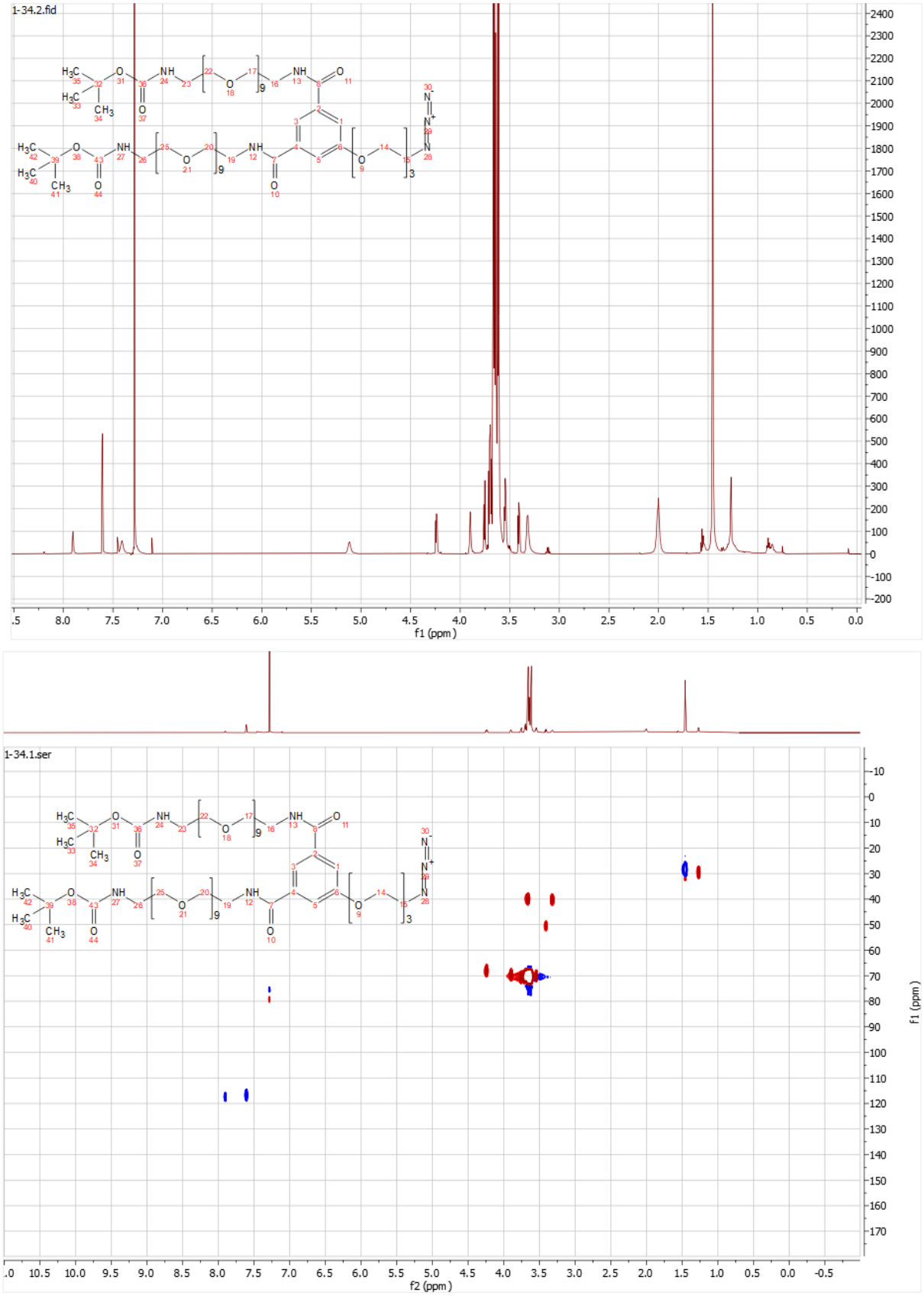

(20) bis-(26-amino-nona(ethoxy))-5-(2-(2-(2-azidoethoxy)ethoxy)ethoxy)isophthalate di-trifluoroacetate

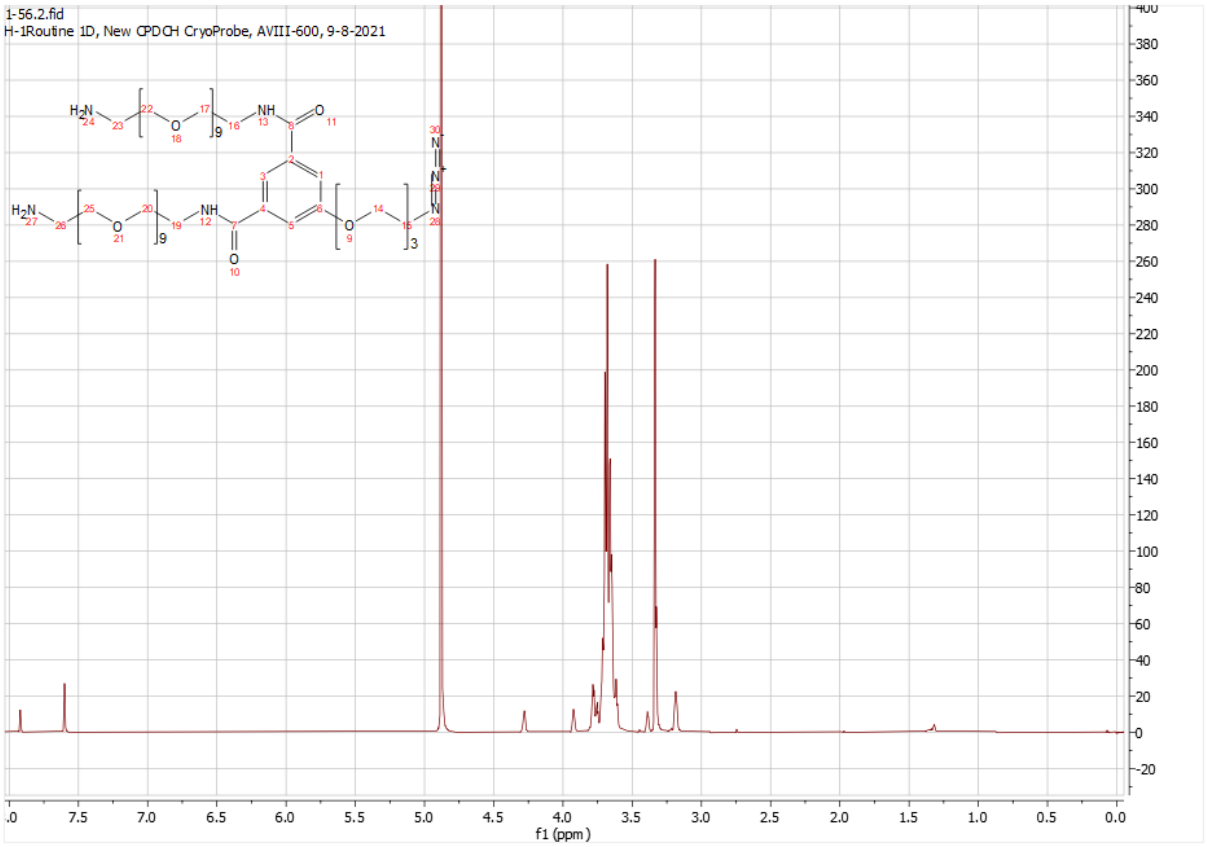

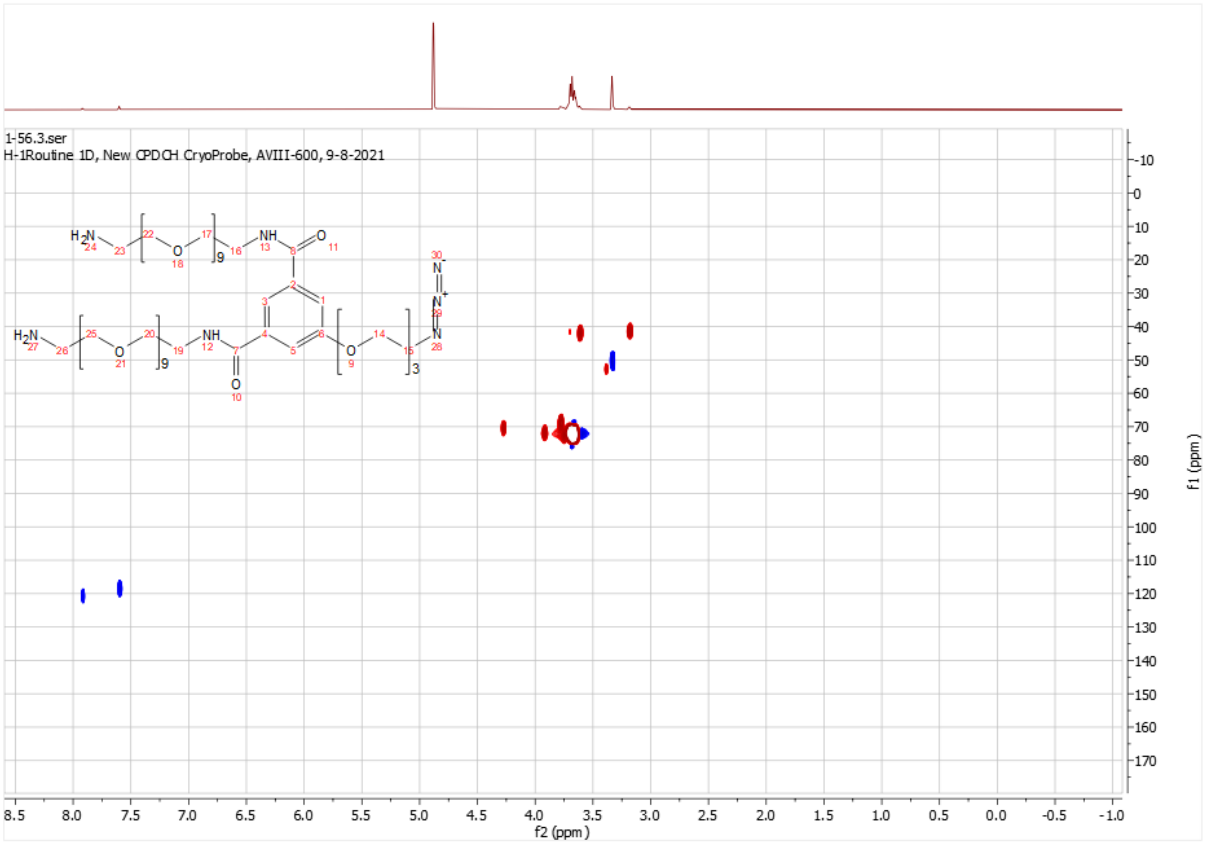

(21) bis-(N-(thiopropionyl)-26-amido-nona(ethoxy))-5-(2-(2-(2-azidoethoxy)ethoxy)ethoxy)isophthalate

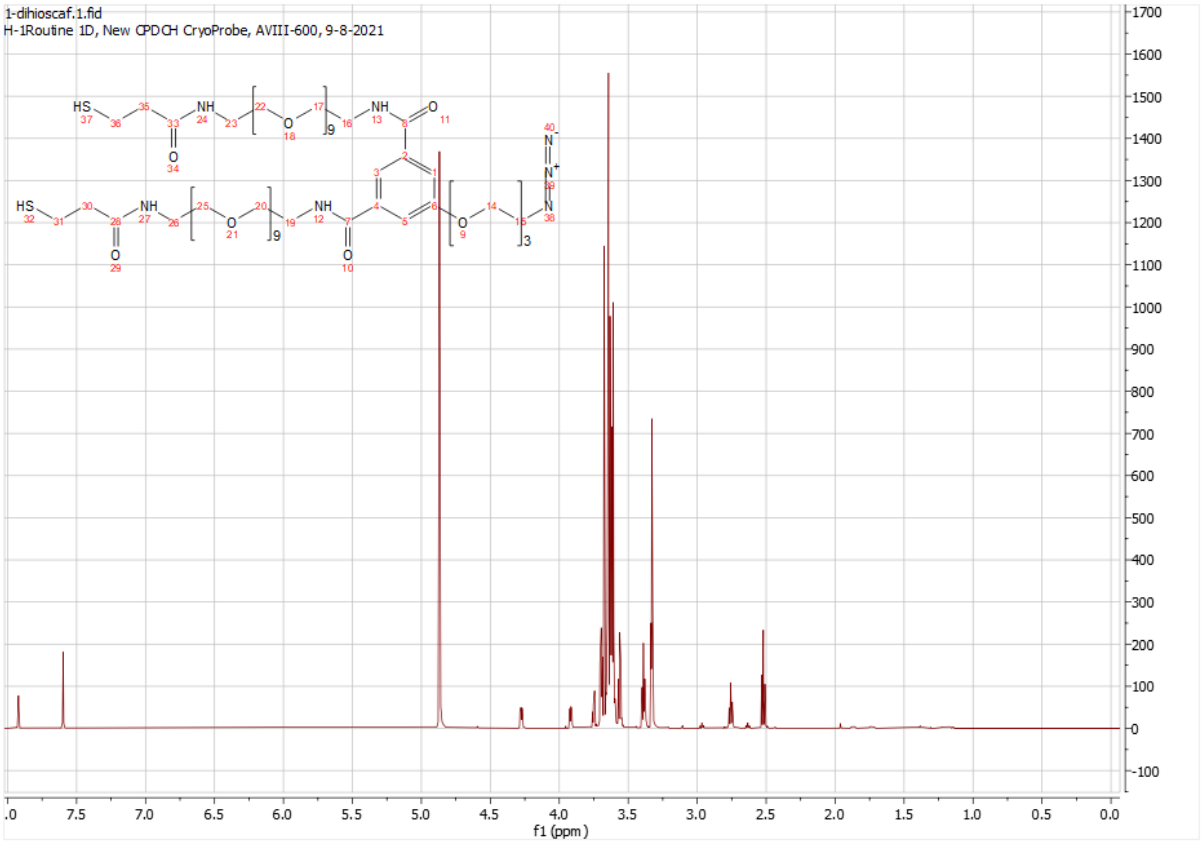

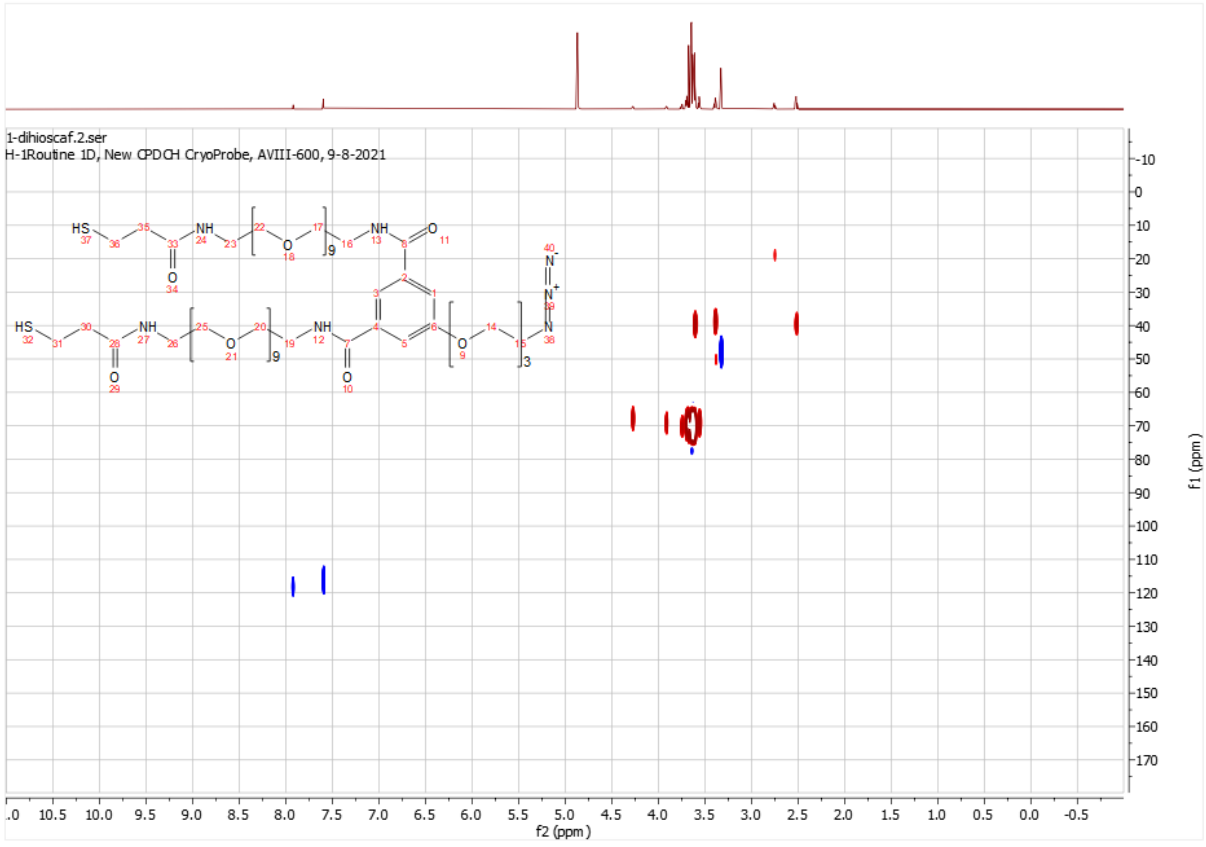

(22) bis-(26-(1,5-di-N-Boc-amido-pentyl-carboxamide)-nona(ethoxy))-5-(2-(2-(2-azidoethoxy)ethoxy)ethoxy)isophthalate

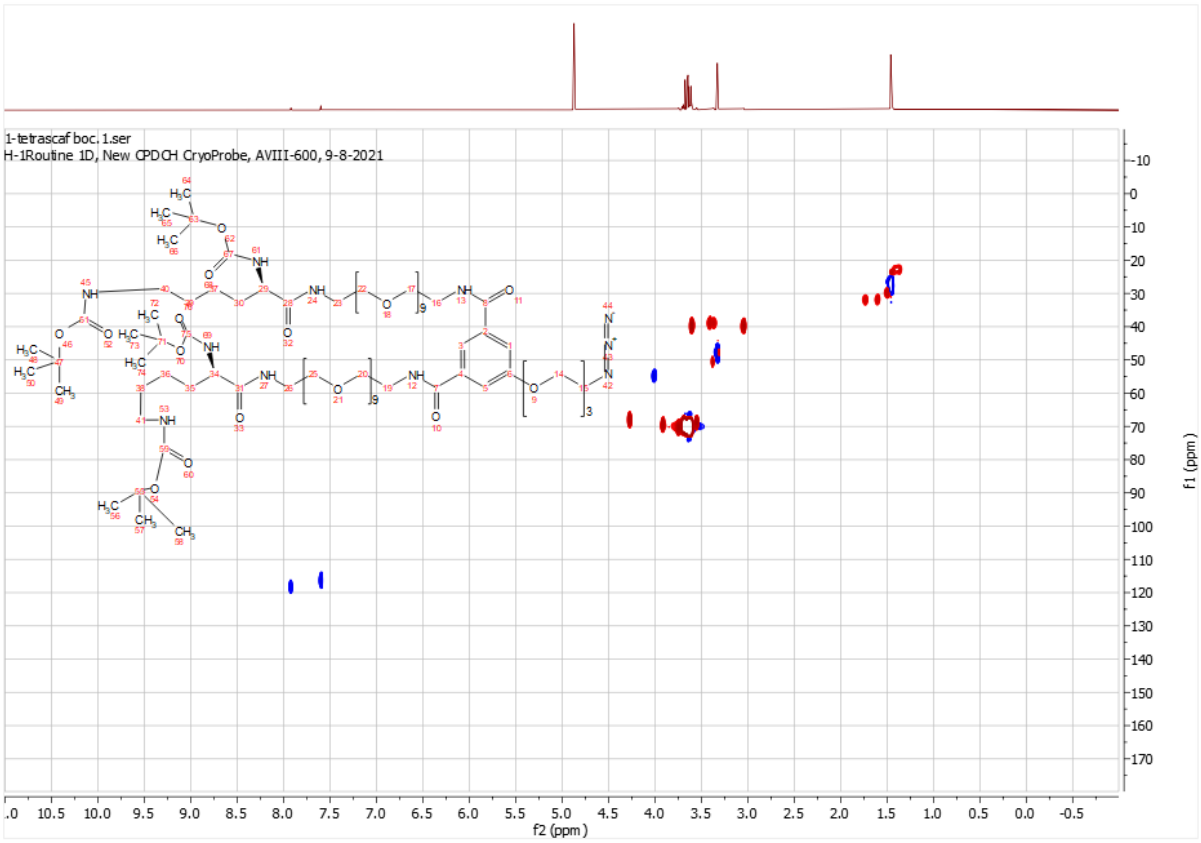

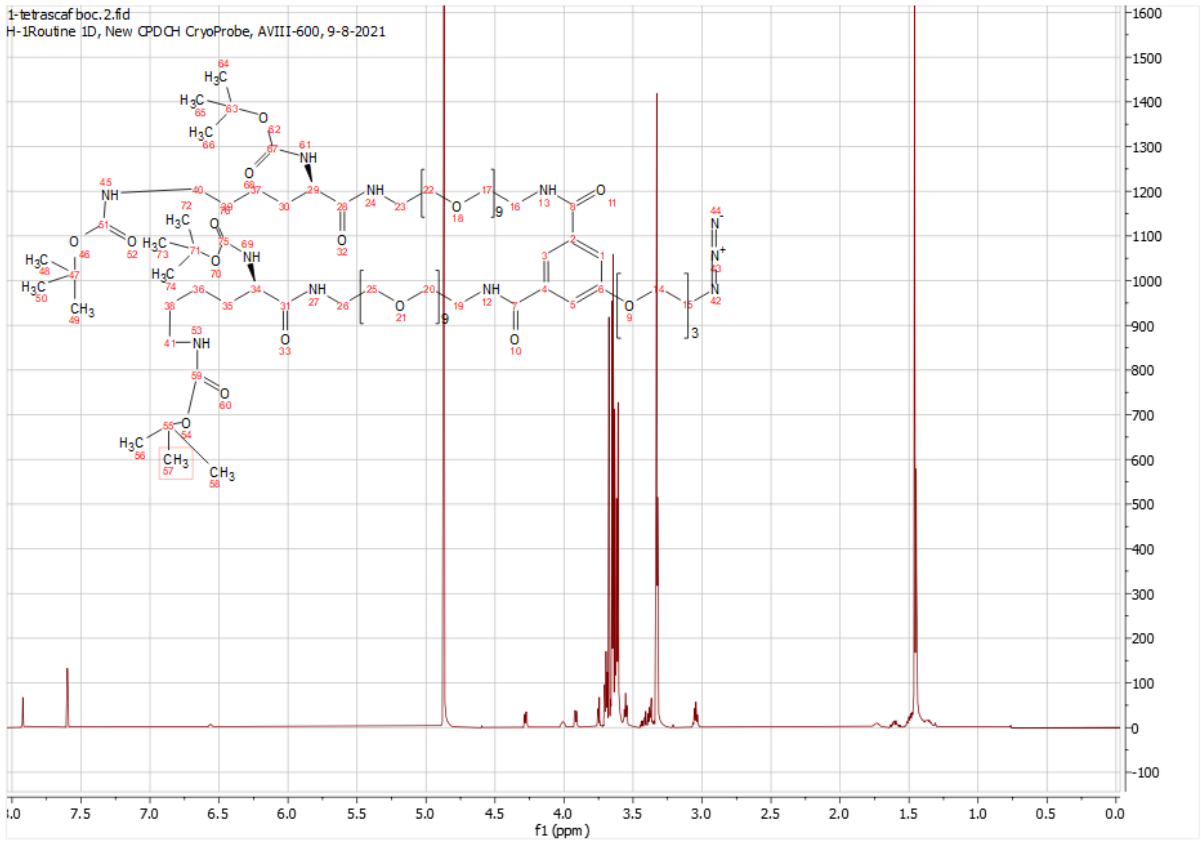

(23) bis-(26-(1,5-di-aminopentyl-carboxamide)-nona(ethoxy))-5-(2-(2-(2-azidoethoxy)ethoxy)ethoxy)isophthalate tetra-trifluoroacetate

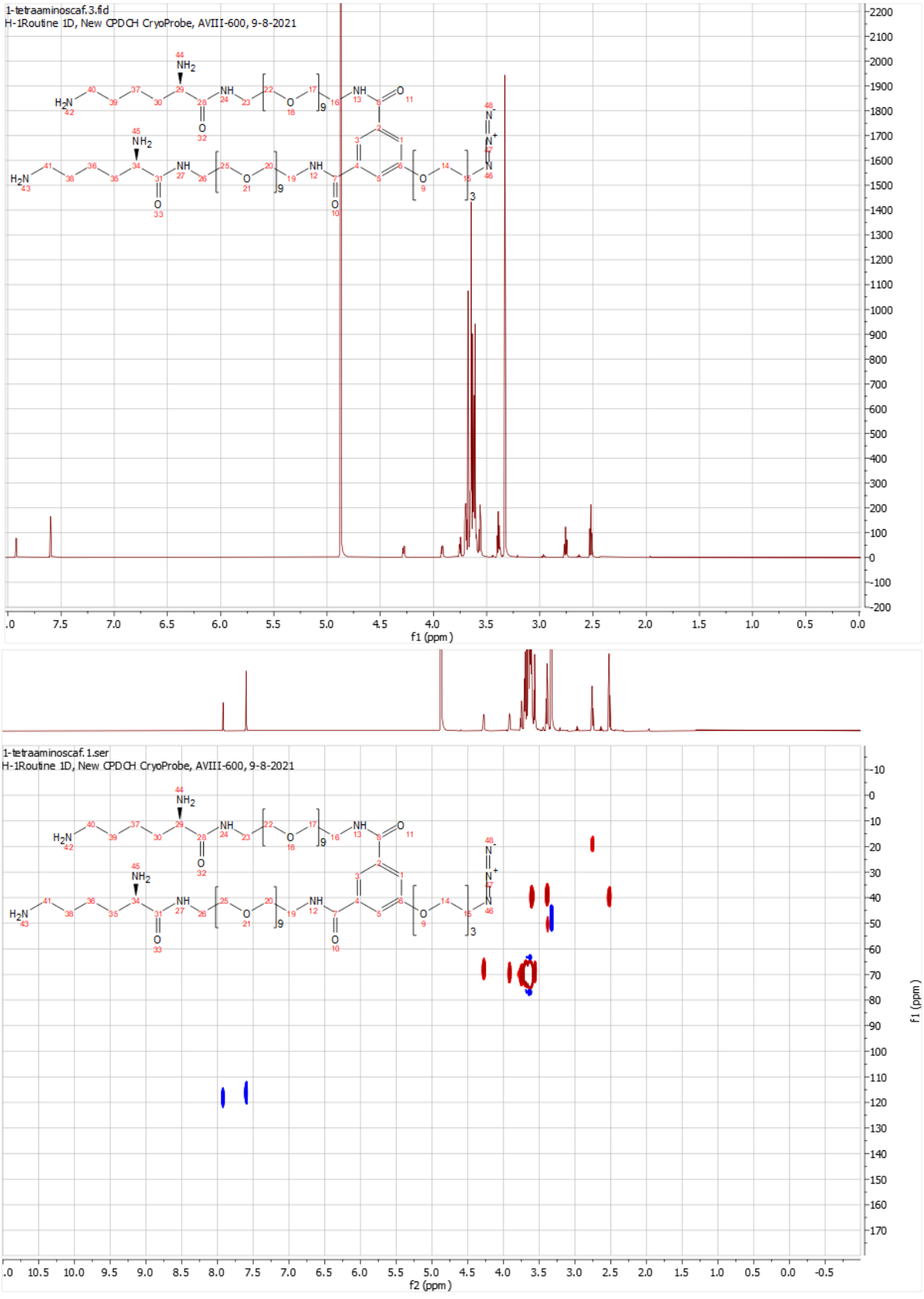

(24) bis-(26-(1,5-di-N-thiopropionyl-amido-pentyl-carboxamide)-nona(ethoxy))-5-(2-(2-(2-azidoethoxy)ethoxy)ethoxy)isophthalate

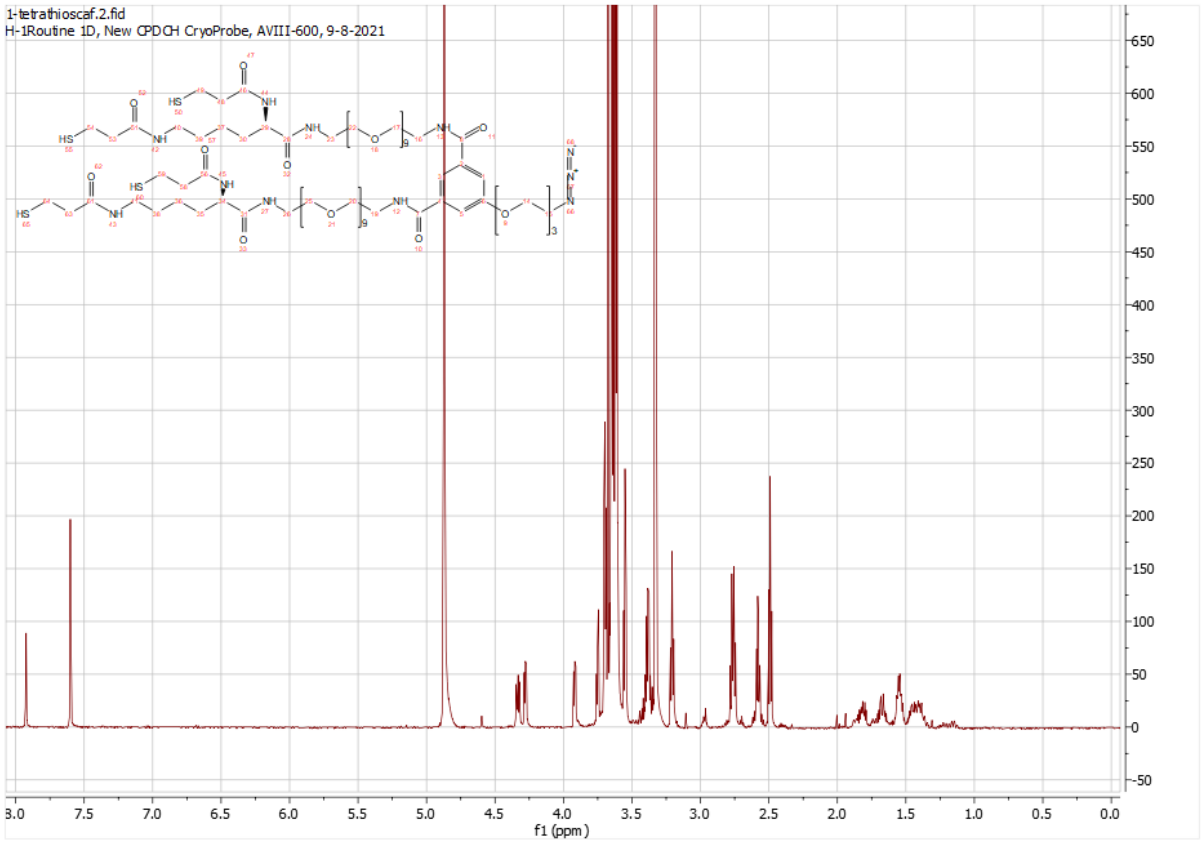

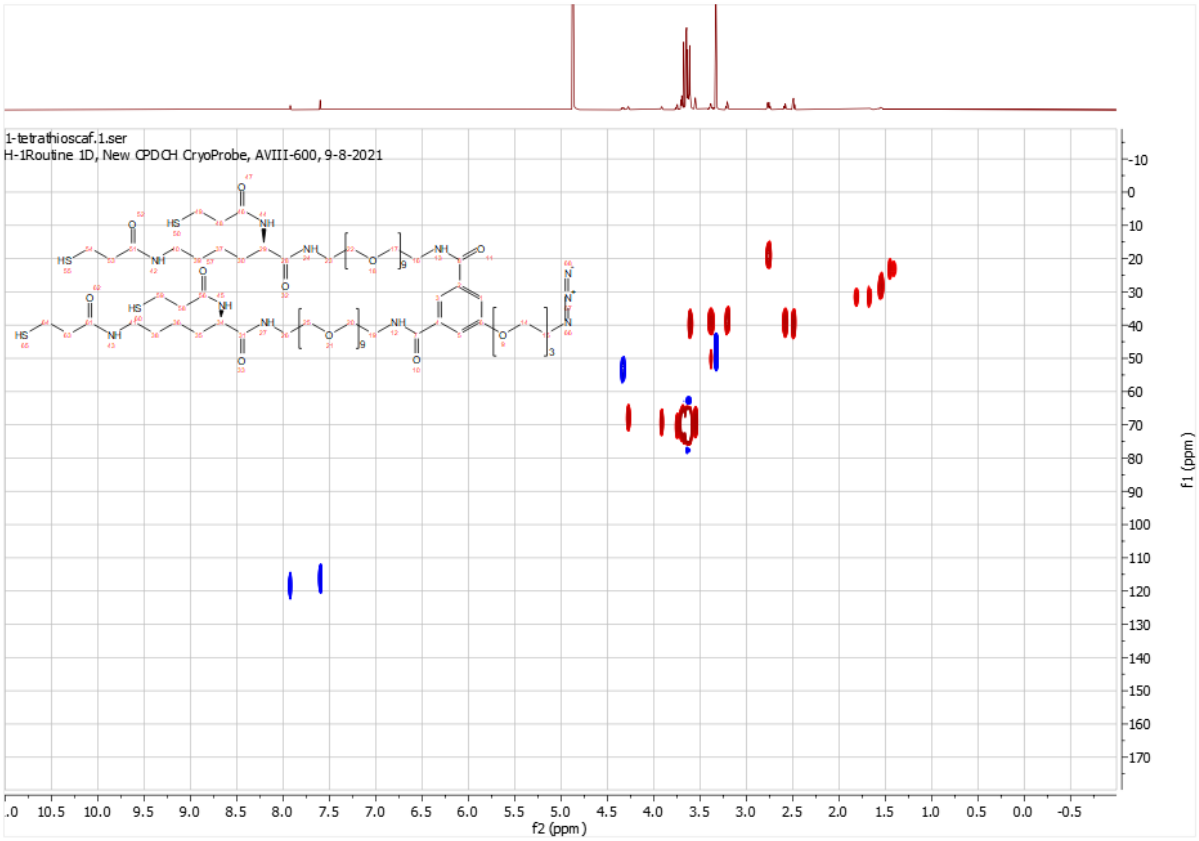

(25) Monovalent-CD22L-N_3

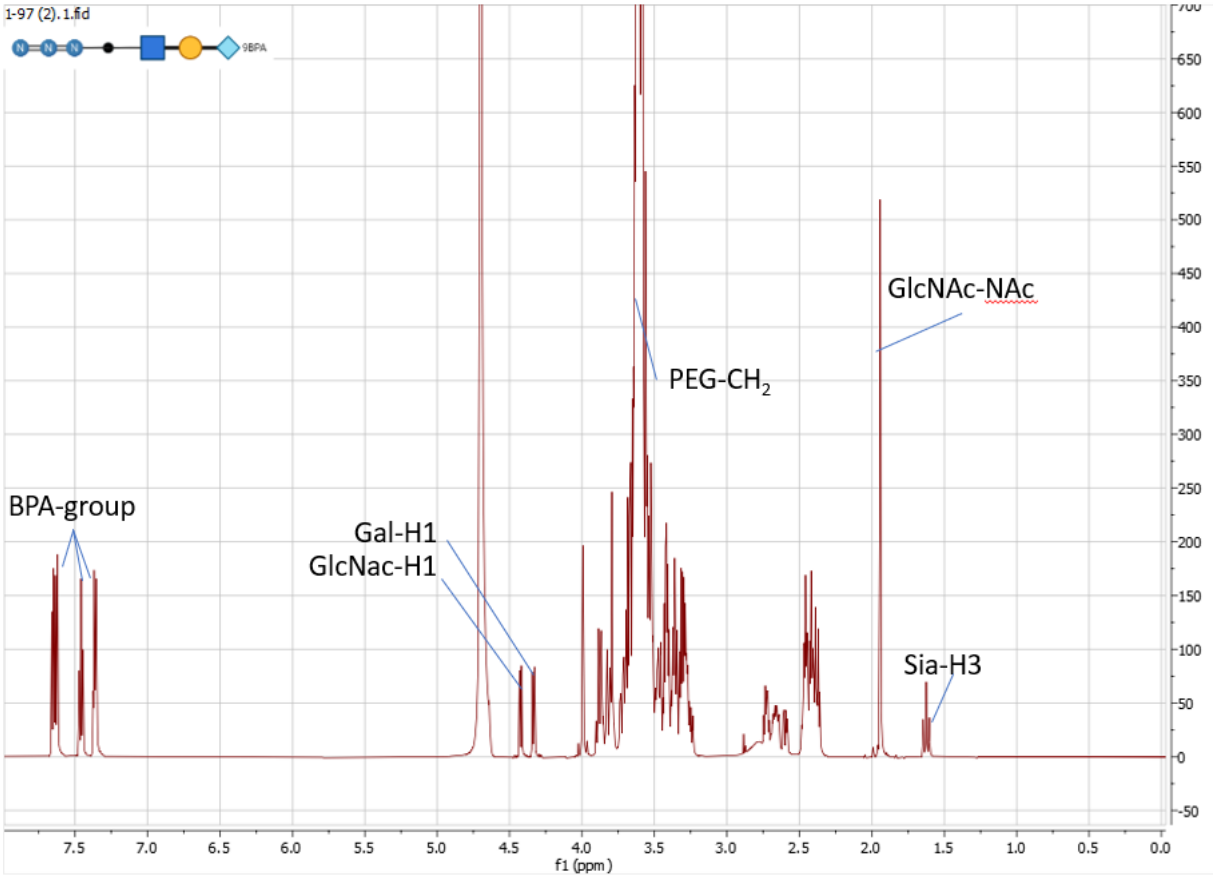

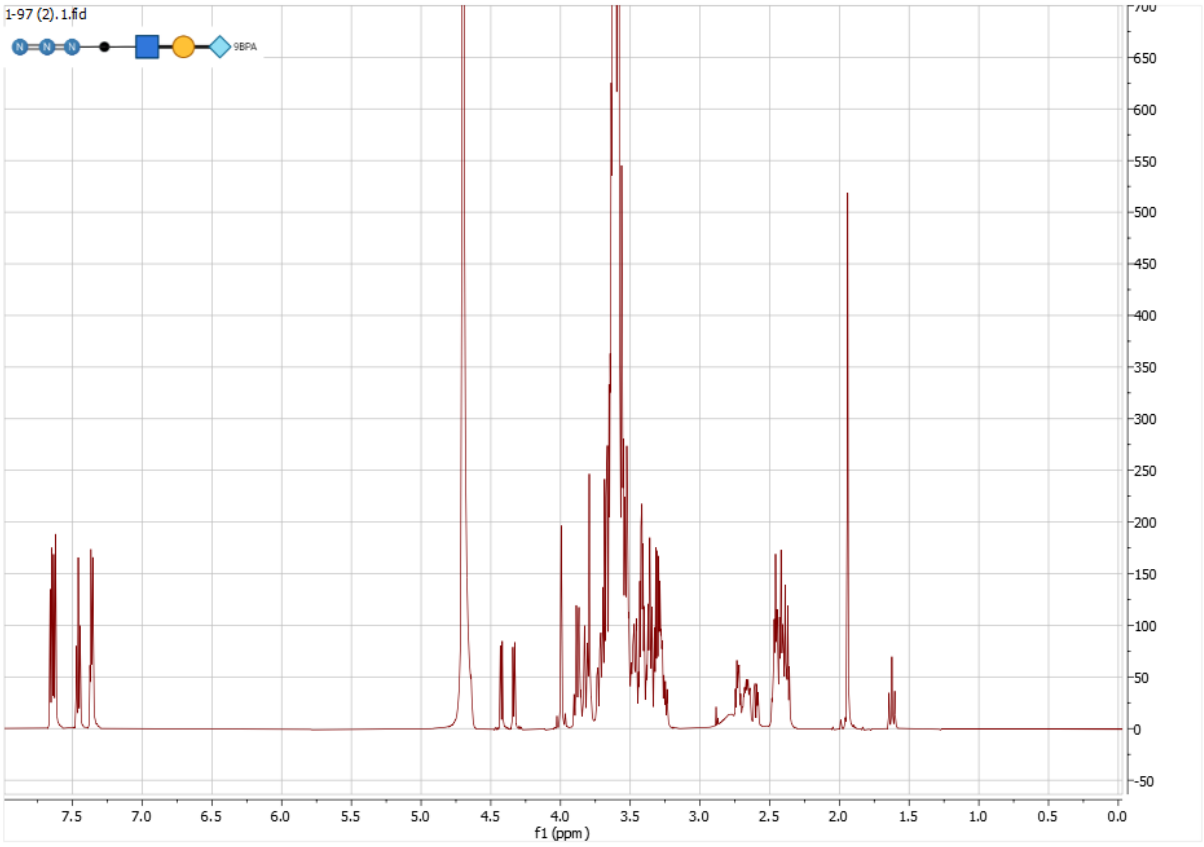
1-97 (2).1.fid
9BPA
f1 (ppm)


1-97 (2).2.ser
9BPA
f2 (ppm)
f1 (ppm)

(26) Divalent-GlcNAc-N_3

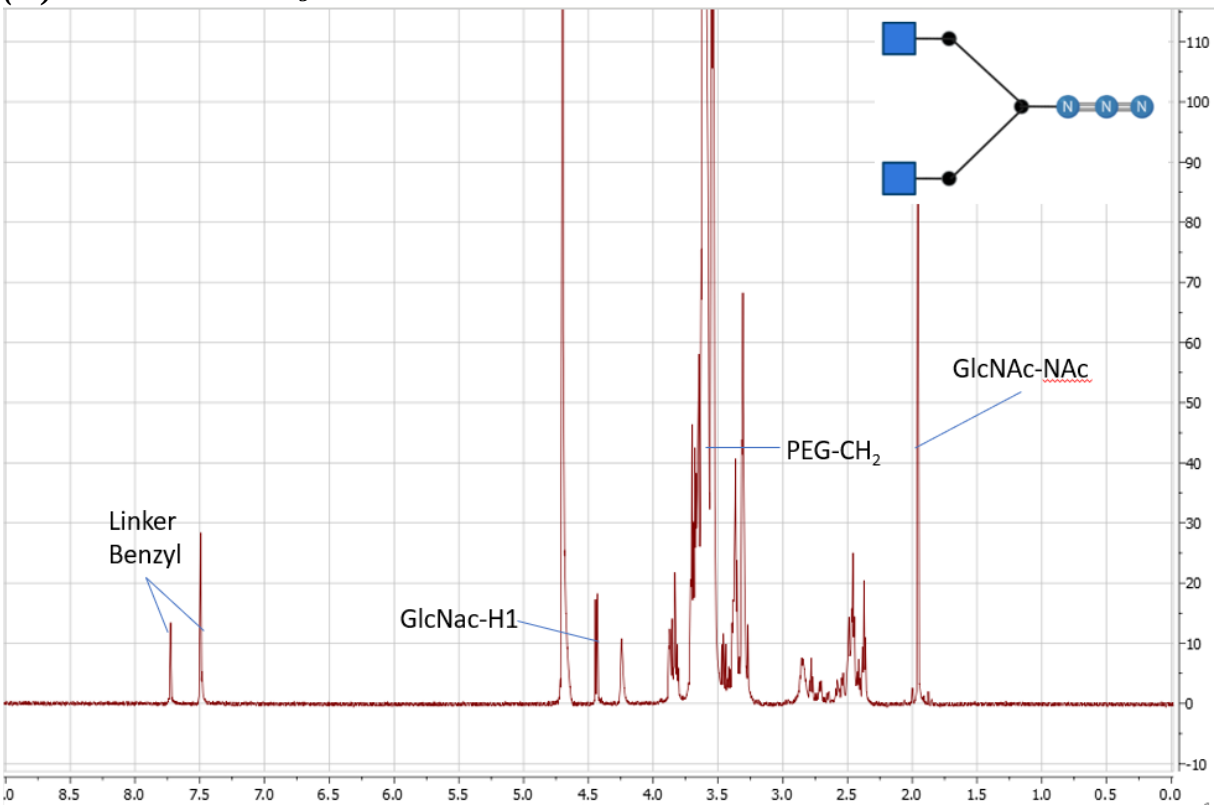

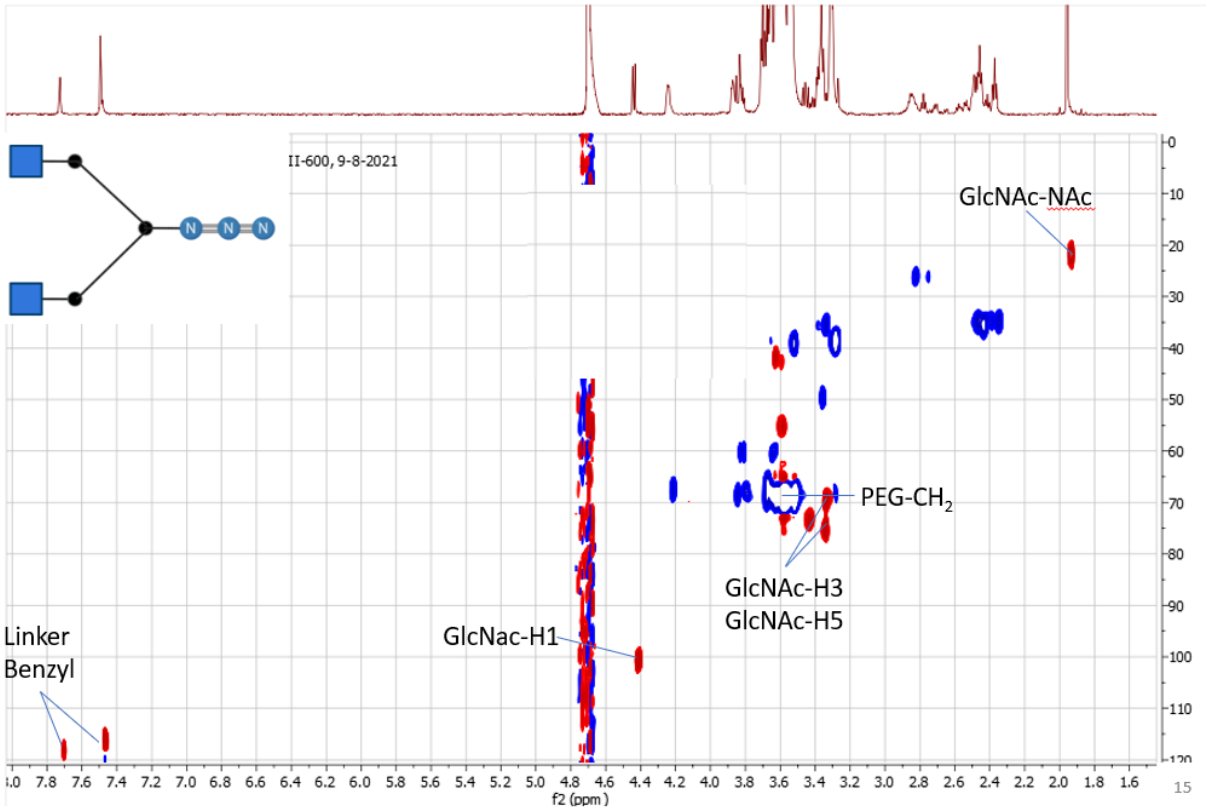

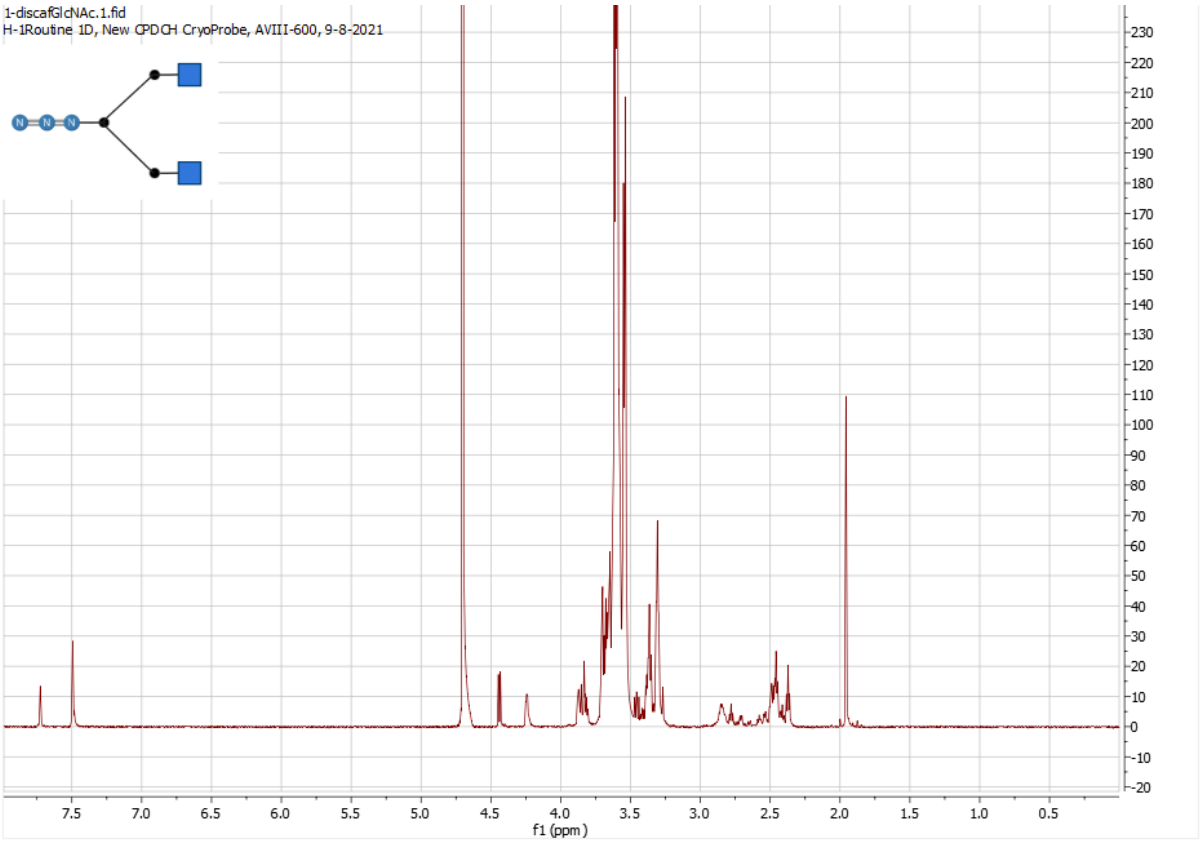
1-discafGlcNAc.1.fid
H-1Routine 1D, New CPDCH CryoProbe, AVIII-600, 9-8-2021
f1 (ppm)

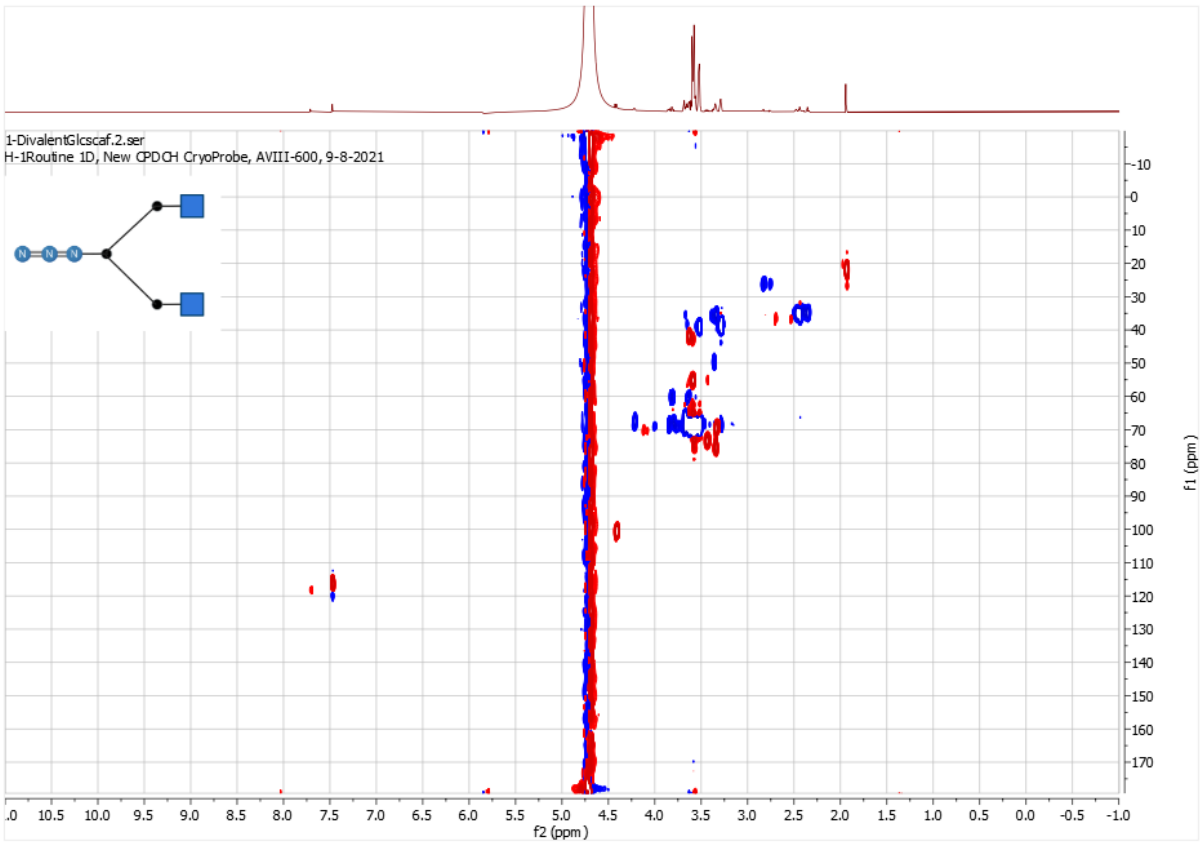
1-DivalentGlcscaf.2.ser
H-1Routine 1D, New CPDCH CryoProbe, AVIII-600, 9-8-2021
f2 (ppm)
f1 (ppm)

(27) Divalent-CD22L-N_3

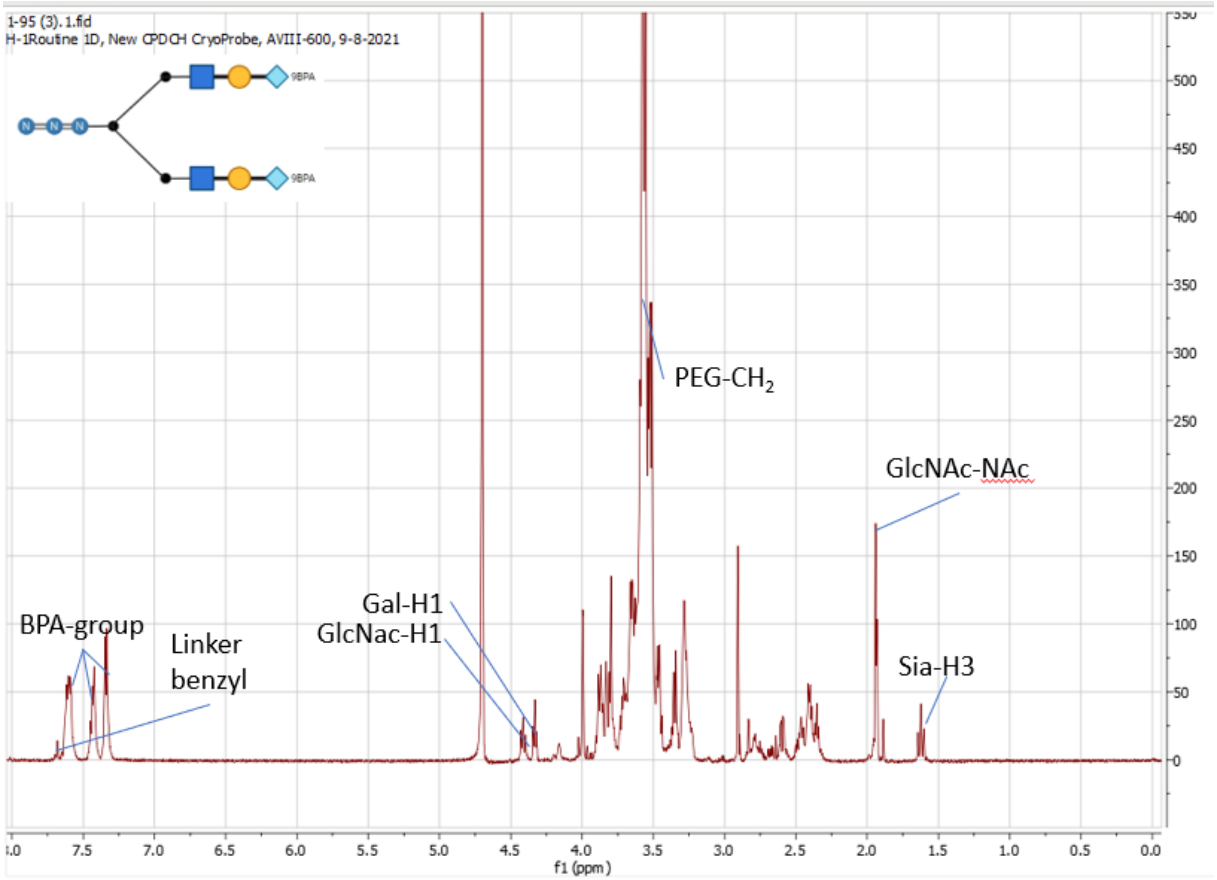

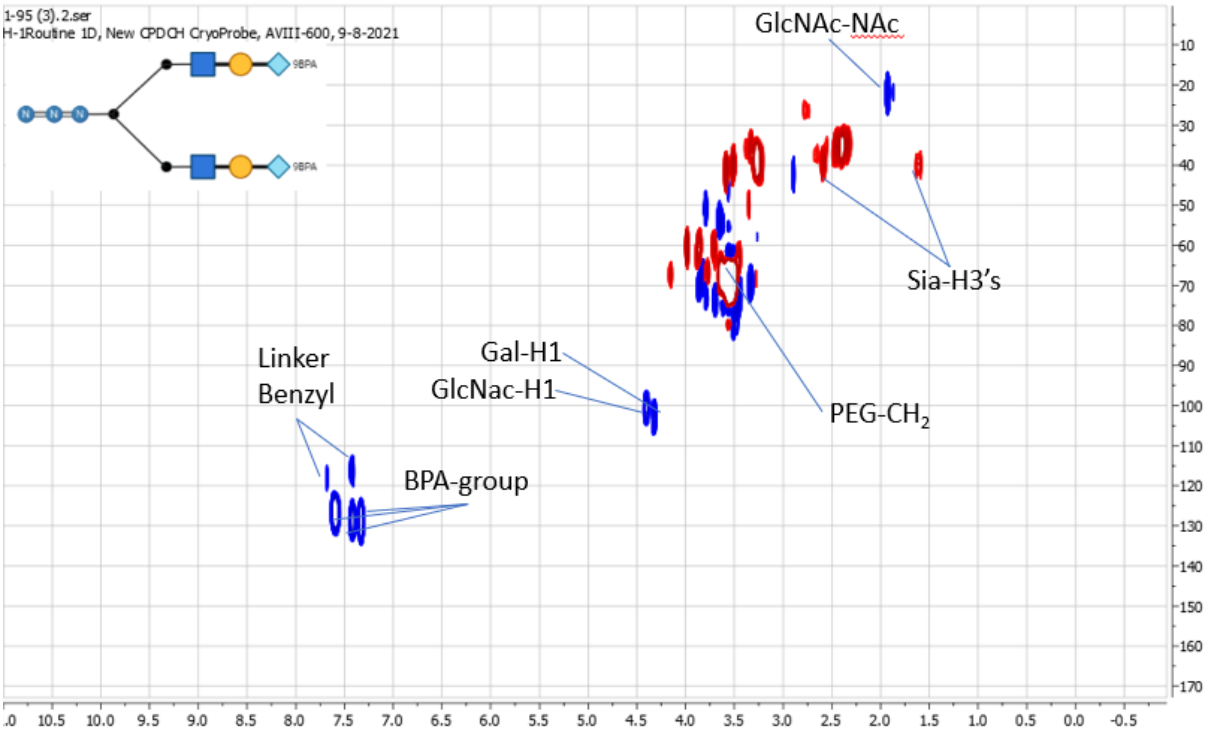

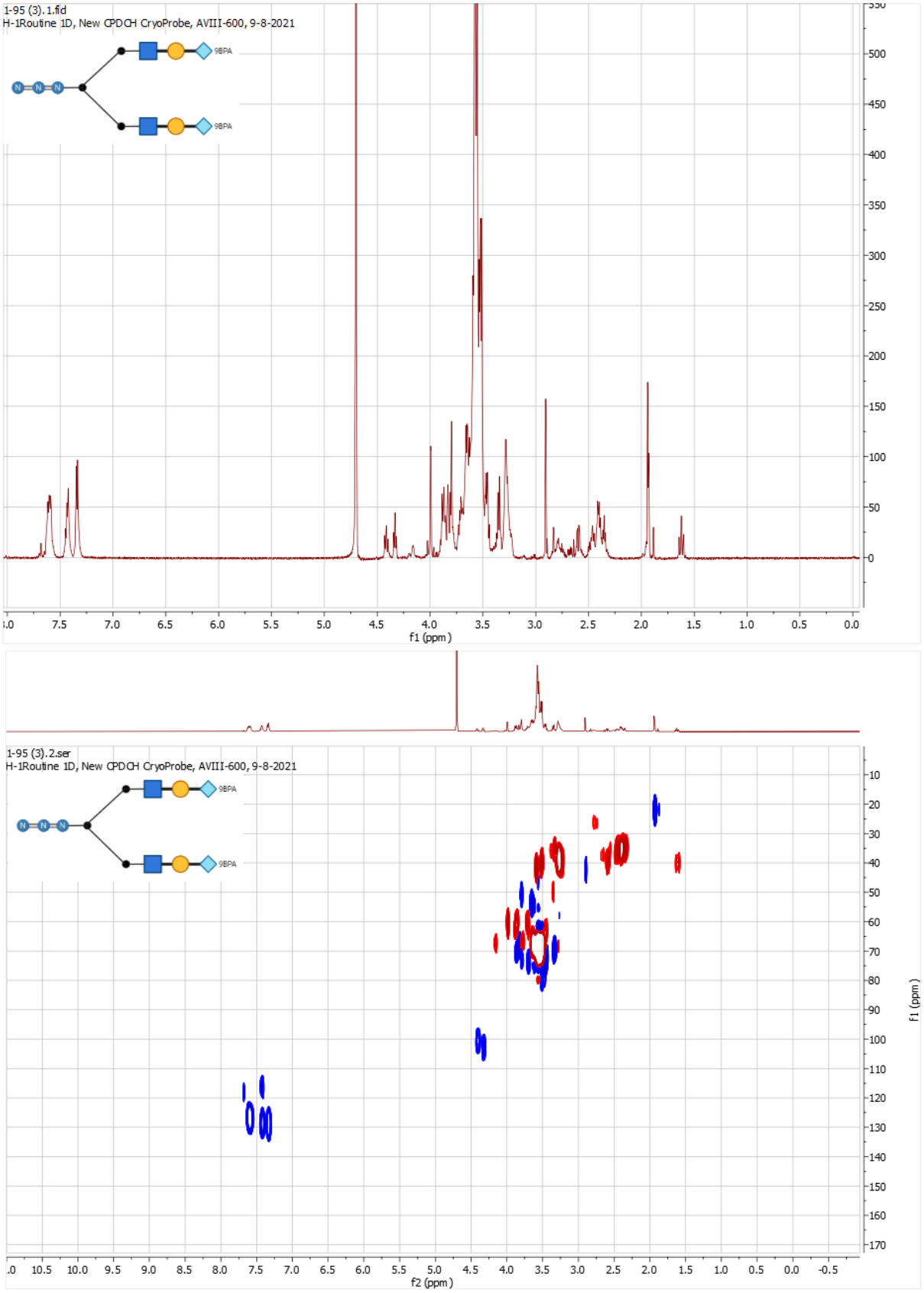
1-95 (3).1.fid
H-1Routine 1D, New CPDCH CryoProbe, AVIII-600, 9-8-2021
9BPA
9BPA
f1 (ppm)
1-95 (3).2.ser
H-1Routine 1D, New CPDCH CryoProbe, AVIII-600, 9-8-2021
9BPA
9BPA
f2 (ppm)
f1 (ppm)

(28) Tetravalent-CD22L-N_3

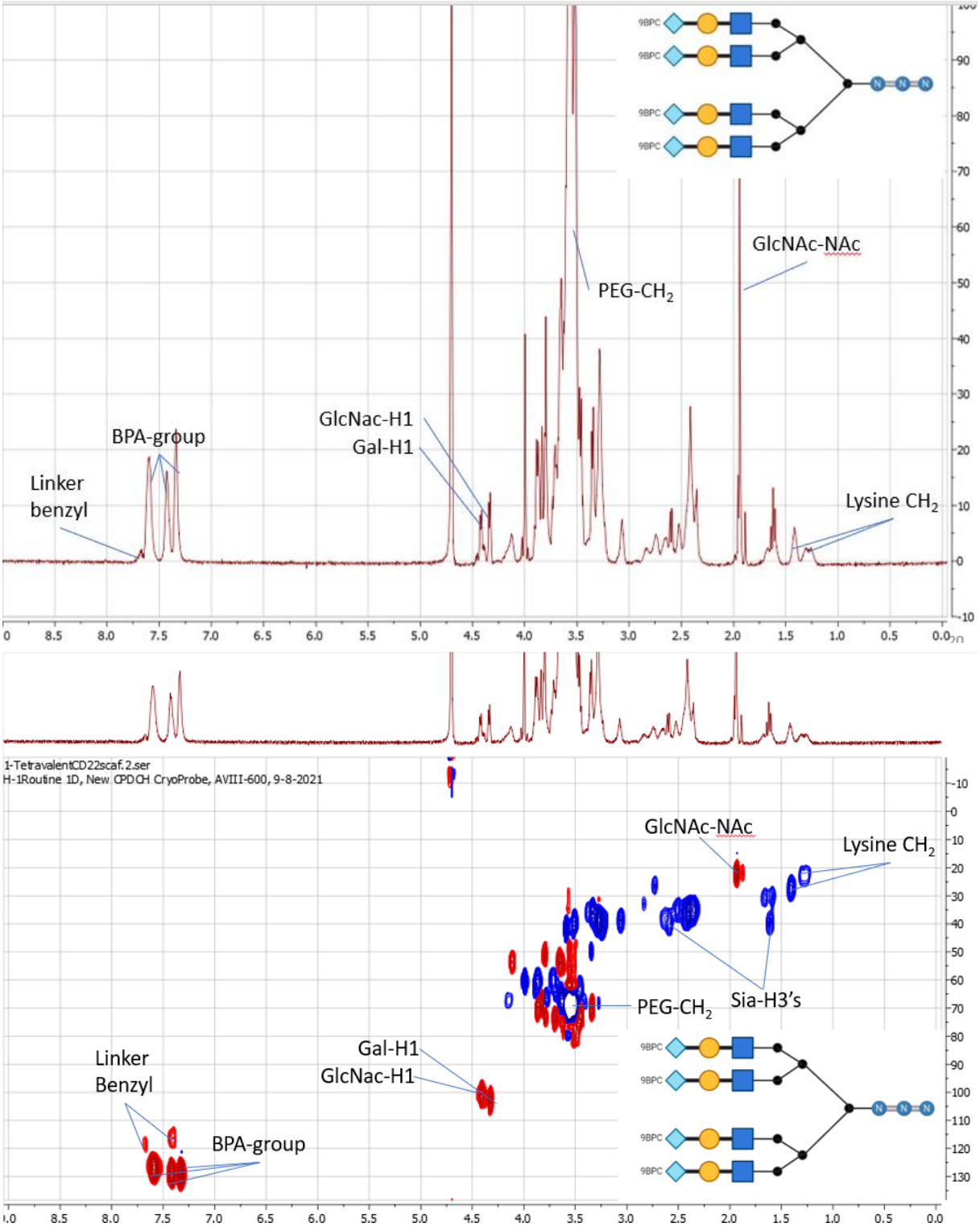

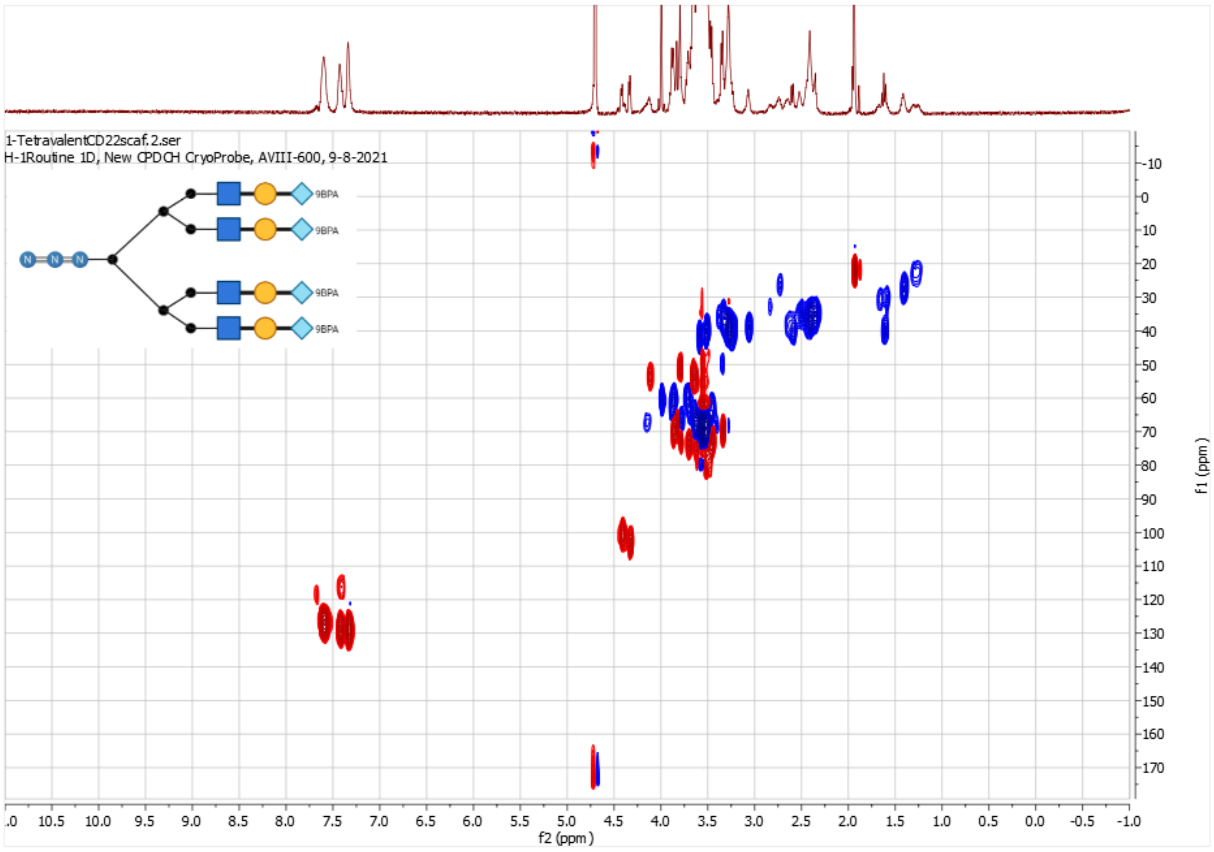
1-TetravalentCD22scaf.2.ser
H-1Routine 1D, New CPDCH CryoProbe, AVIII-600, 9-8-2021
9BPA
9BPA
9BPA
9BPA
f2 (ppm)
f1 (ppm)

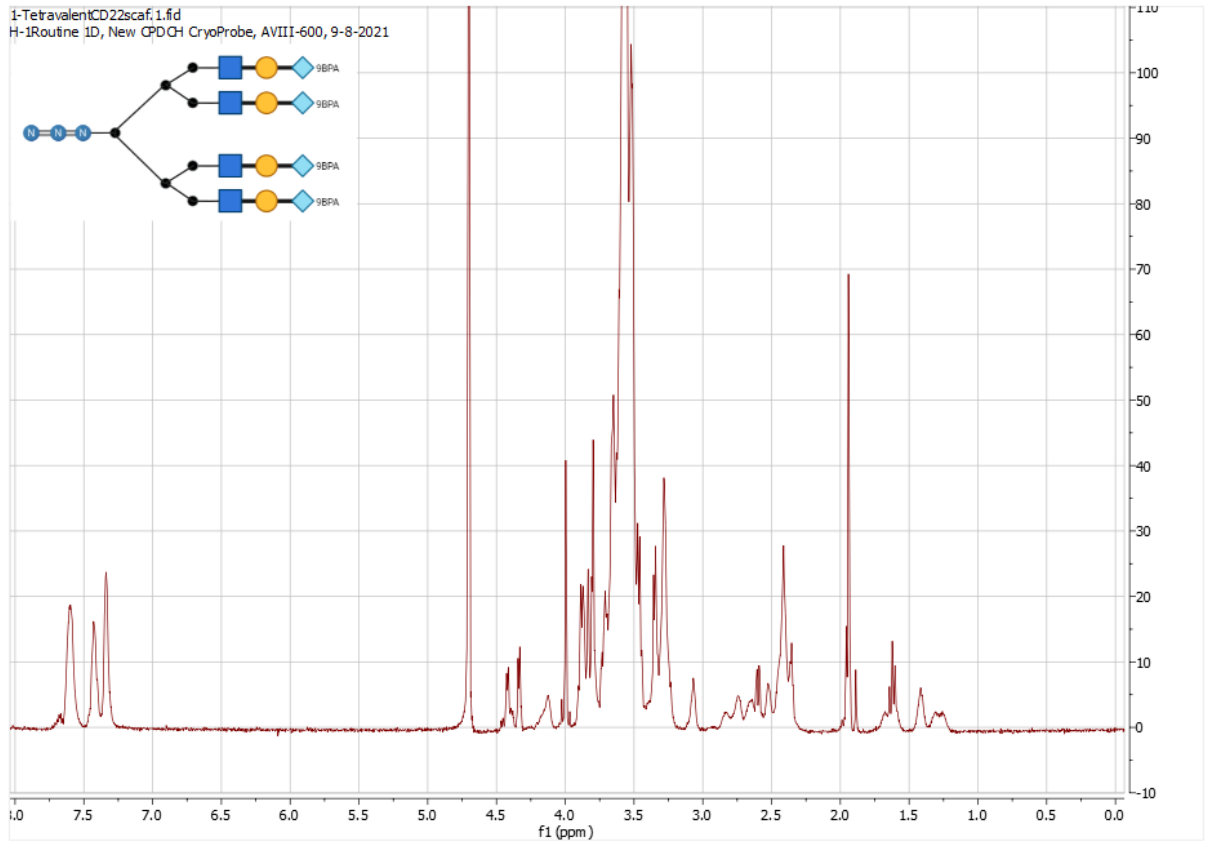
1-TetravalentCD22scaf.1.fid
H-1Routine 1D, New CPDCH CryoProbe, AVIII-600, 9-8-2021
9BPA
9BPA
9BPA
9BPA
f1 (ppm)

11.3 DECONVOLUTED MASS SPECTRA

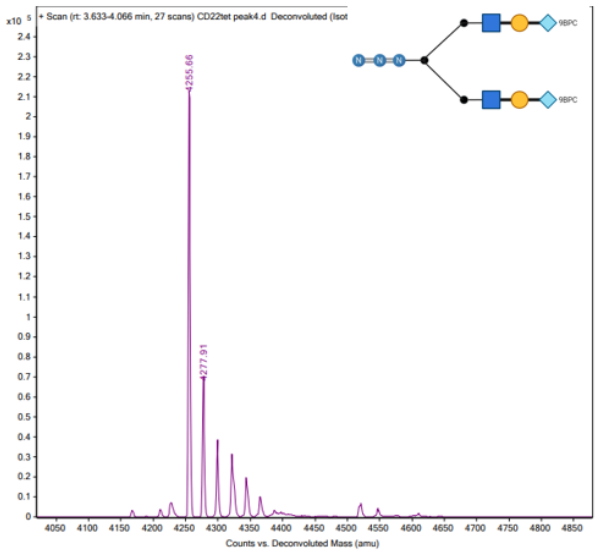

m/z = 4255.66
Calc[+H_2O] = 4255.87

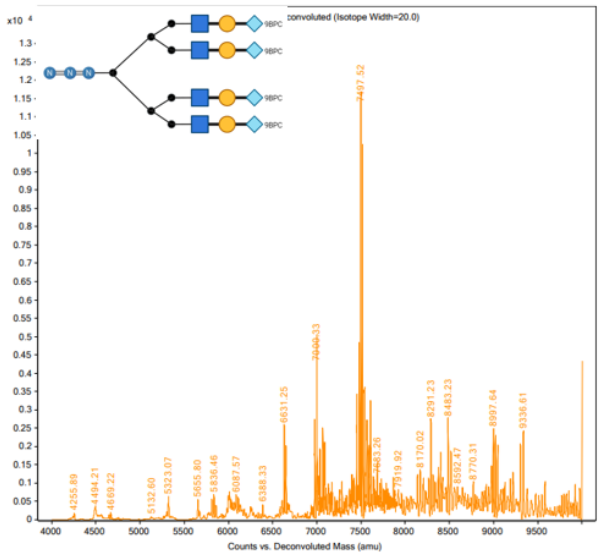

m/z = 7497.52
Calc[+Na] = 7497.86

OVA + 10 equivalent BCN-NHS

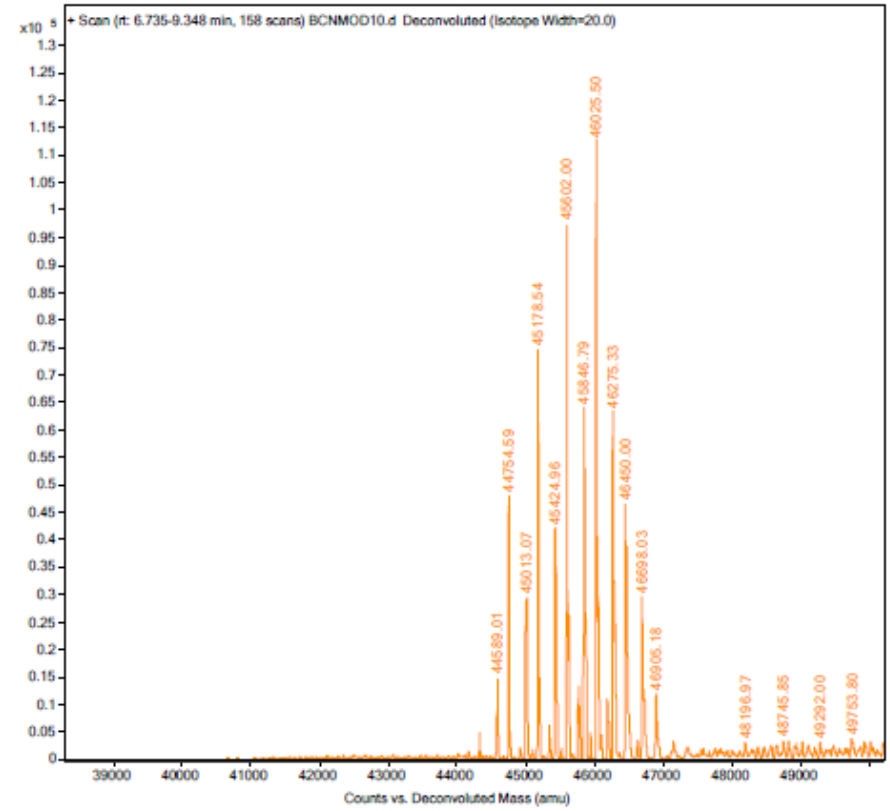

OVA + 15 equivalent BCN-NHS

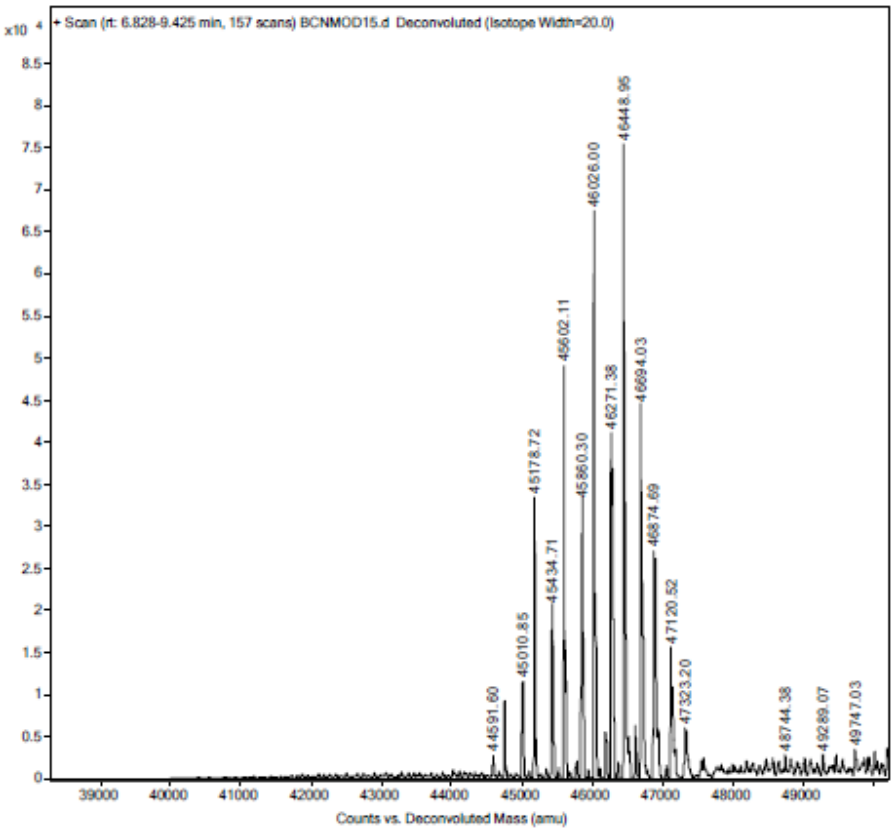

OVA + 20 equivalent BCN-NHS

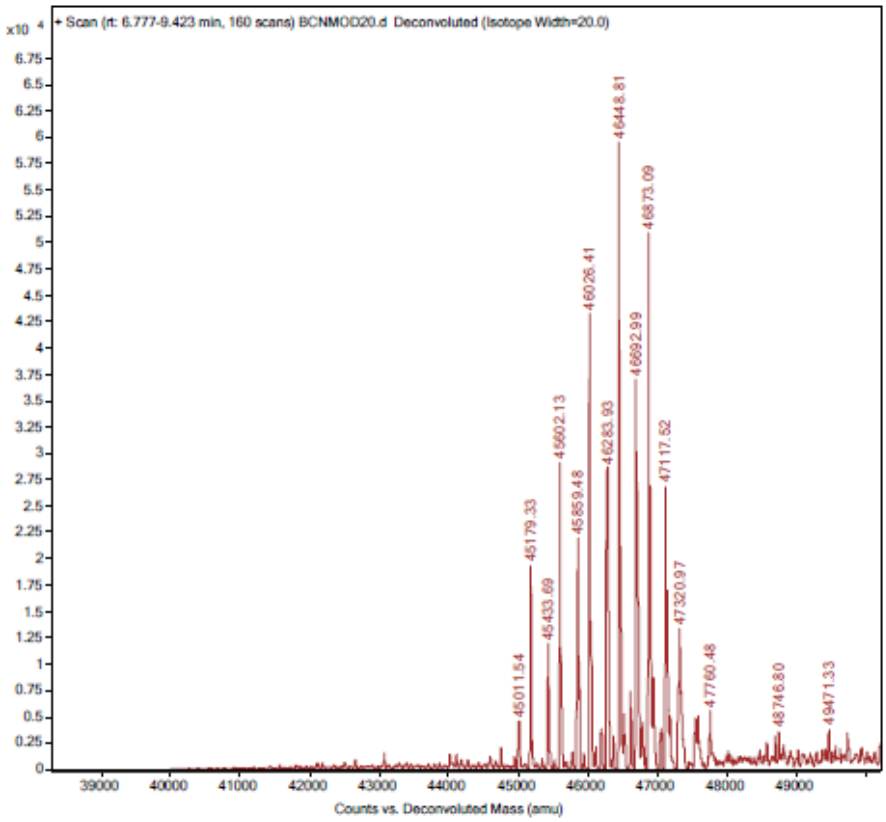

OVA + 25 equivalent BCN-NHS

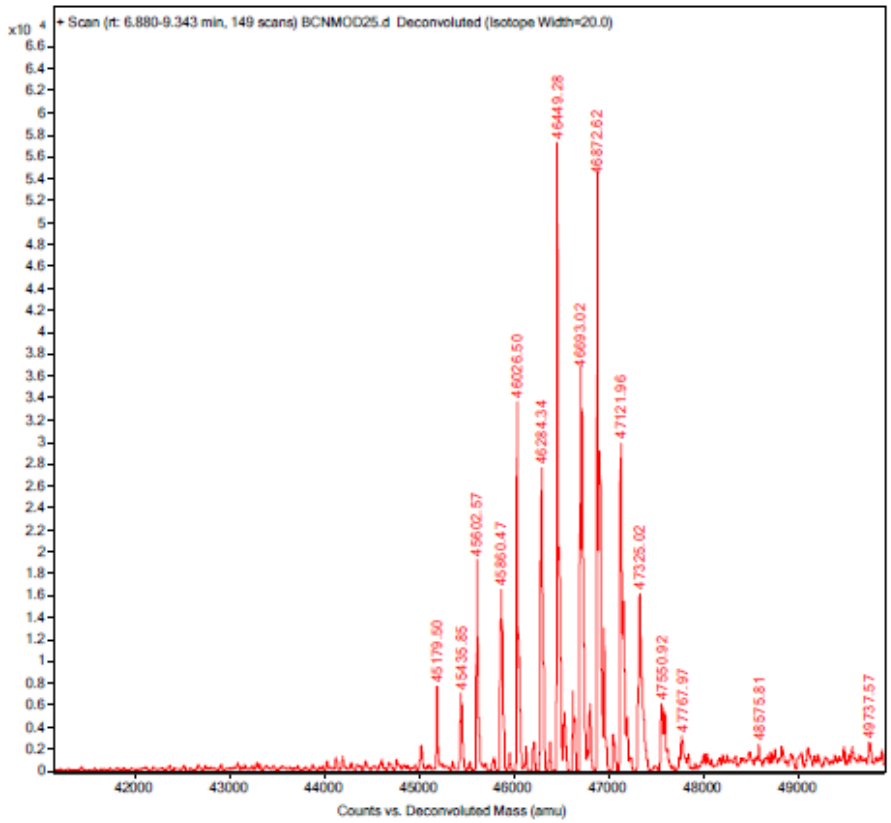

OVA + 30 equivalent BCN-NHS

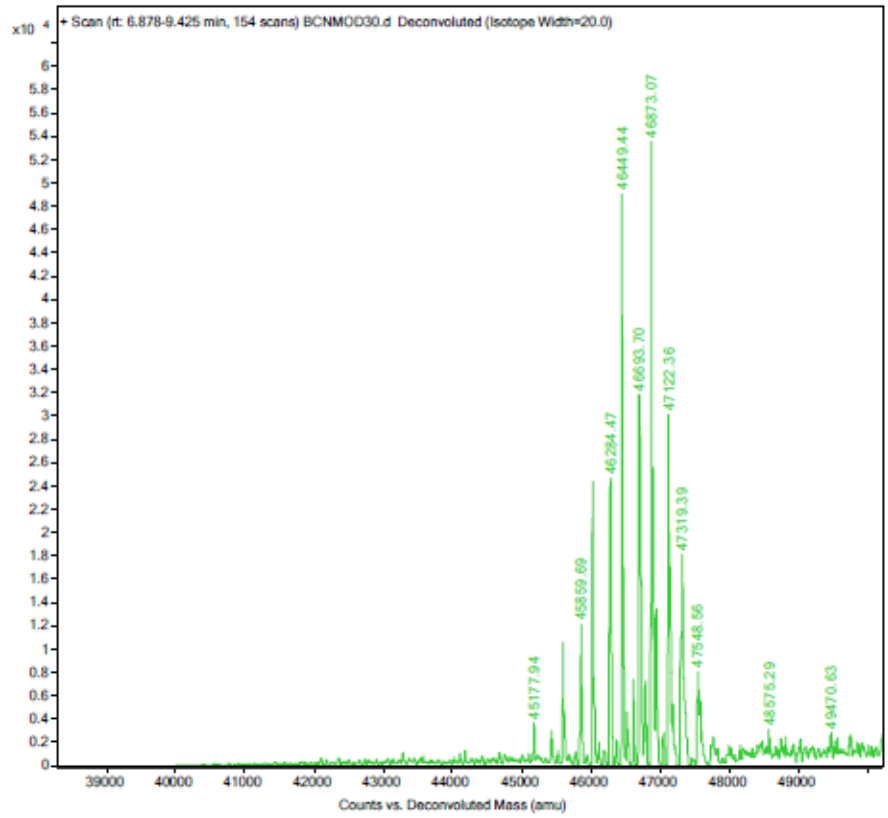

OVA + 40 equivalent BCN-NHS